IMPLEMENTATION OF PRETREATMENT PATIENT – SPECIFIC QUALITY ASSURANCE FOR INTENSITY MODULATED RADIOTHERAPY

BY

ALHASSAN MOHAMMED BAIDOO

(10702652)

THIS THESIS/DISSERTATION IS SUBMITTED TO THE UNIVERSITY OF GHANA, LEGON IN PARTIAL FULFILMENT OF THE REQUIREMENT FOR THE AWARD OF MPHIL MEDICAL PHYSICS DEGREE.

DEPARTMENT OF MEDICAL PHYSICS, SCHOOL OF NUCLEAR AND ALLIED SCIENCES

April, 2021

DECLARATION

I hereby declare that except for the references to other people's work cited, this work is the result of my own research and that it has neither in part nor whole been presented for any other degree elsewhere.

.....

(Alhassan Mohammed Baidoo)

Student

Date: 22-04-2021

.....

(Dr. Samuel N. A. Tagoe)

Principal Supervisor

Date: 26-04-2021

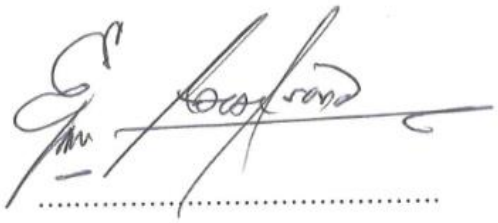

.....

(Mr. Eric K. T. Addison)

Co – Supervisor

Date: 23rd April 2021

DEDICATION

This work is dedicated to my beloved wife, Halimatu Saeed Jallo; daughter, Maryam bint Alhassan Baidoo and Muhammad Shaahid Alhassan Baidoo my son.

ACKNOWLEDGEMENT

I would like to express my deepest and sincerest gratitude to my supervisors: Dr. Samuel N. A. Tagoe and Mr. Eric K. T. Addison for their support, guidance and motivation that have brought me this far in the work.

In the profoundest of gratitude, I express my appreciation to the GNPC Foundation for the sponsorship, leading to the amazing discoveries throughout this research.

I am extraordinarily indebted to Mr. Evans Sassu of the Radiotherapy Department of the KorleBu Teaching Hospital (KBTH), whose support in this research is unparalleled. I am also thankful to the physicists and the entire staff of the Radiotherapy Department of the KBTH for their kind assistance.

I owe this success to my precious family; Mohammed Diafo Baidoo (Father), Mariama Baidoo (Mother), Ishmael Mohammed Baidoo (Brother), Mustapha Mohammed Baidoo (Brother), and my dearest Halimatu Saeed Jallo for her subservient assistance, care and support throughout the journey, and for being there for me.

Finally, I wish to happily and humbly express my sincerest appreciation to my friends Hafiz Saeed, Mujahid Eliasu and Mohammed Awwal Mensah for their support and encouragement.

TABLE OF CONTENT

LIST OF TABLES

LIST OF FIGURES

LIST OF ABBREVIATIONS

2D	2 – Dimensional
3D	3 – Dimensional
3DCRT	3 – Dimensional Conformal Radiotherapy
AAA	Anisotropic Analytical Algorithm
AAPM	American Association of Physicists in Medicine
ABS	Acrylonitrile Butadiene Styrene Plastic
ACR	American College of Radiology
AP	Anterior – Posterior
ASTRO	American Society for Radiation Oncology
BEV	Beam's Eye View
CAX	Central Axis
CD – ROM	Compact Disc Read-Only Memory
CI	Conformity Index
CPU	Central Processing Unit
CT	Computed Tomography
DD	Dose Difference
DICOM	Digital Imaging and Communications in Medicine
DLP	Dynamic Leave Gap
DMLC	Dynamic Multileaf Collimator
DTA	Distance – to – Agreement
DVH	Dose Volume Histogram
D_W	Absorbed Dose to Water

EBRT	External Beam Radiation Therapy
EDW	Enhance dynamic wedge
EPID	Electronic Portal Imaging Devices
EPM	Effective Point of Measurement
ESTRO	European Society for Radiation Oncology
GI	Gamma Index
GP%	Gamma Passing Rate
IAEA	International Atomic Energy Agency
IC	Ionization Chamber
ICRP	International Commission on Radiological Protection
IEC	International Electrotechnical Commission
IMRT	Intensity Modulated Radiotherapy
IPEM	Institute of Physics and Engineering in Medicine
KBTH	Korle-Bu Teaching Hospital
k_{pol}	Polarity Factor
k_q	Quality Factor
k_{sat}	Saturation Factor
$k_{t/p}$	Temperature – Pressure Correction Factor
LCD	Liquid Crystal Display
LED	Light Emitting Diode
MLC	Multileaf Collimator
MPHIL	Masters of Philosophy
NCRNM	National Centre for Radiotherapy and Nuclear Medicine

NCS	Netherlands Commission on Radiation Dosimetry
NPC	Nasopharyngeal Carcinoma
NTCP	Normal Tissue Complication Probability
OARs	Organs at Risk
PA	Posterior – Anterior
PC	Personal Computer
PDD	Percent Depth Dose
PSDL	Primary Standard Dosimetry Laboratory
PTV	Planning Target Volume
Q	Beam Quality
Q_0	Reference Beam Quality
QA	Quality Assurance
QC	Quality Control
RT	Radiotherapy
SAD	Source to Axis Distance
SC	Stealth Chamber
SCD	Source to Calibration Distance
SMLC	Segmented Multileaf Collimator
SPD	Source-Phantom Distance
SSD	Source to Surface Distance
SSDL	Secondary Standard Dosimetry Laboratory
TCP	Tumour Control Probability
TG	Task Group

TMR	Tissue Maximum Ratio
TNC	Threaded Neill – Concelman
TPR	Tissue Phantom Ratio
TPS	Treatment Planning System
TRS	Technical Report Series
VMAT	Volumetric Arc Therapy

ABSTRACT

Clinical implementation of Intensity Modulated Radiotherapy (IMRT) has begun in Ghana, despite this advancement, to date, there has been no implementation of patient-specific IMRT verification Quality Assurance (QA) in Ghana. If this is not addressed, the degree of accuracy and dose conformity in our IMRT plans may not be realized clinically.

The main objective of this study was to verify the actual dose that would be delivered to the patient during an IMRT treatment at the National Centre for Radiotherapy and Nuclear Medicine (NCRNM), based on implementation of patient – specific Quality Assurance for IMRT prior to external beam radiation treatment using Gamma Index method.

Ten (10) IMRT plans were generated for a phantom study using 3, 5, 7 or 8 fields IMRT, based on clinical objectives for the treatment of 10 patients with varying prostate and head and neck cancers. The procedure involved linear accelerator commissioning, absolute dose determination, calibration of patient – specific QA device, IMRT treatment planning, plan verification for IMRT, treatment delivery and data analysis using the gamma index (3%/3 mm, threshold 5%) criteria with 95% passing rate.

All prostate IMRT cases enrolled in the study passed the acceptance criteria, with values that ranged from 95.50 to 98.43%.The mean passing rate, based on the gamma index method ($\gamma \leq 1$) for treatment of each of the cases using the MatriXX was 96.82±1.22%, showing good compliance with the prescribed rates for all 5 cases.The mean value for the pass rate of the head - and - neck IMRT cases was 96.42±1.14% with one case failing the acceptance criteria of the gamma evaluation method, and the passing values ranged from 94.60 to 97.70%.

The reference doses calculated at TPS were accurately delivered by the medical linear accelerator, and the gamma criteria for acceptance were mostly satisfied by the selected cases throughout the research for both cancer sites under study. The measurements and the results demonstrated that the delivery equipment, the treatment planning system, the QA tools and their corresponding software were accurate and therefore acceptable for IMRT implementation at the centre. The analysis made demonstrated that these IMRT results were consistent with peer reviewed baseline data for a well-commissioned IMRT program.

CHAPTER ONE

INTRODUCTION

1.0 Introduction

This chapter gives the background information to the study, statement of research problem, research objectives, the scope and limitation, as well as the justification and relevance of the research work. The systematic arrangement of the entire work is as well outlined in this chapter.

1.1 Background

Intensity Modulated Radiotherapy (IMRT) is an external beam technique that uses multiple radiation beams of non-uniform intensities, characterizing a steep in-field dose gradient in clinical applications for the treatment of diseases, allowing better conformity of dose to the planning target volume (PTV) and better avoidance of organs at risk (OARs) (Agazaryan, et al., 2003).

Physicists, physicians and radiotherapists have over the century been trying to promote means of providing doses of tumour-specific radiation to different tumors appearing in diverse anatomical sites. Various types of devices, technology, software and procedures have been established to meet diverse clinical requirements. In the 1960s, metallic beam modifiers were first used to adjust the spatial distribution of the beam intensity for two-dimensional (2D) radiotherapy treatments (Cheung, 2006). Despite the existence of three-dimensional (3D) techniques, there were no available practical means of delivering intensity modulated beams in radiotherapy until mid-1990s (Cheung, 2006). The advent of

computers into radiotherapy led to the development of new class of computer – controlled medical linear accelerators (linacs) with motorized multileaf collimators (MLC) dedicated to both beam shaping and fluence modulations and this pave the way for Intensity Modulated Radiotherapy (IMRT) (Cheung, 2006).

The potential benefit of this technique to the patient is the reduction of the probability of in-field recurrence, reduction of the degree of morbidity associated with treatment, and the improvement in local control.

However, the complexity of the technique necessitates stringent tolerance levels for random and systematic errors for the achievement of high conformity and high precision treatment. Quality assurance (QA) prior to treatment is therefore a major concern in sophisticated radiotherapy plans like IMRT (Cyriac, et al., 2014).

1.2 Statement of the Problem

Intensity modulated radiotherapy has the dosimetric capacity to deliver planned doses to the delineated target volume with high precision, and with better chances of sparing the critical tissue structures adjacent to the target. However, such a degree of exactness and conformity in dose delivery may perhaps not be realized as a clinical goal due to dosimetry calculation errors, geometrical tolerance of the treatment machine, patient set-up errors, and uncertainties associated with delineation and contouring of the target and critical tissue structures (Cheung, 2006). The dosimetric benefits of IMRT can be clinically realized depending on the exactitude in localizing and delineating the tumour and the adjacent normal structures, understanding the prime connection between dose and response for

specific tumour, and delivery of the prescription doses according to the treatment plans (Son, et al., 2015).

Such an increasing sophisticated treatment that has gathered widespread adoption requires QA verification program that is effective and extensive, in terms of both machine – specific and patient – specific delivery precision (Cyriac, et al., 2014). This is because proper verification of QA procedures for both equipment and individual dosimetry are imperative measures to guarantee that treatment could be delivered in accordance with treatment plans (Ravichandran, et al., 2011). For IMRT, there is sudden increase in treatment parameters and verifying each one prior to treatment delivery is very cumbersome and difficult task to undertake. Also, during IMRT treatment planning, the number of treatment parameters that one needs to control is very colossal making it impossible to use forward planning approach. IMRT treatment planning is therefore based on inverse planning; where the planner provide desired dose distributions and constraints as well as irradiation geometries, and the treatment planning system (TPS) comes out with beam fluence modulations that need to be applied to the various beams to achieve the desired dose distributions. Beam fluence modulations are made possible by the movement of the MLCs during treatment delivery based on coordinates with respect to time and speed of each leaf of MLC transferred from the TPS to the treatment machine. Lot of things may go wrong with this process that would influence the delivered dose distribution. With reference to this, one needs to acknowledge limitations associated with the treatment machine. Since the chosen treatment parameters would culminate into dose distribution, it is therefore prudent to assess the dose distribution in order to verify the treatment parameters. Clinical

implementation of IMRT thus requires a well implemented QA verification system (Cheung, 2006).

It is therefore a critical requirement as a nation to review the dosimetry advantages of IMRT, issues relating to the limitations in the equipment present, clinical QA procedures, and a wide scale implementation of the technique.

Meanwhile, the regular QA protocols for evaluating the accuracy and precision in IMRT are mostly machine – specific. This form of QA does not guarantee treatment precision, as its major goal is the optimal performance of the radiologic device. A careful analysis of recommendations by American Association of Physicists in Medicine task group report 53 (AAPM TG – 53) as well as No. 7 booklet by European Society for Radiation Oncology (ESTRO) reveals deficiencies in the existing IMRT QA regardless of the selected metric (Stojadinovic, et al., 2014).

Patient – specific QA, well thought-out to be the confirmatory phase of the IMRT treatment process must therefore be performed prior to a clinical treatment, as it ensures compliance between planned and treatment dosimetry of the individual patient. This type of QA sanctions the exactness of administered doses using both the transfer of procedural setup and dose – delivery information (Hatford et al., 2016).

Considering the fact that Ghana has approximately 0.1 radiotherapy treatment machine per a million population as opposed the expected 1-3 radiotherapy treatment machines per million population in Africa (Adhanom, 2019), it is extremely relevant to avoid treatment errors at all costs by verifying IMRT techniques based on measurement of dosimetry for individual patients.

Ghana has just begun the clinical implementation of IMRT technique, despite this advancement, to date, there has been no implementation of patient – specific IMRT verification QA in Ghana.

If this is not addressed, the degree of precision and dose conformity in our IMRT plans may not be realized clinically due to errors in dosimetry calculation, patient set-up, and geometrical tolerance of the treatment machine (Cheung, 2006).

1.3 Research Objectives

The main objective of the study was to verify the actual dose that would be delivered to the patient during an IMRT treatment at the National Centre for Radiotherapy and Nuclear Medicine (NCRNM), based on implementation of patient – specific Quality Assurance for IMRT prior to external beam radiation treatment using Gamma Index method.

1.3.1 Specific objectives

a) To verify the TPS being used for IMRT plans by the possibility of newly generated IMRT plans to pass an internationally acceptable gamma passing rate;
b) To verify the accuracy of the entire IMRT setting by comparing doses prescribed at TPS to doses delivered by the medical linear accelerator;

1.4 Relevance and Justification

In order to ensure accurate transfer of the parameters of treatment and confirm the dose delivered by the medical linear accelerator prior to the start of the actual patient treatment, pretreatment verification is highly recommended by several professional societies. It is used to check whether the IMRT plan is deliverable or not, and does not contain deviant shapes, and can ensure that verification and the relationship between dosimetric and geometric parameters are checked to be in tolerance (van der Wal, et al., 2013).

Dosimetric verification of an IMRT plan specific to a patient is an important part of clinical implementation of the technique (Pan, et al., 2019). Patient-specific Quality Assurance for this modality is critical to its successful implementation. It ensures accurate equipment delivery of the planned doses by assessing the accurateness of treatment planning, transfer, plan set-up and delivery (Pan, et al., 2019). It is highly recommended to be part of the clinical process of IMRT by international professional societies such as the American Association of Physicists in medicine (AAPM), the European Society for Radiation Oncology (ESTRO), the American Society for Radiation Oncology (ASTRO), the American College of Radiology (ACR), and the Netherlands Commission on Radiation Dosimetry (NCS) (Pan, et al., 2019).

Realization of fluence distribution across beams prior to treatment delivery is paramount to any IMRT treatment (Tagoe, et al., 2018). Pretreatment dosimetric verification is therefore a requirement in all IMRT treatment plans to relate the beam fluence maps delivered using continuous motion of multileaf collimators (MLCs) (Stasi, 2012).

In order to establish patient – specific QA programs for the clinical implementation of the technique, and for the purpose of detecting potential mismatches between the dose measured by TPS and the dose actually administered by treatment devices, designated patient-specific QA protocols are expected to be followed (Stasi, 2012).

Meanwhile, there has been lack of verification programs on pretreatment patient-specific Quality Assurance for IMRT in Ghana. Therefore, as IMRT plans have been introduced in routine clinical practice in Ghana, it requires the implementation of pretreatment patient – specific QA. (Stasi, 2012).

1.5 Scope and Limitation of the Study

This work begins with commissioning tests on the linear accelerator at the center, absolute dose determination and calibration of the MatriXX IBA detector at the centre to be used for patient – specific QAs.

It also involves computed tomography (CT) scan of a MatriXX IBA detector, generation of IMRT treatment plans of miniPhantom based on specified clinical demands, IMRT plan verification, treatment of the miniPhantom, and the use of myQA Patient SW for the comparison of planned and measured dose distributions.

The work would end with conclusions and recommendations of protocols for patient – specific IMRT QA based on analytical findings.

CHAPTER TWO

2.0 LITERATURE REVIEW

2.1 Introduction

Several technological models exist for the implementation of Intensity Modulated Radiotherapy (IMRT). There is the MLC based system using a conventional linear accelerator, a tomographic system that is based on a helical slice-wise delivery method and robotic systems that use of many small beam segments. These models are relatively different from one another in the manner of their implementation. This research was restricted to the pretreatment patient-specific quality assurance of the MLC based systems of IMRT.

This chapter highlights the relevant literature review pertinent to the contemporary areas of the study. It covers overview of Intensity Modulated Radiotherapy (IMRT); dosimetric advantages of IMRT; IMRT in Ghana; IMRT Treatment Planning Systems; IMRT Quality Assurance; measuring devices; calibration of measuring devices; dose measurement methods; analytical software; Gamma Index, Dose Differences, and Distance to Agreement evaluation; and review of similar work done.

2.2 Overview of Intensity Modulated Radiotherapy

IMRT is a sophisticated clinical technique used to deliver highly conformal radiation doses to the treatment target, while sparing the critical normal tissue structures, and has superior dosimetric advantages over two-dimensional (2D) and conventional three-dimensional conformal radiation treatments (3DCRT) (Cheung, 2006).

During external beam radiation therapy, the spatial distribution of radiation dose within a patient is influenced by factors such as surface topography at the point of beam entrance and tissue inhomogeneities within the irradiated region. These factors along with the complex shape of an irradiated target volume (tumor) call for the modulation of the beam fluence distribution across the individual radiation fields (Tagoe, et al., 2018).

Intensity modulated radiotherapy (IMRT) uses several multiple beams of non-uniform radiation intensities in clinical applications for the treatment and management cancerous diseases. The beams are modulated to the required intensity maps for delivering highly conformal doses of radiation to the treatment targets, while sparing the adjacent normal tissue structures (Cheung, 2006). Thus, the modulation facilitates the optimization of the radiation dose to the intended target volume while minimizing radiation dose to the neighboring normal tissues (Tagoe, et al., 2018). The relevance of the effort in this area is to escalate the dose and reduce the possible risk of severity of complications (Agazaryan, et al., 2003).

The high dose conformity in IMRT enables escalation of dose and a better fortification to normal tissue structures. This makes it principally appropriate for the management and treatment of diseases that have possibility of high rates of local recurrence, toxicity and complications related to treatment. Nasopharyngeal carcinoma (NPC) is an example of the numerous cancer diseases that can benefit from the technique, owing to the acknowledged radio-curability, and the evidence of a relationship between dose and response for the disease. The numerous critical normal tissue structures in close proximity of the tumour also warrant this treatment. It is actually demanding to deliver a agreeable radiation dose to the target volume of the NPC by conventional techniques without leading to significant

irradiation of the adjacent critical structures, such as the spinal cord. This is particularly difficult in locally advanced diseases. Planners of treatment often have to make compromises between protection of normal organ and optimal coverage of dose (Cheung, 2006).

The implementation of IMRT at a facility needs the actualization of basic requirements which begins with the availability of a treatment planning system (TPS) with inverse planning or forward planning competences, possessing direct optimization algorithms to support the provision of the fluence distributions across the beams depending on predefined distribution of doses, and another requirement is the availability to a teletherapy machine containing multi-leaf collimators regulated with dedicated computers and its software to assist the movement of the leaves of the collimator system during treatment (Tagoe, et al., 2018).

The result of an increasingly multifarious computerized process for delivering doses to a patient constitutes the MLC-based intensity modulated radiotherapy (IMRT) (van der Wal, et al., 2013). IMRT uses the multileaf collimators (MLC) to modulate the beam intensity that is delivered to the tumour (Son, et al., 2015).

2.2.1 Equipment and Operation

Clinical implementation of IMRT involves the accessibility of an array of sophisticated equipment. It as well require a range of compatible auxiliary facilities, including imaging paraphernalia, computerized systems, dosimetry and QA systems, patients' immobilization devices, along with a multidisciplinary team of highly proficient staff (Cheung, 2006).

The IMRT modality is mostly administered by medical linacs with multileaf collimators. The machine can be custom-built to deliver treatment for IMRT in diverse modes of operation using MLCs (Cheung, 2006).

One of the most commonly used modes of operation is the step-and-shoot or segmental MLC (SMLC) technique, in which, the modulation of intensity of beam in a treatment field is created by the exposure of a series of MLC shaped discrete segmental fields (Cheung, 2006). The beam of radiation in this mode is automated to be off once the MLCs remain moving from any field to the other, and its automatically turned on once the leaves have reached and stopped at the defined positions (Cheung K. , 2006). The other frequently used method of IMRT delivery is the sliding window or dynamic MLC (DMLC) technique. This IMRT beam is created as a result of the movement of individual leaf – pairs of the MLCs across the treatment field while the beam of radiation is turned on. "The required pattern of intensity fluence for the IMRT beam can be achieved by varying the width of the gap between each of the leaf pairs and the speed of travel of individual leaf pairs" (Cheung, 2006).

Since IMRT treatment requires appropriate control mechanisms of the MLC during irradiation, sufficient caution must be applied in delivering radiation. QA in treatment is therefore essential to evaluate the difference between planned and actual doses (Son, et al., 2015).

2.3 Dosimetric Advantages

Intensity Modulated Radiotherapy has proven to have dosimetric advantages over 2D and 3D CRT techniques over a number of cancer sites based on clinical data (Cheung, 2006). Numerous studies have confirmed the dosimetric advantages of the dose distribution of the technique over other modalities (van der Wal, et al., 2013).

The prevalent interest attracted by IMRT is the consequence of its dosimetric and potential clinical advantages (Cheung, 2006).

Among key qualities of a 3DCRT planning is the beam's eye view (BEV) design of treatment fields and plan evaluation, which allows the discovery of a beam direction that could irradiate the tumor without the beam passing through critical organs closer to the target. In such plan evaluations, dose-volume histograms (DVHs) and isodose distributions became essential tools. In addition to the 3D image processing, the 3D volume information from CT also enabled accurate dose calculation using the convolution-superposition method, allowing the inhomogeneous distribution of tissues to be more accurately handled (Cho, 2018).

IMRT has superior dosimetric advantages over treatments from 2D and 3DCRT techniques. It has the potential benefit of improving conformity with target dose, reducing exposure to normal tissues, and escalation of dose. (Cheung, 2006).

In as much as 3DCRT employs field shape conformity to improve dose conformality to the treatment target, the organs at risk situated in the groove region of a concave target volumes cannot be saved from the target dose. This is because, in conventional 3DCRT, the irradiation field shape coincides with the shape of the target according to the incidence

direction of the irradiation beam. The intensity of the beam in IMRT is modulated in accordance with the positions and the arrangements of the treatment target and the surrounding organs. The intensities of the photon beam passing through OARs are therefore reduced, while the intensities of the photon beam that primarily pass through the target are escalated, and this deliberate inhomogeneity is compensated for by beams from other directions (Cho, 2018).

IMRT have reliable dosimetric benefits over conventional treatments based on several dosimetry studies on linac – based IMRT treatments of diverse anatomical sites. These clinical data have also shown that the treatment is relatively safe and effective. In the treatment of nasopharyngeal carcinoma (NPC) for instance, early clinical results have proven to have survival and other clinical benefits compared with 2D and 3DCRT treatments. A large scale application of this technique for treatment is therefore justifiable. The technique has also aided treatment of prostate cancer by reducing difficulties related to treatment, compared with conventional treatment, even though survival benefit is yet to be observed. This implies that replacing 2D treatment with IMRT can therefore be justified. A number of different disease sites have also established similar benefits in the reduction of technical hitches related to treatment based on clinical data reports (Cheung, 2006).

According to Cheung, IMRT appears to be more beneficial for diseases located at various anatomical sites that have recognised radio-curability and evidence of an established relationship between dose and response for dose escalation, as well as the several normal tissue structures that are in close proximity to the tumour that exclude the use of other treatment techniques (Cheung, 2006).

Due to its higher dose conformity indices, the technique is comparatively more sensitive to errors associated with geometrical tolerance of the treatment machine in relation to conventional treatments (Cheung, 2006).

2.4 Intensity modulated radiotherapy (IMRT) in Ghana

Africa on the whole is the least developed world region with respect to radiotherapy services, with an average capacity of less than one teletherapy machine per million people. In contrary, the North American and western European regions have capacities of 14·89 and 6·12 teletherapy machines per million people, respectively (Abdel Wahab et al., 2013).

Ghana has approximately 0.1 radiotherapy treatment machine per a million population, as opposed the 1-3 radiotherapy treatment machines per million population expected in Africa. It is extremely relevant to however state that as at the end of the year 2019, the nation has not yet to embarked on the radiotherapy techniques using IMRT (Adhanom, 2019).

Meanwhile, a July 2020 press statement issued from the National Centre for Radiotherapy and Nuclear Medicine of the Korle – Bu Teaching Hospital indicates that the Centre has for the first time treated its first patient with the IMRT technique as the first in the country.

2.5 IMRT Treatment Planning Systems and Processes

The dose distributions in the target are generally calculated with the aid of dosimetric functions determined in a full scatter water phantom and mathematical algorithms that are aimed to explain the physics of the radiation interactions with a medium or matter (Tagoe, et al., 2018).

Treatment processes are simulated with dedicated computers known to be treatment planning systems (TPSs), to improve the efficiency of dose computation while speeding up the process, in order to realize the clinical objectives of the treatment delivery. The process of simulating the treatment delivery process with a computer is referred to as treatment planning (Tagoe, et al., 2018).

The process is extended to the determination of dose distribution in the patient, typically connected with treatment duration, and as well involves the steps required for an effective patient management. The treatment planning steps include patient diagnoses, imaging, radiation dose optimization, and treatment plan evaluation (Tagoe, et al., 2018).

TPSs are therefore used for optimization of radiation dose for treatment delivery in EBRT. The procedure can be categorized into forward and inverse planning techniques. (Tagoe, et al., 2018).

Forward planning involves the planner selecting based on experience the required number of open or wedged treatment beams of appropriate beam geometries (Cheung, 2006).The TPS calculates the resultant dose distribution within the irradiated region based on the selected irradiation geometries (Tagoe, et al., 2018). If the dose and the distribution of dose are unsatisfactory, the planner repeatedly varies the beam parameters and geometries and repeats the calculation for each variation (Cheung, 2006).

In comparison to the convex-shaped coverage achieved with 3DCRT, where geometric conformal shaping of a uniform intensity beam is carried out, the method of adding intensity modulation to geometric shaping will make the IMRT dose distribution concave. Therefore, IMRT will allow organs at risks (OARs) located within a concave region of the

planning target volume (PTV) to reduce doses. A beamlet is called the minimum unit of the irradiation region that can be individually monitored. In an irradiation area, the intensity distribution of the beamlets is referred to as an intensity map. For example, in the case of a field of 20 cm × 20 cm, for 400 different beamlets of 1 cm × 1 cm, intensity modulation may be necessary, and in the case of a 5-field treatment, this amount reaches 2000 beamlets for which the intensity needs to be individually allocated. For treatment planners, this is often not possible, and so machine optimization is important (Cho, 2018).

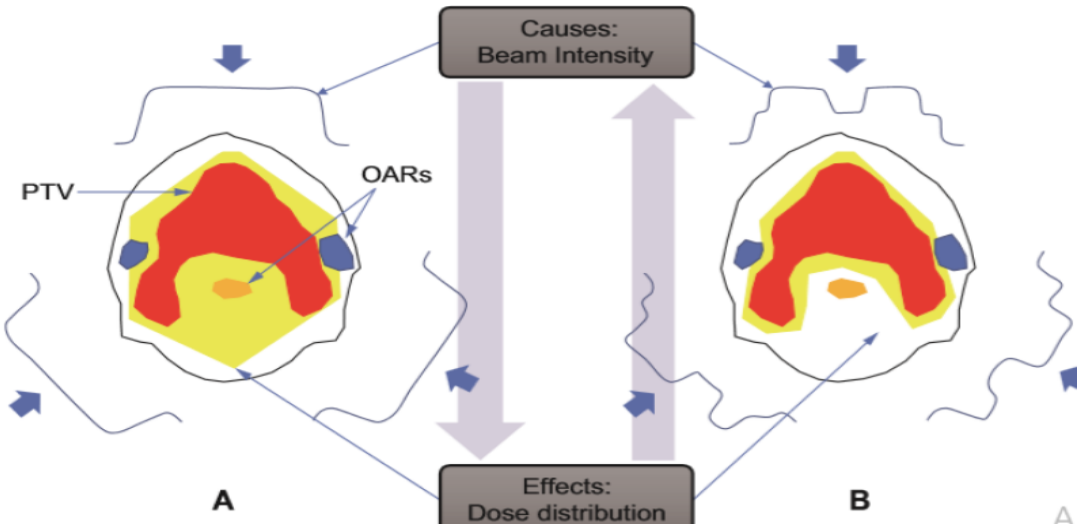

Figure 2.1: Comparison of the principle of 3D-CRT (A) and IMRT (B) with illustrations of forward vs. inverse planning (Cho, 2018).

In this case, the dose distribution in the target and the OARs as in the case of Figure 2.1 for instance are first assigned by the treatment planner, and then the intensity of the irradiation beam is determined by the optimization method, and this is referred to as 'inverse' planning (Cho, 2018).

In reverse planning, the requested dose and dose distribution shall be specified by the planner for the target volumes and the acceptable tolerance dose for individual normal

organs of interest, in the form of a dose constraint table or TPS template. In addition to the dosage specification, the treatment planner needs to determine the appropriate MLC opening for each IMRT beam that covers the target volume, portal and collimator angles (Cheung, 2006). In this technique, the required beam weightings and modulations that necessary to give rise to the expected dose distributions in the patient are applied by the TPS (Tagoe, et al., 2018). The TPS can create a number of MLC leaf motion pattern for each of the beams, upon sufficient calculation of the needed map of the intensity of the beam. In order to achieve the required beam intensity map and, thus, the dose and dose distribution during treatment, these codes can be transferred to the MLC controller of the linac to drive the specific movements of the MLC leaf (Cheung, 2006).

It may not always be possible for the inverse planning system to generate a satisfactory treatment plan based on a given dose constraint table. This is because, the extent to which the treatment plan is sophisticated depends on the number of vital normal organs needing protection, the shape of those organs, the target for treatment, and the geometric margin available between the normal organs and the target for treatment. Therefore, the treatment planner may need to adjust the dosage restriction parameters and repeat the dosage optimisation iteration process multiple times until a satisfactory plan can be achieved (Cheung, 2006).

A standardized or optimized dose constraint template is a prerequisite for specific target sites in order to minimize the number of optimization approaches and, therefore, to minimize planning time. However, for complex treatment sites, such as NPC, where a large number of critical tissue structures are required to be protected, this is very difficult to implement (Cheung, 2006).

There are currently several instruments for assessing plans, such as the dose-volume-histogram (DVH) and the dose conformity index (CI), in addition to the 3D dose and delivery instruments for dose analysis. For objective evaluation and comparison of treatment strategies, these methods may be used. To calculate these biological indices from DVH data, software tools based on mathematical models of tumour control probability (TCP) and normal tissue complication probability (NTCP) are also available. This information can serve as a useful guide for treatment planners, dose optimization, and plan evaluation (Cheung, 2006).

Doses in IMRT are calculated with beamlets, having varying intensities. These varying intensities are created by the movement of MLC leaves across the beam (Ezzell, et al., 2009).

Factors such as transmission of collimators, the shape at the end and sides of the leaf, and physical limitations to motion have effect on the doses delivered.

TG 82 explains that one should expect dose inhomogeneity in the target to increase as

- The required dose differences between target and adjacent critical structures increases;
- The distance between target and critical structures increases;
- The concavity of the required dose distribution increases;
- The number of available beam directions increases.

2.6 Dosimetric Commissioning of an IMRT Planning System

Commissioning of IMRT dosimetry planning system requires that the user is allowed to specify and apply to a phantom, a desired intensity pattern for resulting doses to be measured and confirmed. It is appropriate to advance from simple to more multifaceted tests. The objective is to examine the accuracy of the beam parameters in both simple and clinical situations. The second objective is to develop an understanding of the dosimetric uncertainties so that clinical plans for critical structures especially can be evaluated meaningfully (Ezzell, et al., 2009).

Cylindrical ion chambers are preferred to parallel plates in multiple beam irradiation due to the axial symmetry, and small – volume are best recommended.

The IMRT setup has to be commissioned through an initial verification by phantom studies, to prove that treatments can be planned, prepared, and delivered with sufficient accuracy (Ezzell, et al., 2009).

Commissioning studies should be done by defining target and normal structure shapes on CT images of the dosimetry phantom. Treatment should be planned, and measured doses in the phantom should be compared to the planned doses from the computer system.

Commissioning exercise is supposed to:

- Mimic the varieties of targets and structure geometries alongside the target doses and dose constraints likely to be clinically encountered.
- Be performed with extra cautiousness to minimize uncertainties in measurement.

2.7 IMRT Quality Assurance

IMRT happens to be a multifarious technique that imposes higher demands on a delivery system and its treatment planning system. However, these demands are not always met in practice since there is an indication that IMRT treatments may not always be as accurate as practitioners believe. This is due to reports from two different groups confirming this assumption through dosimetry audits of IMRT treatments based on phantom irradiation of the head and neck in the United States of America and Europe, in which approximately 1/3 of the contributing institutions did not meet the criteria for accuracy, even though the criteria for dose tolerance were not very strictly defined (van der Wal, et al., 2013).

Accurate planning of dose delivery in cancer treatment by radiation becomes indispensable in the advent of sophisticated treatment options with innovative technology using linacs, making it very crucial for patient management. Treatment performance in a patient is subject to the professional participation of staff and implementation of an accurate plan. This is based on the IAEA's highlights on the mishaps in radiotherapy involving: incorrect manual parameter transfer; reversal of images in treatment planning; use of inappropriate measuring detector; erroneous calculation for soft wedge; incorrect Intensity Modulated Radiotherapy (IMRT) planning; and mis-calibration of a stereotactic unit (Ravichandran, et al., 2011).

These reports strongly suggest that some radiotherapy centres have not effectively implemented the QA of their delivery systems and treatment planning for IMRT. Consequently, it becomes an overriding concern that with the introduction of IMRT in a country, quality of IMRT treatments is evaluated and upheld over time (van der Wal, et al., 2013).

The MLC motion and collimator rotations in IMRT have the tendency of being influenced by gravity shift when the linac is in nonzero gantry angles. This is more severe in IMRT treatments where the critical organs are closely covered using MLCs (Stasi, et al., 2012). Thus, Quality Assurance in IMRT is necessary to ensure patient safety (Pan, et al., 2019).

Proper dosimetry verification and treatment QA protocols are essential steps to ensure that treatment can be administered in accordance with the treatment plan (Cheung, 2006).

Quality assurance (QA) is therefore an essential component to ensure safe and accurate treatment delivery of this technique, in spite of the fact that linear accelerator and its computerized system will certainly proceed in the path of self-checking and IMRT automation (van der Wal, et al., 2013).

A careful analysis of recommendations by AAPM TG – 53 as well as No. 7 booklet by ESTRO reveals deficiencies in the existing IMRT QA regardless of the selected metric (Stojadinovic, et al., 2014).

Proper acceptance testing and commissioning of the IMRT systems should be carried out to ensure that the performance of the IMRT meets clinical requirements. This involves both the treatment delivery systems and the treatment planning system. Moreover, it is imperative to select suitable equipment and measurement methods to fit the complex nature of IMRT in performing these tests (van der Wal, et al., 2013).

In IMRT treatment, the performance of the devices used for treatment, along with the precision and reliability of dosimetry and MLC systems in the delivery of intensity modulated beams, are important. It is especially important for the implementation of the

virtual dosimetry verification method, which assumes that the devices used for treatment are working properly and accurately. Therefore, dedicated and strict QA programs should be designed to verify and ensure the proper operation of the devices used for IMRT beam delivery in treatment, with a specific emphasis on testing the efficiency and integrity of the dynamic IMRT mode operating MLC system (Cheung, 2006).

In radiation therapy, and particularly in IMRT technique, managing quality includes much more than only focusing on technological issues. It encompasses the description and succeeding analysis of the whole procedure of delivering the IMRT treatment. For any new technique, it is recommended that a potential risk of IMRT delivery is performed and analyzed, from which all measures to be taken to ensure safe and correct delivery of IMRT technique should follow. These will involve technological issues, the organization of the process, and the training and maintenance of the personnel that is involved in IMRT treatments (van der Wal, et al., 2013).

Conventionally, QA is categorized into periodic equipment QA and routine patient-specific QA. With the introduction of IMRT, patient-specific QA has had an extension to pretreatment QAs. A third category of QA has, emerged in the practice of the pretreatment patient-specific QA known as the class solution. Despite the fact that these categories exist, they do not remain or operate in isolation (Wagter, 2006).

IMRT workflow, including TPS beam modeling and commissioning, QA preparation, QA system and linac output monitoring, as well as end-to - end checks, should be thoroughly investigated. Gamma passing rates should be monitored between patients at the same sites

to decide if the errors are unique to a treatment site or delivery equipment (Pan, et al., 2019).

2.7.1 Equipment QA

Linear accelerator commissioning is the process of preparing the treatment machine for clinical use. During this process physical parameters are acquired to enable the TPS generate a virtual model of the treatment machine. Also, certain beam data are acquired to assist with the characterization of beams from the treatment machine. Data to be acquired are therefore dependent on treatment modalities the treatment machine would be used for and requirements for TPS algorithm for dose calculation.

The American Association of physicists in Medicine (AAPM) describes machine – QA as machine specific tests performed repeatedly to check that the performance of the delivery system does not deviate significantly from their baseline values acquired at the time of acceptance and commissioning, and are generally performance – oriented (Klein, et al., 2009).

This generally has a chart and is ideally configured with the upkeep and upgrade processes applied to the machine band on information from the acceptance testing and commissioning face of the equipment. It may comprise of periodic checks on laser system alignment, stability of position of the treatment isocenter as well as the integrity of machine mechanical travels (Wagter, 2006).

2.7.1.1 Acceptance Testing

Performance of acceptance tests as a quality assurance measure before using a linear accelerator clinically is a statutory requirement in many states. The licensee is obliged to ensure that before a new, or a changed linear accelerator or technique will be put to use, an acceptance test has been conducted by an expert medical physicist or a radiation protection officer for his approval. The framework of acceptance tests for linacs have been described in several international reports covering the harmless use of the machine from the trend of radiation protection, functional performance of the linac in relation to the standards distinct as part of the agreement, as well as recording of baseline values for QC procedures in future (van der Wal, et al., 2013).

The requirements for an acceptance testing is usually more stringent than regular quality control for linacs, since the results are used as baseline values for QC in future. It places much emphasis on the aspects of dosimetry and technical dose delivery as well as the safety checks like beam interruptions caused by the verification as well as the control system (van der Wal, et al., 2013).

2.7.1.2 Commissioning

The initial procurement and documentation of the relevant dosimetric and automated data required for clinical use is referred to as Commissioning of IMRT. This includes a verification step with phantom studies to show that IMRT treatments can be planned, transferred, and delivered with sufficient accuracy (van der Wal, et al., 2013).

Commissioning of equipment performance specific to IMRT may involve the possible repetition of some tests (such as MLC transmission) that had been done during acceptance

phase of the linac, in which case they might be extended or made precise. Measurements that are beyond the acceptance protocols will also be taken (van der Wal, et al., 2013).

2.7.1.3 Performance Quality Control

The accuracy of IMRT dose delivery can be validated by regular assessment of how stable the system is in terms of the baseline data obtained from the acceptance and commissioning. The frequency of this assessment with respect to the baseline information depends on the predictable stability of the system's constituents, which are adaptable over time in relation to the stability observed for the individual machine parameters (van der Wal, et al., 2013).

2.7.2 Patient Specific QA

In spite of the inadequacy of published literature addressing the issue of how patient-specific IMRT QA should explicitly be performed, several guidelines and recommendations testifying the necessity of patient-specific for IMRT QA have been published. (Pan, et al., 2019).

Patient – specific QA is done to ensure that intended dose distributions for a specific patient is physically verifiable, and that the intensity modulated beams are clinically feasible (Moretti, et al., 2017).

Once commissioning of the whole array of treatment planning system, data transfer as well as delivery has been completed, a therapist needs to make sure that an appropriate treatment plans for patient – specific delivery are made, and ensure that these plans are correctly transferred to the medical linear accelerator to be accurately administered. It is

imperative to define the tools desired for appropriate patient-specific QA in the clinic, and the performance of pretreatment verifications (van der Wal, et al., 2013).

The demands for QA rely on the experience of the institute with IMRT and the technique's complexity. Where there are anomalies between expected and calculated values outside agreed limits, an expert medical physicist must be consulted and the issue must be investigated (van der Wal, et al., 2013).

2.7.3 Pre-treatment verification

Patient – specific QA can be considered as the confirmatory stage of the treatment process of IMRT, and has to be done prior to clinical treatment, as it ensures compliance between planned and treatment dosimetry of the individual patient. Such treatment confirmation is connected to a successful implementation of the technique through an entire process starting before the commencement of treatment along with the continuation throughout the treatment duration. This provides documentation of all implementation-related components, as well as diagrams of treatment ports and measurements of physical doses. Verification data confirms the exactness of the dose administered with the transfer of the technical setup along with the dose – delivery data (Hatford et al., 2016).

In order to ensure that treatment parameters are correctly transferred and dose verification is performed before the actual treatment of the patient, pretreatment verification is highly recommended by several professional societies. It can be used to ascertain the deliverability of the IMRT plan, and ensures that the plan does not contain deviant shapes, and can ensure

that both dosimetric and geometric agreement between prediction and verification are well checked and are within tolerance (van der Wal, et al., 2013).

In complicated radiotherapy care plans like IMRT, pretreatment QA is a major concern. For beneficial results from IMRT procedures, higher monitor units and continuous motion of multileafs during the beam on time need to be strictly controlled prior to treatment (Cyriac, et al., 2014).

The current standards of IMRT patient – specific QA based on recommendations made by ACR and ASTRO imply verification of plan parameters for IMRT treatment and the use of measurements for dosimetry to validate the exactness of the dose administered. Both the ACR and ASTRO recommend that these tests should be done prior to the commencement of treatment of any given plan due to safety considerations (Moretti, et al., 2017).

This is done by delivering the intended patient treatment plan to a demonstrative standard phantom containing detectors (Wagter, 2006).

2.7.3.1 Effect of Gantry Angle on Pretreatment Verification

Many studies investigating the effect of gantry angles on the quality assurance have reported that gravitational pull of the head of the linac and the electronic portal imaging device (EPID) tail can have tremendous influence at non-zero gantry angles. It is however noticed that if the sagging is negligible, we can realize the actual delivery positions, and this aids us to acquire the authentic dose mapping (Cyriac, et al., 2014).

The same study has also indicated that the advantages of actual gantry pretreatment QA over zero – degree gantry pretreatment QA are purely machine dependent. It also emphasizes that there is no difference obtained once the mechanical QCs are performed

for gantry sagging and MLC leaf positions in addition to other relevant checks (Cyriac, et al., 2014).

While EPID pretreatment plan verifications are preferred to be in positions based on the angle of the gantry, it has also shown that such a requirement is not strictly essential. It has essentially been established that if periodic quality assurances are carried out, the IMRT QA pretreatment may also be carried out at zero-degree gantry angles, with a substantial reduction in time for each patient to perform quality control. However, the zero-degree pretreatment analysis is much better than the real degree of gantry angles in less situations. (Cyriac, et al., 2014).

Meanwhile, the gantry-dependent QA using 2D detectors may be limited to zero degree gantry angles for pretreatment verification in treatment facilities where there is no on-board EPID (Cyriac, et al., 2014).

Nonetheless, due to limitations of current equipment, the dosimetric benefits of IMRT are not projected to be fully realised clinically in the next few years. This potential advantage can only be accomplished if it is possible to find realistic solutions for reliable and correct delineation of target volumes, proper compensation for organ movements during care and changes in the location of these structures over time, and clinically implement corrective measures (Cheung, 2006).

In spite of this, the research and progress work carried out by academic institutions and manufacturing industries and the exciting developments made in the fields of biological imaging, dosimetry techniques, and IMRT driven by images look promising to increase the technique's efficiency and effectiveness. The treatment technique, especially in locally

advanced cancer diseases, has the potential to have a positive effect on the clinical outcome. This would have an effect on reducing treatment-related complications and increasing overall survival rates as these innovations become more advanced and IMRT is more commonly used in hospitals as a routine treatment (Cheung, 2006).

2.7.3.2 Verification Data of Treatment Unit

In the real clinical environment, correct verification of the IMRT plan requires proper comprehension, analysis, transfer and documentary evidence of all aspects of the clinical setup, positioning and immobilization of the patient, as well as parameters of the treatment unit such as jaw settings, MLC settings, patient positioning devices, gantry angles, collimator angles, table angles of patient support and positive positions (Hatford et al., 2016).

2.7.3.3 Image-Based Verification Data

For accurate treatment delivery, there is a need for coherence between regular on-treatment images and accepted simulation CT images. This approach involves matching the simulation images with the images collected from the treatment unit when the patient is in a treatment role. These images include conventional CT, megavoltage CT, cone-beam CT, orthogonal kV images, portal images generated with the treatment beam, and MR images that could be obtained through technological innovations (Hatford et al., 2016).

Such patient position confirmation should be done initially and then regularly, at least weekly, during the course of treatment of the patient. In order to check the initial settings of the collimator, MLC, and portal for that field, verification images for each field should be collected for each treatment field (Hatford et al., 2016).

2.7.3.4 Dose-Delivery Verification by Physical Measurement

The accuracy of dose delivery should be documented by irradiating a phantom containing a calibrated dosimetry system prior to the start of treatment and using all the parameters of the patient's treatment plan to verify that the dose delivered is the planned dose. As can be achieved through the patient-specific end-to - end testing procedure, multiple points in the delivered distribution should be compared against the planned distribution. In this process, the Qualified Medical Physicist should ensure that the actual radiation doses received during treatment delivery are verified (Hatford et al., 2016).

2.8 Measuring Devices

2.8.1 Instruments and Laboratories Classification

The international atomic energy agency (IAEA) technical report series (TRS) 398 describes a primary standard instrument as "an instrument of the highest metrological quality that permits determination of the unit of a quantity from its definition, the accuracy of which has been verified by comparison with the comparable standards of other institutions at the same level". The report also describes a secondary standard instrument as "an instrument calibrated by comparison with a primary standard" (IAEA, 2000).

Primary Standard Dosimetry Laboratory (PSDL)is however defined by the IAEA TRS 398 as a national standardizing laboratory designated by the government for the purpose of developing, maintaining and improving primary standards in radiation dosimetry. Meanwhile, a Secondary Standard Dosimetry Laboratory (SSDL) has been defined by the agency as a dosimetry laboratory designated by the competent authorities to provide

calibration services, and which is equipped with at least one secondary standard that has been calibrated against a primary standard (IAEA, 2000).

2.8.2 Dosimeters

The measurement equipment for IMRT QA should be able to perform within the tolerance level of the measured parameters, having in mind the stringent demands on tolerances for IMRT. Emphasis should be laid on the performance of the equipment in terms of precision, repeatability and uncertainties in measured parameters (van der Wal, et al., 2013).

The three-dimensional spatial accuracy in IMRT QA has introduced the concept and the creation of new detectors for the verification of radiation dose distributions and patient positioning. This is because the quality of the dose distributions in IMRT and its techniques for delivery may actually complicate measurements of doses. The dose gradient that occurs in intensity modulated beams requires detectors that have a good spatial resolution and a response which is independent of the energy spectrum for is analysis (Wagter, 2006).

According to the AAPM TG142 that the measurement system and procedure repeatability be such that two standard deviations for three or more repeated consecutive measurements are less than the tolerance value. The Netherlands Commission on Radiation Dosimetry (NCS) report 22 explains the above statement to indicate the need of quality control on devices and equipment used for measurements (van der Wal, et al., 2013). It also elaborates further that one should familiarize oneself with the suitability of its use in terms of possibilities as well as limitations (van der Wal, et al., 2013).

A cylindrical ionization chamber type is more suitable for radiation quality measurements of radiotherapy beams and can be used to calibrate electron beams with energy above 10 MeV. It is because this type of chamber is tough and quite simple to use for measurements using a water phantom (IAEA, 2000).

There should also be a cautious collection of the measurement equipment and its conditions for small field dosimetry, to prevent deviation of the scanning device in depth from the real central axis of the beam, and result in an accurate percentage depth dose curve. Since it is practically impossible to acquire a commercially available detector that can produce an excellent spatial resolution, dose response independent of energy, as well as dose and dose rate excellent stability, linearity and reproducibility, measurement should be done by selecting detectors with complementary features and with several overlapping field sizes (van der Wal, et al., 2013).

The farmer-type chamber is the best in the category of point detectors in regions of shallow dose gradient and for the measurement of low doses. However, its accuracy may be affected during IMRT since there can be moments that the ionization chamber is outside the actual beam. Nonetheless, several studies have indicated that the measuring error may amount to a few percent for individual beamlets, but the overall error depends on the IMRT plan (Wagter, 2006).

When selecting a cylindrical ionization chamber, the user should pay attention to whether it is to be used as a reference instrument (calibrated in a standard laboratory and used in a user beam for beam calibration) or as a field instrument (cross-calibrated against a reference chamber and usually used for routine measurement) (IAEA, 2000).

Meanwhile, the more suitable detectors for the dosimetry of IM beams are detector arrays (1D or 2D) and EPID (2D). This is because these devices have to be irradiated with the beam axis perpendicular to the surface, and have the advantage of short acquisition time (Wagter, 2006).

In spite of the fact that radiographic film is widely used as composite film for treatment dose verification, its validity is still a controversial literature of conflicting data (Wagter, 2006).

Conventionally, IMRT QA is performed by applying the patient plan to a phantom and comparing the measured and calculated dose distributions in the phantom. This was traditionally implemented by taking a point-dose measurement using an ion chamber or a planar measurement using a radiographic film for dosimetric QA of treatment plans (Agazaryan, et al., 2003). Although film has the great advantage of high resolution, it has several disadvantages, including the need to change film for every beam test and the fact that it is dependent on beam energy, processing conditions, and external light (Son, et al., 2015).

There are at the moment advanced products that allow the acquisition of absolute dose distribution measurements using either an ion chamber or a diode-based detector arrays in a 2D or 3D geometry (Agazaryan, et al., 2003). This study is based on the determination of the absolute dose distribution measurement using a 2D detector array.

2.8.3 Phantoms

In the IAEA Codes of Practice, for measurements of the absorbed dose for both photon and electron beams, water is recommended as the reference medium and should stretch to at least 5 cm beyond all four sides of the largest field size used at the measuring depth (IAEA, 2000).

The Dosimetric verification of intensity modulated beams is carried with many phantoms including slab phantoms (Wagter, 2006).

Preferably, the phantoms used for pre-treatment verification should be the same scale as the site of treatment under consideration. Therefore, relative to prostate IMRT, a separate phantom should be used for head and neck IMRT (van der Wal, et al., 2013).

2.8.4 The role of SSDLs

According to the IAEA's TRS398, the main role of the SSDLs is to bridge the gap between PSDLs and the users of ionizing radiation by enabling the transfer of dosimeter calibrations from the primary standard to user instruments (IAEA, 2000).

It further states that "One of the principal goals of the SSDL network in the field of radiotherapy dosimetry is to guarantee that the dose delivered to patients undergoing radiotherapy treatment is within internationally accepted levels of accuracy. This is accomplished by ensuring that the calibrations of instruments provided by the SSDLs are correct, emphasizing the participation of the SSDLs in quality assurance programmes for radiotherapy, promoting the contribution of the SSDLs to support dosimetry quality audits

in therapy centres and assisting if needed in performing the calibration of radiotherapy equipment in hospitals" (IAEA, 2000).

2.9 Calibration of Measuring Devices

Every equipment should be properly calibrated for use, with the acknowledgement of their limitations in terms of dosimetric and spatial accuracy (van der Wal, et al., 2013).

Furthermore, for IMRT QA study, absolute dose mode should be used since significant differences can go undetected using relative dose mode. In order to rule out the effect of detector reaction and accelerator performance variance, absolute dose calibration of the ion chamber or diode arrays should be performed prior to each measurement (Pan, et al., 2019).

2.9.1 Output factors

For a given electron beam, the output factors should be estimated at d_{max} for the non-reference field sizes and SSDs used for patient care. Under the required reference conditions, they can be calculated as the absorbed dose at d_{max} for a given set of non-reference conditions relative to the absorbed dose at d_{ref} (or d_{max}) (IAEA, 2000).

2.9.2 Measurements under Non-Reference Conditions

For both reference and non-reference situations, clinical dosimetry includes measurements of central axis percentage depth dose (PDD) distributions, tissue phantom ratios (TPR) or tissue maximum ratios (TMR), isodose distributions, transverse beam profiles and performance factors as a function of field size and form. For all possible combinations of

field size and SSD or SAD used for radiotherapy treatment, such measurements should be made (IAEA, 2000).

2.9.3 Choice of beam quality index

The tissue phantom ratio $TPR_{20,10}$ is defined by the beam quality Q for high-energy photons emitted by clinical accelerators. $TPR_{20,10}$ is the average of the doses consumed in a water phantom at depths of 20 and 10 cm, determined with a constant SCD of 100 cm and a field scale of 10 cm × 10 cm in the chamber plane (IAEA, 2000).

The most important feature of the beam efficiency index $TPR_{20,\ 10}$ is the freedom of the electron contamination in the incident beam. It is also a measure of the effective coefficient of attenuation that defines the approximately exponential reduction of the dose curve of the photon depth beyond the maximum dose depth. As $TPR_{20,10}$ is obtained as a ratio of doses, when cylindrical chambers are used, it does not require the use of displacement correction factors at two depths. In addition, $TPR_{20,10}$ is not affected by minor structural errors in placing the chamber at each depth in most clinical set-ups, as the settings in the two positions would be affected in a similar manner (IAEA, 2000).

2.9.4 Calibration standards

Calibrations may necessarily be carried out against a secondary standard of absorbed dose to water at an SSDL (IAEA, 2000).

It is an observation that for ^{60}Co gamma rays, the absorbed dose of water, D_w, is known at a depth of 5 g/cm^2 in a water phantom. This is done in a water phantom at the SSDL by

means of a calibrated cavity ionization chamber conducting measurements. In a water phantom, the consumer chamber is located with its reference point at a depth of 5 g/cm^2 and its calibration factor $N_{D,w}$ is obtained from equation 1 below.

$$N_{D,w} = \frac{D_W}{M}, \quad (1)$$

where M is the dosimeter reading corrected for influence quantities, in order to correspond to the reference conditions for which the calibration factor is valid (IAEA, 2000).

2.9.5 Standards of absorbed dose to water

Water calorimetry, chemical dosimetry and ionization dosimetry are the three basic methods explained by TRS398 as the only methods that are sufficiently accurate to form the basis of the primary criteria for measurements of the absorbed dose of water. The system used in this analysis is the ionization dosimetry system (IAEA, 2000).

The ionization chamber used for this standard consists of a precisely recognized chamber volume graphite cavity chamber built to fulfill the specifications of a Bragg-Gray detector to the extent possible. At the reference point, the chamber is put in a water phantom and the absorbed water dose is extracted from the mean real energy imparted to the cavity air (IAEA, 2000).

2.9.6 Calibration formalism

The geometric arrangement (distance and depth), the field scale, the material and dimensions of the irradiated ghost, and the ambient temperature, pressure and relative

humidity are designated in the IAEA TRS398 as the reference conditions for the calibration of the absorbed water dose. By this designation, reference conditions are defined by a set of effect quantity values for which the calibration factor is true without additional correction factors (IAEA, 2000).

Absorbed dose to water, D_w is the fundamental quantity in the dosimetry for radiation therapy (IAEA, 2000).

The TRS398 defines absorbed dose to water at the reference depth Z_{ref} in water for a reference beam of quality Q_o and in the absence of the chamber is given by$D_{w,Q_0} = M_{Q_0} N_{D,w,Q_0}$, where$M_{Q_0}$ is the reading of the dosimeter under the reference conditions used in the standards laboratory and N_{D,w,Q_0} is the calibration factor in terms of absorbed dose to water of the dosimeter obtained from a standards laboratory. Since conditions of measurements in most clinical situations do not match the reference conditions used in the standards laboratory, the response of the dosimeter may be affected. It is therefore necessary to differentiate between the reference conditions used in the standards laboratory and the clinical measurement conditions (IAEA, 2000).

When a dosimeter is used in a beam whose quality, Q is different from that used in its calibration, Q_o, the absorbed dose to water is given by equation 2 below.

$$D_{w,Q} = M_Q \times N_{D,W,Q_0} \times k_{Q,Q_0}, \qquad (2)$$

where the factor k_{Q,Q_0} corrects for the effects of the difference between the reference beam quality Q_o and the actual user quality Q. This beam quality correction factor k_{Q,Q_0} is defined

as the ratio, at the qualities Q and Q_o, of the calibration factors in terms of absorbed dose to water of the ionization chamber as displayed in equation 3 below.

$$k_{Q,Q_0} = \frac{N_{D,W,Q}}{N_{D,W,Q_0}}, \quad (3)$$

and thus $$k_{Q,Q_0} = \frac{D_{w,Q}/M_Q}{D_{w,Q_0}/M_{Q_0}} \quad (4)$$

M_Q is the dosimeter reading that has been corrected to the reference values of influence quantities, other than beam quality, for which the calibration factor is valid (IAEA, 2000).

2.9.7 Calibration at other qualities

Calibration of high energy photon and electron beams can only be performed in standards laboratories with an accelerator. The user may be given a series of calibration factors $N_{D,w,Q}$ at various beam qualities or a calibration factor N_{D,w,Q_o}, with measured values for k_{Q,Q_o} (IAEA, 2000).

2.9.8 Determination of absorbed dose to water

If the user has an ionization chamber or a dosimeter with a calibration factor N_{D,w,Q_o} in terms of absorbed dose to water at a reference quality Q_o, the chamber is positioned according to the reference conditions, and the absorbed dose to water is given by equation 5.

$$D_{w,Q} = M_Q \times N_{D,W,Q_0} \times k_{Q,Q_0} \quad (5)$$

2.9.9 Correction for influence quantities

Influence quantities are quantities that are not the focus of the calculation, but also affect the measured quantity (IAEA, 2000).

However, the ionization chamber calibration factor is true only for the reference conditions which apply to the calibration. The ionization chamber in the consumer beam should be corrected using sufficient factors when there is a change in the reference conditions" (IAEA, 2000).

2.9.9.1 Pressure, temperature and humidity

Since the mass of air in the cavity volume of all chambers open to the ambient air is subject to atmospheric variations, the cavity air mass should be converted to the reference conditions by applying the factor k_{TP} as applied in equation 6.

$$k_{TP} = \frac{(273.2+T)}{(273.2+T_0} \frac{P_0}{P}. \quad (6)$$

Where P and T are the cavity air pressure and temperature at the time of the measurements, and P_o and T_o are the reference values (generally 101.3 kPa and 20 °C) (IAEA, 2000).

2.9.9.2 Polarity effect

The effect on a chamber reading of using polarizing potentials of opposite polarity in charged particle beams such as electrons may be very significant (IAEA, 2000). This effect on the chamber for each user beam quality Q can be accounted for by using a correction factor k_{pol} in equation 7.

$$k_{pol} = \frac{|M_+|+|M_-|}{2|M|} \quad (7)$$

Where M+ and M– are the electrometer readings obtained at positive and negative polarity, respectively, and M is the electrometer reading obtained with the polarity used routinely (positive or negative) (IAEA, 2000).

2.9.9.3 Ion recombination

The incomplete collection of charge in an ionization chamber cavity owing to the recombination of ions requires the use of a correction factor k_{sat} (IAEA, 2000). The recombination correction factor k_{sat} at the normal operating voltage V1 is obtained from equation 8.

$$k_{sat} = a_0 + a_1\left(\frac{M_1}{M_2}\right) + a_2\left(\frac{M_1}{M_2}\right)^2 \qquad (8)$$

Where the constants a_i are given in Table *9* for pulsed and for pulsed–scanned radiation (IAEA, 2000).

2.10 Dose Measurement Methods

2.10.1 Measurement Quantity

Absorbed dose, a quantity acting as an intermediary between physics and medicine is the fundamental function in quality assurance of any radiotherapy technique, including IMRT. Unlike many biological quantities such as tumour control probability or normal tissue complication probability, the distribution of absorbed dose in IMRT combines the positional and intrinsically dosimetric end points (Wagter, 2006).

The end result of IMRT is the 3D planned dose delivery that the radiation oncologist needs to deposit at a particular location. It is usually difficult for the patient to make a clear determination by calculating the absorbed dose. In vivo dosimetry, the associated quantity,

such as the input dose or output dose at a point, is calculated and compared to the expected dose distribution quantity as planned by the computational model, which is preferentially independent of the model used to develop and calculate the planned dose distribution (Wagter, 2006).

2.10.2 Dose Verification

The leakage current should be corrected for point dose verification as small volume ion chambers are used in point dose verification. It is important to pick and locate an ion chamber with adequate spatial resolution in a plateau dose region, taking into account the dose gradient and positioning errors (Pan, et al., 2019).

Generally, for homogeneous dose distributions, the dose gradient around the ion chamber should be less than 5 percent of the mean chamber dose. The estimated dose for the volume of the chamber should be compared with the recorded dose instead of the dose at the effective measurement point or in the center of the active volume of the chamber (Pan, et al., 2019).

If the angular dependency of the 2D array is negligible or can be correctly corrected, TC measurements can be used to check the planar dose. Otherwise, due to the anisotropic dose reaction of the array detectors, the measurements should be done using the PFF process. Due to the risk of masking distribution defects, the PC approach should not be used (Pan, et al., 2019).

2.11 Gamma Index (GI or γ) , Dose Differences (%DD) and Distance to Agreement (DTA) Evaluation

2.11.1 Comparison between Two Dose Distributions.

This comparison exercise comprises of both geometric and dosimetric correlation. An extra-ordinary concept introduced by Low et-al explains this phenomenon using an approach defined as the gamma (γ) index method (Wagter, 2006).

Gamma Index (GI) is a very common process to quantitatively compare measured and calculated dose maps. It represents the minimum multidimensional distance between the measured and calculated points in a space composed of dose and coordinates of physical distance, scaled by preselected confines called acceptance criteria for distance to agreement (DTA) and dose differences (DD) (Stasi, et al., 2012).

The evaluated dose distribution in gamma index analysis should have the same or higher resolution than the reference distribution. In such analysis, DD, DTA, dose profiles and isodose distribution should be reviewed in addition to the gamma pass rate (Pan, et al., 2019).

The effectiveness of a treatment plan is estimated through the evaluation of the gamma passing rate (% GP), representing the percentage of dose points per plan that comply with the acceptance criteria. A GI smaller than unity indicates that the measured absorbed dose agrees with the calculated one within the passing criteria (Stasi, et al., 2012).

It is quite difficult to institute the acceptance limits for IMRT QA because of the usage of different delivery systems, planning systems, and verification devices. The impact of

discrepancies can be judged by analyzing gamma pass rate with different DD/DTA criteria (Pan, et al., 2019)

The limitation of GI method is that it only determines the number of points out of tolerance without giving any information about their spatial location. It is therefore extremely difficult for one to assume that the %GP of the entire plan corresponds to that of the single organ (Stasi, et al., 2012).

Along with the accelerator and MLC QA, tighter tolerances should therefore be used. Due to its clinical importance, global normalization should be used. The point of normalization should be placed in a high dose, low gradient region, often the maximum dose point, not necessarily the isocenter of the plan , especially where the isocenter is located in the low dose or high gradient region (Pan, et al., 2019).

2.11.2 The Acceptance Criteria

The acceptance criteria for initial machine and TPS commissioning are well established in literature. However, the acceptance criteria for patient – specific IMRT QA are more difficult to establish due to large variations among IMRT planning and delivery systems as well as measurement tools (Miften, et al., 2018).

GI provides an excellent measure of disagreement between measured and calculated doses for complex intensity distributions. Several institutions specify 3% dose difference and 3 mm distance-to-agreement as acceptance criteria. Their dose distributions are analyzed based on dose gradients. Low dose gradient regions are required to meet the acceptance criteria placed on dose difference, whilst high dose gradient regions are required to meet

the acceptance criteria placed on distance-to-agreement DTA. However, tolerance levels for most photon beam calculations in homogeneous media are 3% and 4 mm, respectively (Agazaryan, et al., 2003).

Generally, gamma evaluation is used to verify the actual dose distribution that will be delivered to the patient during IMRT. The method is based on a comparison of the calculated 2D dose map from TPS with the measured 2D dose map from each dosimetric tool. QA results are considered acceptable without general consensus that when the passing rate is greater than 95% using as criteria a tolerance of dose difference (DD) of 3% and a tolerance for distance to agreement (DTA) of 3 mm (Son, et al., 2015).

2.11.3 Gamma Passing Rate and Acceptance Criteria Protocols

The use of gamma method for IMRT QA has been widely investigated, in which there have been countless studies on suggested acceptance levels for planar IMRT QA. A recent report of the AAPM Task Group 119 and some other papers have reported that the 3% dose difference and 3mm DTA criteria is most commonly used by physicists in pretreatment IMRT QA (Ezzell, et al., 2009). IMRT action level proposed by TG119 for % GP is 90% for per-beam planar analysis and 88%–90% for composite irradiations. A survey analysis also showed that when the institutions used 3%/3 mm criterion, %GP action level most commonly used is 95% (Stasi, et al., 2012). The AAPM uses universal tolerance limits of the gamma passing rate ≥ 95%, with 3%/2 mm and a 10% dose threshold. Additionally, the AAPM uses universal action limits of the gamma passing rate ≥95%, with 3%/2mm and a 10% dose threshold (Miften, et al., 2018).

The European Society for Radiotherapy and Oncology (ESTRO) recommends tolerance and action limits of 3% and 5% respectively for ion chamber measurements. AAPM also recommends tolerance and action limits to be within ≤ 2 % and ≤ 3%, respectively (Pan, et al., 2019).

In order to achieve a distance to agreement (DTA) of 3 mm or better, the NCS recommends performing the dose computation with a resolution of 3 mm or better, depending on computation times, and states that the slice thickness of the imaging dataset used for dose computation should be considered to meet this criterion (van der Wal, et al., 2013).

CHAPTER THREE

MATERIALS AND METHODS

3.1 Introduction and Overview

This chapter highlights the descriptions of the major devices and equipment used in this study. In addition, it outlines in a comprehensive manner, the procedure and methods employed throughout the research.

3.2 Study Design

This work was a phantom study carried out at a Radiotherapy Unit of the National Centre for Radiotherapy and Nuclear Medicine, Korle-Bu Teaching Hospital (KBTH) at Accra, Ghana. The research study was conducted with a medical linear accelerator equipped with 120 MLC producing 6 MV photon beam. The phantom study was designed to mimic the clinical objectives for the treatment of 10 patients with prostate and head and neck cancers. Prior to the study, a letter (as displayed in Appendix) requesting for the permission to embark on the study was written to the Director of the Radiotherapy Unit of the KBTH by the Head of the Medical Physics Department of the University of Ghana, and was positively responded by the Unit.

3.2.1 Study Site

The National Centre for Radiotherapy and Nuclear Medicine (NCRNM) is considered as one of the Centres of excellence of the Korle Bu Teaching Hospital (KBTH), Accra, Ghana, and the Centre from time to time is referred to as the Radiation Department of the Korle-Bu Teaching Hospital. The Centre is one of the two public Radiotherapy Centres within

the country. It is the first Radiotherapy Centre to be established among the three Radiotherapy Centres currently operational within the country. The Centre was established with assistance from the International Atomic Energy Agency (IAEA) and the Chinese government. The Chinese government donated equipment: telecobalt machine and conventional radiotherapy treatment simulator machine during the initial set-up of the Centre. This benevolence was complemented by the IAEA by providing the needed financial and technical supports: ancillary equipment donations and the development of the requisite manpower to man the Centre. Since radiotherapy services were new to the country, majority of the labour force was trained oversees and to sustain the Centre, the IAEA brought in expatriates to attend to things until the return of the beneficiaries of the various trainings. The Centre was commissioned in May 26, 1998. The pre-occupations of the Radiotherapy Centre are the management and treatment of solid tumours with radiotherapy (ionising radiations) and chemotherapy, as well as utilizing radioactive substances for diagnosis and treatment of diseases.

The Centre had gone through a lot of transformation, and between 2012 to the later part of 2016, the radiotherapy equipment donated by the Chinese government which had lived their effectiveness were decommissioned and removed from the premises of the Centre. These equipment had since been replaced with new ones under a project with the objectives to upgrade and expand Radiotherapy and Nuclear Medicine services within the country. This had also made it possible for the Radiotherapy Centre to acquire the single energy (6 MV) medical linear accelerator (Varian Medical Systems linear accelerator) with IMRT and VMAT capabilities (advanced treatment techniques). The Radiotherapy Oncology Centre started computerized treatment planning (where treatment simulations are done

with computers) in 2000 with a 2D Prowess Panther (Prowess Inc., USA), which was later upgraded to 3D TPS of the same manufacturer in 2006. Computerized treatment planning (where computers are use to simulate treatment prior to its delivery) started at the Radiotherapy Centre in 2000 with the stand-alone Prowess 2D TPS. In the later part of 2006, 3D conformal radiotherapy had start with the telecobalt machine at the Centre. Though the Radiotherapy Centre did not have dedicated computed tomography (CT) scanner within its premises for patient image data acquisition for treatment planning, there were mutual agreements with diagnostic centres around the environs of the hospital, to make it possible for patients of the Radiotherapy Centre who were candidate for 3D treatment planning to have access to 3D imaging. Patient data for treatment planning acquired with the CT scanners were loaded onto CD-ROM and then exported into the TPS for the treatment planning process. Physicists from the Radiotherapy Centre occasionally visited the facilities with CT scanners earmarked for image acquisition for treatment planning, to perform CT number to electron density calibration with CIRS tissue characterization phantom (CIRS, USA): to enable the TPS account for tissue heterogeneities in dose computation process. Also, a locally designed and fabricated flat-board with wood had been provided for the various CT scanners to make the couch top of each individual CT scanner flat to ensure that a patient was scanned in treatment position. To ensure set-up reproducibility, patients were always accompanied by at least a staff (Radiation Therapist) from Radiotherapy Centre for the CT scanning. This is no more the situation at the Radiotherapy Centre as the Centre had procured and installed a dedicated CT-simulator (the GE Healthcare Discovery RT CT scanner). Embracing advanced treatment techniques by the Centre had been very smooth and less stressful owing to the

fact that the Centre was doing 3D conformal radiotherapy with the limited resources available. Before installing the linac, Varian Medical Systems provided offshore training and proctoring of key faculty members of the Radiotherapy Department to acquire requisite knowledge and skill to ensure effective implementation of the advanced radiotherapy techniques. The major treatment modality in use at the Centre for the management of cancer is external beam radiotherapy (EBRT), and brachytherapy may be offered as a sole treatment or a boost for the EBRT depending on the stage of the disease. On the average 100 patients (60 patients with telecobalt machine and 40 patients with linac) are treated daily with EBRT at the Centre. Cancer cases that are treated at the Centre are: breast, cervix, prostrate, head and neck, anorectal, lung and others (arranged in decreasing orders of prevalence).

The choice of the study site for this research was based on its proximity to the researcher and the fact that the Centre is striving to put into practice IMRT to improve on the quality of life of patient to be treated at the Centre.

3.3 Equipment and Materials

The radiation detectors for the IMRT measurements were selected based on the AAPM TG – 120 recommendations (Low, et al, 2011).

3.3.1 Discovery RT CT 590 Scanner (CT simulator)

Discovery RT CT 590 Scanner (GE Healthcare, 3000 N. Grandview Blvd, Waukesha, WI 53188 USA) is a dedicated 16-slice multifunction CT scanner for patient image (or data) acquisition for computerized treatment planning. In reference to the aforementioned role of the CT scanner, it has the following features: a wide bore or aperture (80 cm), movable

external laser system to define the coordinates of the patient beyond those inbuilt into the CT scanner, and a carbon fibre flat couch top insert to flatten the surface of the CT scanner couch to ensure that a patient is scanned in treatment position. Owing to the wide aperture, the CT scanner is configured to have a large field of view (FOV) which is achieved through the use of the General Electric (GE) Healthcare's proprietary algorithm that generates an approximate CT image reconstruction outside of the CT measurement field of view. The FOV is 80 cm. The CT scanner is built on the platform with GE's microVoxel™ imaging and using the 100 kW Performix™ Pro VCT 100 x-ray tube, make it possible for the CT scanner to deliver 2D and 3D images with superb image quality through the optimum choice of sub-millimeter slice thickness and reconstructed voxel size (https://www.gehealthcare.com/). The scanner is able to provide slice thickness as small as 0.625 mm helping clinicians to effectively delineate organs. Patient dose indices (Dose Length Product and Dose Efficiency) are displayed during scanning providing patient dose information to the operator. Peak tube voltage (kVp) and tube current (mA) selectable during a scan protocol ranges from 80 to 140 kVp (increments of 20 kVp) and 10 to 800 mA (5 mA increments), respectively. The CT scanner was installed at the National Centre for Radiotherapy and Nuclear Medicine, Korle Bu Teaching Hospital in August, 2019. A picture of the CT scanner is shown in Figure 3.1.

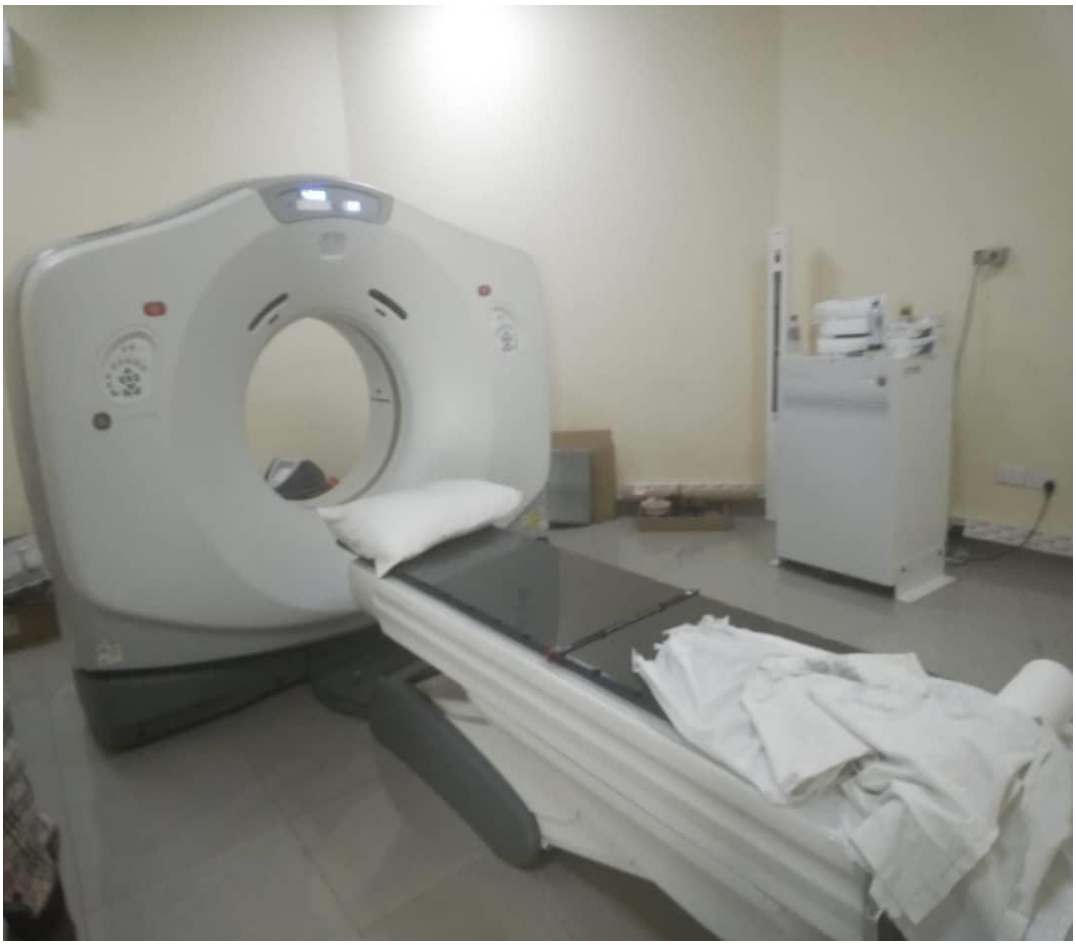

Figure 3.1:GE Healthcare Discovery RT CT scanner (KBTH)

3.3.2 Varian Unique Performance Linear Accelerator

The Varian Unique Performance linear accelerator (Varian Medical Systems Inc. Palo Alto, CA, USA) is a 6 MV single energy medical linear accelerator which is equipped with the Varian Medical Systems 120 leaves millennium multileaf collimator system (MLC-120). The MLC-120 offers 0.5 cm leaf resolution at the isocenter for the central 20 cm of the 40 cm x 40 cm field and 1 cm leaf resolution for the remaining. The leaves of the multileaf collimator (MLC) are designed to have average leaf transmission ranging from 1.5 to 2% of the non-attenuated beam. The leaves of the MLC are arranged in two separate

opposing banks of 60 leaves per bank with a bank mounted on a movable carriage give the leaves additional travel span. The maximum leaf speed at the isocenter is 2.5 cm/s and maximum over-travel distance for a leaf is 20.1 cm. The maximum leaf extension from the bank is 15 cm, and the leaf position accuracy is ± 0.1 mm. The leaves in a bank are interlocked with each other using a tongue and groove arrangement to reduce interleaf transmission, but the leaves can move independently of each other. The linear accelerator is configured to have capabilities for both intensity modulated radiotherapy (IMRT) and volumetric arc therapy (VMAT). On the opposite end of the treatment head of the linear accelerator is a flat panel amorphous-silicon electronic portal imaging device (EPID) mounted on foldable robotic arm, which is dedicated for treatment verification purposes. The linear accelerated was installed at the National Centre for Radiotherapy and Nuclear Medicine, Korle Bu Teaching Hospital on April 2014, and was commissioned for clinical use on April 2019. Beam characteristics of the linear accelerator are provided in Table 3.1. A pictured of the linear accelerator is shown in Figure 3.2.

Table 3.1. Dosimetric characteristics of beams from the Varian Unique Performance linear accelerator

Dosimetric Parameter	**Specification**	**Measured value**
Depth of Maximum Dose (D_{max}). (cm)	10 cm x 10 cm field size	1.45
Percentage Depth Dose at depth of 10 cm (D10). (%)	10 cm x 10 cm field size	66.80
Maximum Field intensity at D_{max} for 40 cm x 40 cm field size. (%)	Diagonal plane (D + +/- -)	106.90

	Diagonal plane (D + +/ - -)	107.00
Photon field flatness for 40 cm x 40 cm field size at depth of 10 cm. (%)	In-plane	± 2.20
	Cross-plane	±2.00
Photon field flatness for 10 cm x 10 cm field size at depth of 10 cm. (%)	In-plane	1.40
	Cross-plane	0.80
Photon field symmetry for 40 cm x 40 cm field size at depth of 10 cm. (%)	In-plane	1.40
	Cross-plane	0.60
Beam output at depth of 10 cm (source to detector distance of 100 cm) (cGy/MU)	10 cm x 10 cm field size	0.80

Figure 3.2: Varian Unique Performance Linear Accelerator (KBTH)

3.3.3 Eclipse treatment planning system (TPS)

Eclipse treatment planning system (Varian Medical Systems, Inc. 3100 Hansen Way Palo Alto, CA 94304-1038, USA) is a Microsoft Windows (Microsoft Corporation, USA) based computerized treatment planning system (TPS), with interface synonymous to the Windows operating system. Principal hardware components of the TPS are: central processing unit (CPU) with high capacity memory and high processor speed, graphics display (very high resolution LED panel screen monitor), input/output devices, archiving devices and network communication devices. The TPS is used for external beam radiotherapy treatment simulations to help clinicians to realise the intent of treatment prior to treatment delivery. The TPS is used to generate beam shapes and dose distributions helping in the optimization of radiation dose to the intended target (tumour) with the intent to maximize tumour control and minimize normal tissue complications. The TPS is linked to the GE CT simulator, a DICOM server, the Unique linear accelerator and other computers through a local area network. Communications among the various devices within the network are managed and made possible with the use of the Varian Medical Systems record and verify system: ARIA® oncology information system, which makes it very convenient to access and transfer patient data across devices and platforms. ARIA® helps to review images and send treatment setup information remotely, as well as checks dosimetric images for IMRT pre-treatment quality assurance and documents activities for evidence-based.

The version of the Eclipse TPS is 13.6, and it uses the Anisotropic Analytical Algorithm (AAA) for photon dose calculation. Implementation of the dose calculation algorithm is convoluted into: photon beam source model- determines the fundamental physical

parameters required for dose calculation, and dose calculation algorithm- calculates the dose deposition using the fundamental physical parameters.Monte Carlo simulations of the radiation generated by treatment head are used to determine the fundamental medical linear accelerator model used in the photon beam source model. The model parameters are adapted for each clinical beam by a source model configuration program. These parameters determine a customized phase space that defines the fluence and energy spectrum specific to each treatment unit and energy. The input of the source model configuration program consists of specific measured beam data and parameter values that are either defined by the user or read in from a parameter library. The parameters describe the measurement geometry and the physical characteristics of a beam (https://www.varian.com). Planning window interface of the TPS is depicted in Figure 3.3.

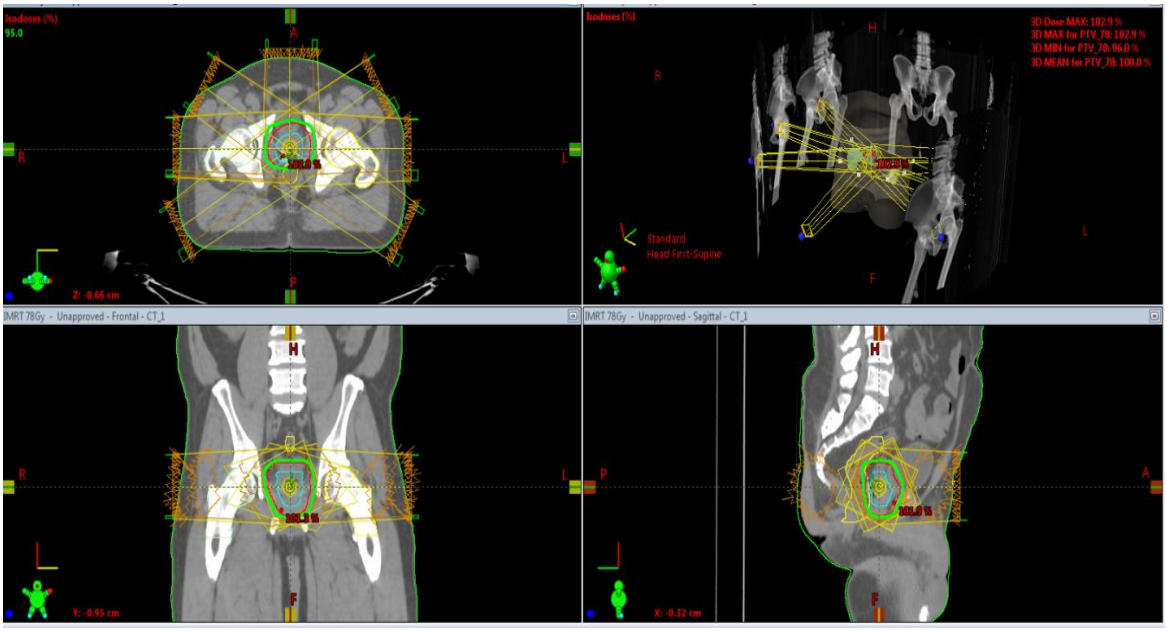

Figure 3.3: Varian Eclipse TPS (KBTH)

3.3.4 Solid Plate Phantom

The solid plate phantom (SP34) (IBA Dosimetry GmbH, Germany) is made up of white polystyrene (type RW3) plates with the same dimensions: 30 cm x 30 cm, with the exception of thickness. The composition of the SP34 is 98% polystyrene and 2% titanium dioxide (TiO_2), giving the phantom and effective density of 1.045 g/cm^3 (mass density of 0.557 ± 0.001 e-^{1}/cm^{3}NA and relative electron density of 1.000 ± 0.005 (compared to that of water))(https://www.lap-laser.com). The plate phantoms consist of one plate of 0.1 cm thickness, two plates of 0.2 cm, one plate of 0.5 cm and twenty-nine plates of 1.0 cm. There are also two plates each having thickness of 2.0 cm with a hole at one side running central to a plate to accommodate a CC13 and a FC65-P ionization chambers (IBA Dosimetry GmbH, Germany), respectively. These plates are referred to as adapter plates. The phantom is designed to provide quick setups for photon and electron dosimetry measurements. The phantom also offers solutions for very accurate and reproducible measuring depths. The phantom is recommended for both absolute and relative dosimetry measurements, and may be used for the following energy ranges:0.1–50 MV and 2–50 MeV for photons and electrons, respectively. A picture of the phantom in different configurations is shown in Figure 3.4.

(a) *(b)*

Figure 3.4: Solid plate phantom: (a) https://www.lap-laser.com, and (b) KBTH

3.3.5 Blue Phantom^2

Blue Phantom^2 is a three dimensional motorized water tank designed by the IBA Dosimetry (IBA Dosimetry GmbH, Germany) to provide complete solution for teletherapy machine commissioning and quality assurance.

The phantom is made up of a water tank having exterior dimensions of $(L \times W \times H) 67.5\ cm \times 64.5\ cm \times 56.0\ cm$, giving the phantom a scanning volume of $48.0\ cm \times 48.0\ cm \times 41.0\ cm$. The water tank can hold approximately 200 litres of water. The water tank has wall thickness of 1.5 cm and it is made from acrylic (Perspex). A detector support system is mounted on top of the water tank which is capable of automatically moving a coupled radiation detector holder in the horizontal, lateral and vertical directions. The detector support system has leveling knobs to assist with the alignment of the detector relative to the surface of the water (figure 3.5. A). The water phantom comes with set of universal holders to enable fast and flexible mounting of all known ionization chambers and detectors appropriate for the water tank in the vertical and horizontal orientation. The movement of a detector has position resolution of 0.1 mm and both position accuracy and reproducibility of $\pm\ 0.1\ mm$. During measurements the water tank is placed on a lifter table having table top dimensions of $63.5\ cm \times 63.5\ cm$ which is mounted on a leveling frame. The leveling frame has three knobs at the base to enable leveling of the surface of water within the tank. The top of the lifter table can be adjusted to a height ranging from 66.0 to 102.0 cm, and can be rotated about the xy-plane. The water phantom carriage has electric (telescopic) lifting mechanism and also doubles as a storage compartment for auxiliary equipment. The water phantom carriage has dimensions (L x W x H) of $79.0\ cm \times 63.0\ cm \times 66.0\ cm$ with two fixed and two steerable rollers with brakes at its

base to make it possible to easily manoeuvre and set up the water phantom for measurements. A picture of the carriage is shown in Figure 3.5 B.

The water phantom also includes separate tank trolley on wheels with a polyethylene water reservoir having dimensions (L x W x H) of $97.0\ cm \times 66.0\ cm \times 83.0\ cm$ and it is capable of storing 220 litres of water. The wheels are similar to those found on the water tank carriage. The reservoir is fitted with bi-directional automatic pump with a flow control rate of 20 litres/min (HA05) to transport water to and fro the reservoir to fill or empty the water tank as well as adjusting the height of water in the tank. The level of water can be adjusted at a rate of 5.0 cm/min. The height level adjustment has position reproducibility of ± 0.3 mm. The reservoir also comes with its independent hand control to facilitate filling and draining of the water tank. A picture of the reservoir is shown in Figure 3.5 C.

A common control unit (CCU) is attached to the water tank which controls the movement of the detector holder and lifter table as well as filling and draining the tank during measurements. Within the water tank is a temperature measurement sensor which is used in combination with the pressure measurement (built-in pressure sensor provided in the CCU) to provide automatic corrections of temperature and pressure ($K_{t,p}$) for vented ionization chambers whose readings are influence by variations in air density. There is also a high-accuracy contact-less sensor technology to accurately measure the changing water level in the tank. A remote hand control unit is connected to the CCU to enable the user to set up the water tank for measurements. The compact design of the CCU integrates two independent electrometers, such that simultaneous support of diodes (example of detectors which do not need bias voltage to operate) and ionization chambers can be achieved.

The CCU is connected to a computer with windows operating system via Ethernet (RJ-45) connection and with the manufacturer of the water tank OmniPro-Accept software, facilitate fast and automatic beam data acquisition, data handling, analysis and processing. Predefined measurement task queues can be created for automatic data acquisition for all major TPS. To save time, smart sorting algorithm had been incorporated for optimized measurement sequences; sorting, prioritizing and multiple edits of measurement queues to maximize efficiency.

Figure 3.5. Blue Phantom^2 motorized water phantom components; A. water tank, showing leveling knobs for detector holder, common control unit, hand control unit and detector holder mechanism; B. water tank carriage; and C. water reservoir, showing nozzle for filling the water tank on top and an independent hand control to fill and drain the tank at the side.

3.3.6 Ionization Chambers

Ionization chambers used to acquire beam data from the linear accelerator (Unique Performance) to facilitate effective commissioning of the treatment planning system are listed in Table 3.2 Types of ionization chambers used and their technical specifications are provided in the table. Pictures of the ionization chambers are shown in Figure 3.6 A-C.

A Stealth Chamber was also used in the beam data acquisition process. The Stealth Chamber (SC) is specifically designed to be mounted on the collimator system of a medical linear accelerator to resolve one of the most challenging tasks in small-field (field with one side less than 4 cm) dosimetry; the positioning and use of a reference chamber in a small-field. The dimensions and position of other reference chambers in the beam path, together with the selection of an appropriate detector in order to avoid partial-volume effects, represent a major challenge for physicists. The SC is also designed to be transparent to the beam that traverses its sensitive volume. The SC has a thickness equivalent of 0.5 mm of Aluminium and a rectangular design that can be used in the data acquisition of fields ranging from 0.5 cm × 0.5 cm to 25 cm × 25 cm. A picture of the SC is shown in Figure 3.6 D.

All the detectors were designed and manufactured by IBA (IBA Dosimetry GmbH, Schwarzenbruck, Germany).

Table 3.2 (a). Technical specifications of ionization chambers

Manufacturer preferred name	**Type**	**Cavity volume (cm^3)**	**Cavity length (mm)**	**Cavity radius (mm)**	**Wall material**	**Wall thickness (g/cm^2)**	**Central electrode material**	**Quantity used**
CC13	Water-proof cylindrical IC	0.130	5.800	3.000	C552	0.070	C552	2.000
Razor Chamber	Water-proof nano cylindrical IC	0.010	3.600	1.000	C552	0.088	Graphite	1.000
FC65-G	Water-proof Farmer type IC	0.650	23.100	3.100	Graphite	0.073	Alumimium	1.000

Table 3.2 (b). Technical specifications of CC13 ionization chamber

Item	**Characteristics**
Polarizing voltage	±300 V (max. ±500 V)
Typical leakage current	3 fA
Recommended pre-irradiation	5 Gy
Typical sensitivity	3.6 nC/Gy
Guard potential	±300 V (max. ±500 V)
Temperature range	15 – 35 ^{0}C
Relative humidity range	20 - 80%

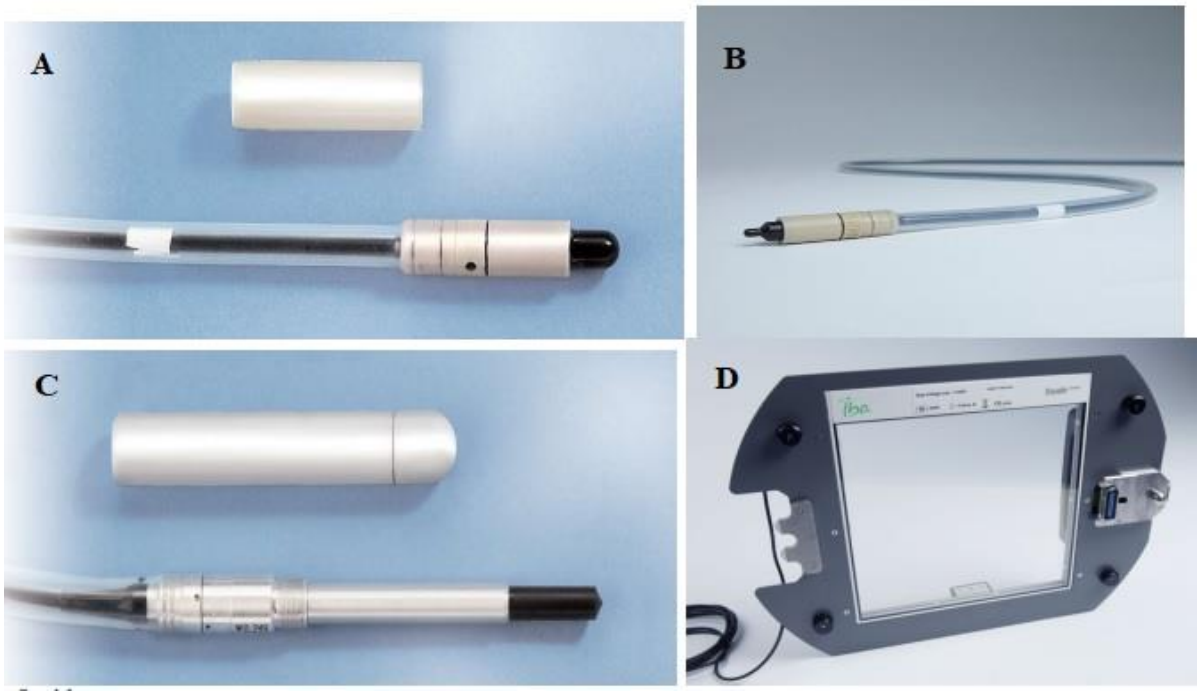

Figure 3.6: Ionization chambers: A. CC13, B. Razor chamber, C. FC65-G, and D. Stealth Chamber

3.3.7 Diode Detector

A Razor™ diode detector (IBA Dosimetry, GmbH, BahnhofstraBe, 5, Germany) was also utilized in the beam data acquisition. The diode was specifically designed for small field dosimetry similar to those encountered in stereotactic radiotherapy, IMRT, and volumetric arc radiation therapy (VMAT), and regions with high dose gradients- choice for measurements where high spatial resolution is required. The detector is appropriate for relative dosimetry of photon and electron fields in radiotherapy, and may be used for depth dose and off-axis ratio measurements in air, solid phantoms and water phantoms. It could be used for the measurement of output factors of small to medium field sizes. It is suitable for the measurement in beam qualities ranging from ^{60}Co-15 MV for photon beams, and 6 to 15 MeV for electron beams. The Razor diode is a high doped p-type silicon detector

chip, which is designed to be rigid and long-lasting. The stem and enclosure materials are made with stainless steel and acrylonitrile butadiene styrene plastic (ABS) and epoxy, respectively. The position of measurement point is indicated by a cross-hair marked on top of the detector. The effective point of measurement is located 0.8 ± 0.2 mm from the surface. The active diameter of the Razor is 0.6 mm and the active detector thickness is 0.02 mm. The other dimensions of the detector are the following: - head diameter 4.0 mm, head length 15.0 mm, stem diameter 4.0 mm and total length 60.0 mm. It is made by infusing n-type semiconductor into p-type semiconductor such that the resultant p-n junction can function in photovoltaic mode without any bias voltage. With reference to this, external stimuli such as an ionizing effect of radiation can be used to generate electron–hole pairs within the diode. The signal of the diode is obtained by electrons diffusing freely through the crystal and are able to cross the p-n junction region with the aid of the built-in electric field of the depleted region. Electron-hole pairs that are produced directly in the depleted region contribute marginally to the signal of the diode. The diode is a shielded diode and therefore requires to be used with its long-axis parallel to the direction of propagation of the beam in which the diode is placed. Pictures of the diode are shown in Figure 3.7.

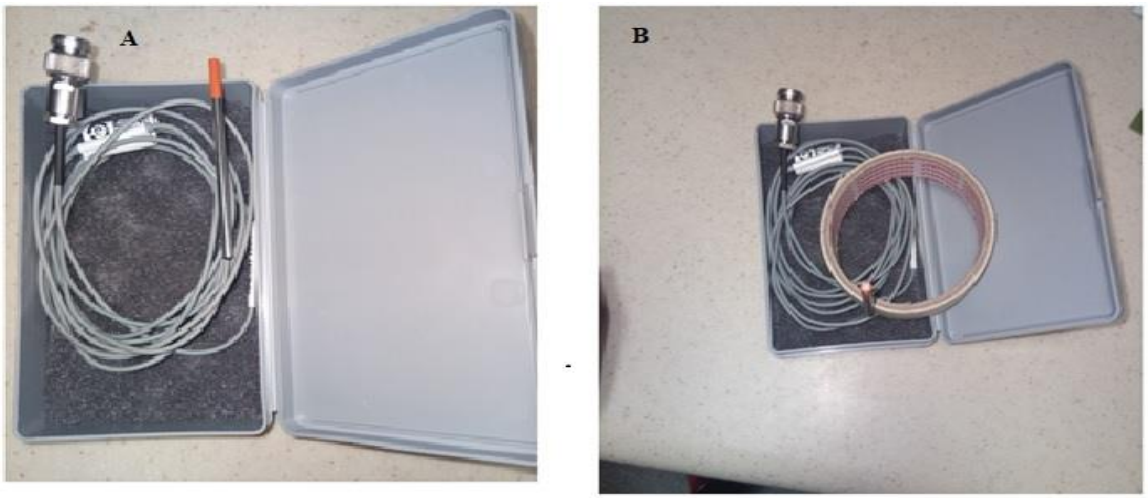

Figure 3.7: Pictures of Razor diode detector in it storage box; A. placed horizontally to show its metallic stem and enclosure material (orange portion), and B. in vertical orientation to show its surface (top) and the cross-hair marked on the surface of the diode

3.3.8 PTW UNIDOS Electrometer (Freiburg GmbH electrometer (PTW 10008))

The PTW UNIDOSelectrometer (model: 10008; PTW Freiburg GmbH, Germany) is an economical high quality dosimeter for universal use in radiation therapy and diagnostic radiology. It complies with IEC 60731 as a field class as well as a reference class dosimeter. It also complies with both IPEM guidelines on dosimetry transfer instruments and IEC 61674 as a secondary standard dosimeter and a diagnostic dosimeter, respectively. It has high accuracy, excellent resolution (1fA) and wide dynamic measuring ranges. It could be connected to an ionization chamber or a diode with a male Threaded Neill–Concelman (TNC) connector (W type) to form a dosimeter system. The electrometer amplifies the small signal from a connected detector to be displayed on its large LCD screen with backlight. The electrometer also provides required bias voltage (HV) for an ionization chamber to ensure movement of the charge carriers to the respective electrodes culminating in flow of charges. The bias voltage supply ranges from 0 to ±400 V (increments of ±50 V). A switch at the back of the electrometer is used to reverse the bias voltage and vice

versa. The electrometer could be set to measure integrated dose (or charge) and dose rate (or current) simultaneously. It also possess RS232 interface at the back for device control and data output (https://www.ptwdosimetry.com). A picture of the electrometer is shown in Figure 3.8

Figure 3.8: PTW UNIDOS electrometer

3.3.9 IBA miniPhantom

The IBA miniPhantom (IBA Dosimetry GmbH, Bahnhofstrasse 5 DE-90592, Schwarzenbruck, Germany) is made of water–equivalent polystyrene (RW3) with mass density of 1.045 g/cm^3 and an electron density of $3.386 \times 10^{23}/\text{cm}^3$. The phantom has dimensions of: 30 cm × 38 cm and height is 14 cm. The phantom was specifically designed for treatment plan verification of both conventional and IMRT techniques, but the phantom can also be used for patient specific quality assurance for VMAT technique. At a distance of 6.4 cm from the top of the phantom is a rectangular insert hole to accommodate an IBA MatriXX detector or rectangular RW3 block for holding a film or FC65-P Farmer type ionization chamber. Various lines are inscribed on the top and side surfaces of the phantom

to facilitate alignment of the phantom within a beam. Sectional schematic diagram of the phantom is depicted in Figure 3.9.A. A picture of the phantom without an insert is shown in Figure 3.9.B. (https://www.iba-dosimetry.com).

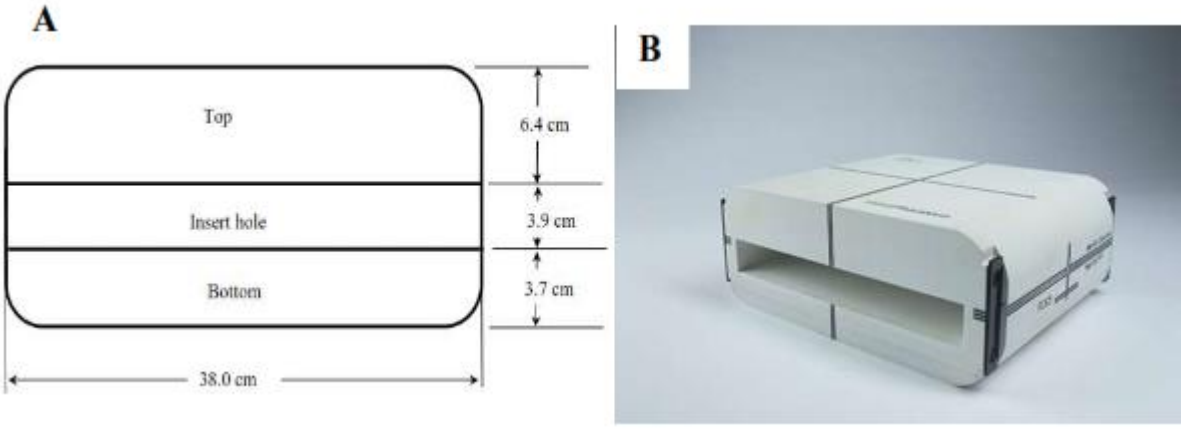

Figure 3.9: IBA Dosimetry miniPhantom: A. sectional schematic diagram of phantom showing dimensions, B. picture of phantom without insert.

3.3.10 IBA MatriXX^{Evolution} 2D Array Detector

The MatriXX^{Evolution} two-dimensional (2D) array detector (IBA Dosimetry GmbH, Schwarzenbruck, Germany) is designed for fast and accurate verification of patient dose and also for Linac QA. The 2D array detector contains 1,020 miniature ionization chambers within its sensitive area. The ionization chambers are aligned in a parallel pattern forming a 32 x 32 grid, with active measurement area of 24.4 cm × 24.4 cm. The detector has dimensions of: 56 cm x 32 cm x 3.8 cm and a weight of 10.5 kg. The detector is provided with inbuilt temperature and pressure sensors to ensure automatic correction of the influence of variation in air density on the responses of the ionization chambers within the detector which are vented to the environment. Each ionization chamber volume is 0.08 cm^3 with a height of 5.0 mm and a diameter of 4.5 mm. The separation between the chambers is 7.6 mm. The locations of the ionization chambers are marked with crosses on

the surface of the detector. Lines are also inscribed on the surface of the detector to indicate the major axes of a beam. Indentation marks are placed on the sides of the detector which are used together with the surface lines indicating beam major axes to align the detector within a beam. Dose rates and doses Ranging from 0.02 – 12 Gy/min (measured with a dose resolution of 0.5 mGy/min) and0 – 10 Gy, respectively can be measured with the detector. Nominal sensitivity of the detector is 2.0 nC/Gy. The detector has dose rate dependence of < ±1.0%, and read-out time of 20 ms without dead time (parallel read-out of all chambers).

The detector charge collection efficiency (pulsed beam at 300 - 360 Hz PRF) are ≥ 99.0%, ≥ 98.5% and ≥ 97.0% at 0.3 mGy/pulse, 0.6 mGy/pulse and 1.1 mGy/pulse, respectively. Applied bias voltage of the detector was 500 ± 30 V. The detector sensitive area has a 3.1 mm water equivalent depth build-up material with 3.5 mm effective point of measurement (P_{eff}) below the surface. Deviation from Linearity for the detector response is ≤ 1% for dose ≥ 0.02 Gy. The 2D array detector during operation is connected to a laptop having the IBA Dosimetry myQA software through Ethernet connection (via standard network cable) at the back of the detector where AC power connector and a switch to put on the detector are located. (https://www.iba-dosimetry.com). Picture of the 2D array detector is shown in Figure 3.10.

Figure 3.10: IBA Dosimetry MatriXX 2D array

3.3.11 myQA Patients

The myQA Patients is one of the applications of the myQA® software package (IBA Dosimetry GmbH, Bahnhofstrasse 5 DE-90592, Schwarzenbruck, Germany), which is specifically designed for patient pre-treatment verification (patient specific QA). The myQA Patients is integrated as a system consisting of a software and supported dose measurement device (such as the MatriXX^{Evolution}) and its associated accessories, such as the miniPhantom and gantry sensor. With the myQA Patients system, the dose distribution of a treatment plan can be measured and compared with dose data from a Treatment Planning System (TPS) (IBA, 2017).

The myQA Patients is a Windows 10 (Microsoft Corporation, USA) based software with intuitive windows/dialogs similar to its Windows based. The software has windows to

enable the user to: set up treatment machine to be used to irradiate a patient and create detector output calibration,create a patient and a project (Figure 3.11.A) ,import the data to be verified (e.g., DICOM data), perform measurements, and perform verification comparison (data analysis). Project creation under a specific patient allows one to do multiple data analyses for the same without the need to create the patient again which can create confusion. Dialog to enable one importsdata and performsmeasurement and data analyses is shown in Figure 3.11.B. The software version of myQA Patients used is 2.9.

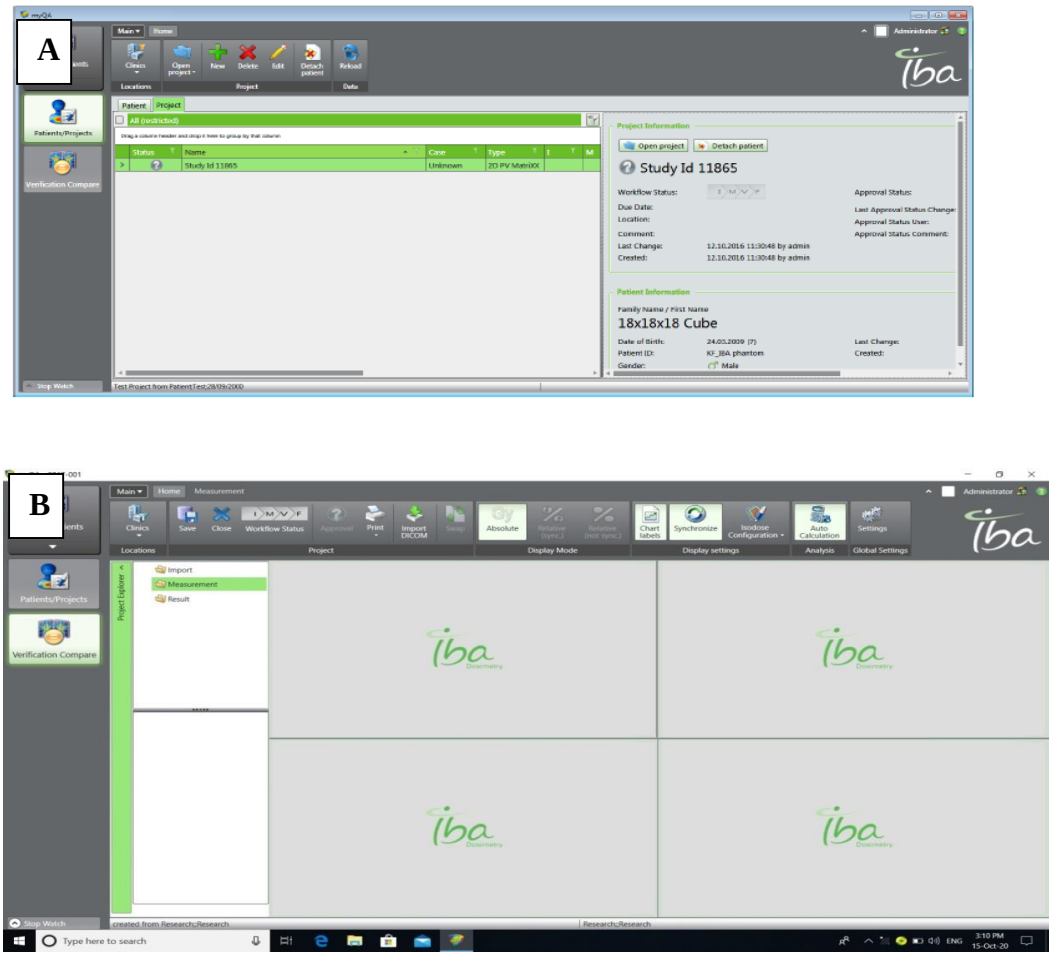

Figure 3.11: IBA Dosimetry myQA Patient software dialogs: A. dialog for creating patient and project, and B. dialog for data import, measurement and analysis

3.4 Methods

The methodology involved end – to – end QA verification tests, tolerance limits, action limits, and pass rate criteria were all defined to evaluate the acceptability of the IMRT QA verification plans. It was systematically organized for linear accelerator commissioning, absolute dose determination, calibration of patient – specific device, IMRT treatment planning, plan verification for IMRT, treatment delivery and data analysis.

3.4.1 Linear Accelerator Commissioning

With the Eclipse TPS there was no need to acquire physical parameters of the Unique linear accelerator (linac) as the TPS already had a virtual model of the linac as both the linac and the TPS were from the same manufacturer. Measurements needed for Eclipse TPS algorithm configuration were therefore acquired. All beam data were acquired with the Blue Phantom 2 motorized water phantom which was connected to a laptop having the IBA Dosimetry myQA Accept software.

At the start of the measurements, lot of time was spent to get the phantom accurately aligned within the beam to ensure integrity and accuracy of the measured data. To ensure this, after filling the phantom to the required level the CC13 chamber placed in its holder provided by the manufacturer was mounted on the movable detector holder arm of the phantom. Accessory (in the form of a cap) provided by the manufacturer to facilitate the location of the water surface relative to the long axis of the chamber was placed on the ionization chamber (IC), and the IC moved to the various corners of the phantom. At each corner, the leveller on top of the phantom was used to adjust the level of water surface by looking in the opposite direction a cross inscribed on the cap (along the long axis of the

IC) place on the detector, such that a perfect cross was seen when the detector was partly submerged. Prior to this, the surface of water in the phantom (water tank) was levelled with the aid of a spirit level using the levelling knobs on the water tank carriage. To check the alignment of the detector within the beam, profile scans (off-axis measurements) were performed at two different depths (1.5 and 2.5 cm) along the major axes (in-plane and cross-plane) of a beam with field size of 10 cm x 10 cm, and "CAX" correction performed with myQA Accept software for both profiles to obtain deviations in alignment of the detector from the beam central axis. From the deviations obtained, the detector was re-aligned perfectly. The measurements were performed at source-phantom distance (source to surface distance) of 100 cm. Percentage depth dose (PDD) measurements along the central axis were also done with this set-up to obtain the depth of maximum dose (d_{max}) for the beam energy as illustrated in Figure 3.12.

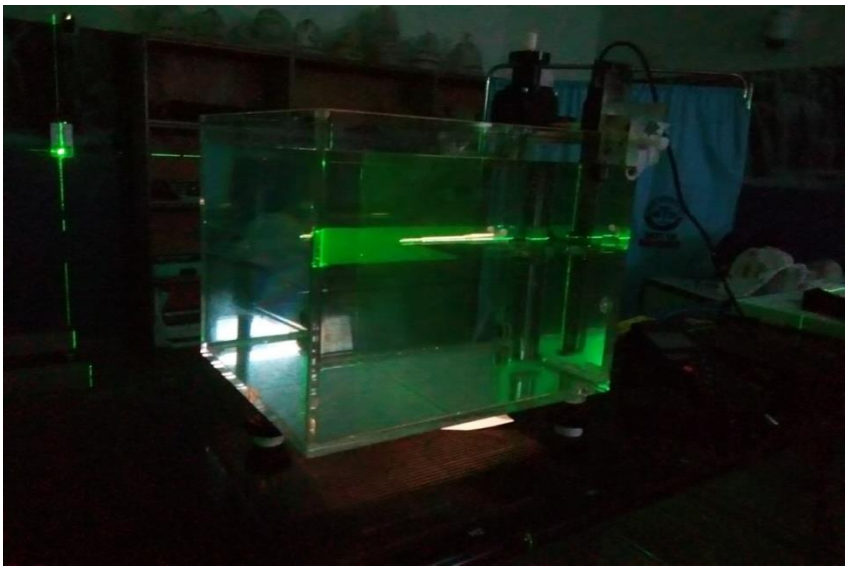

Figure 3.12: Linac commissioning with a water phantom (Korle – Bu Teaching Hospital)

PDDs and profiles were acquired with the CC13 IC in continuous mode at source-phantom distance of 90 cm for field sizes ranging from 4 cm x 4 cm to 40 cm x 40 cm using spacing

(space between measuring points) of 1 mm in high gradient region (penumbra and dose buildup region) and 2 mm elsewhere. The profiles were measured for both in-plane (radial) and cross-plane (transversal) at depths of d_{max}, 5, 10, 20 and 30 cm for each field size. For the largest field size, the phantom was offset to obtain half profiles at the required depths and the half profiles merged with the myQA Accept software to obtain the full profiles. In doing this it was ensure that the offset edge of the water tank from the beam central axis was at least more than 5 cm in the direction of scanning. This was done to maintain lateral charged particle equilibrium at all times with respect to the size of the phantom. Also, for the deepest depth (30 cm) of measurement it was ensured that there was enough water (at least depth of 10 cm) underneath the detector to provide the needed full backscatter. Diagonal profile scans were also taken at stated depths for the largest field size, which is used by the TPS to calculate doses for asymmetric fields. During the measurements one of the CC13 ICs was used as a field detector for the measurements and the other as a reference detector which was placed within the radiation field close to the collimator opening (in air) such that it did not overshadow the field detector during any of the measurements, per the AAPM TG 142 guidelines (Klein, et al., 2009). PDDs and profiles were also measured for field sizes less than 4 cm x 4 cm up to 2 cm x 2 cm using the Razor chamber as the field detector and the Stealth chamber as the reference detector. For All the IC measurements the effective point of measurement (EPM) was used to determine each depth similar to that stated (Wegener, et al., 2019). EPM is illustrated in Figure 3.13, which is from the physical middle (C) of the detector toward the surface by a distance equal to $0.6r_{cyl}$, where r_{cyl} is the cavity radius of the cylindrical ionization chamber of the detector. This shift in depth was incorporated automatically by the myQA Accept software. The measurements for the small

field sizes were repeated with the Razor diode as the field detectors to enhance the accuracy of the measured values obtained.

Output factors were measured for field sizes ranging from 4 x 4 cm to 40 x 40 cm at a depth of 10 cm with the CC13 IC connected to the UNIDOS electrometer without a reference detector in the path of the beam using source-phantom distance (SPD) of 90 cm. The output factor measurements were repeated for the small field sizes (the least being 2 cm x 2 cm) using the Razor diode detector. Output factors were also measured for rectangular field size combinations with appropriate detectors to establish collimator exchange effect associated with the linac. The daisy-chaining method (Azangwe, et al., 2014) was used to link the output factors for the two detectors into one output factor table (or curve). This was done owing to the fact that the TPS requires a single output factor table per beam energy. The output factor measurements were done on the beam central axis (CAX) and geometry for the measurement is illustrated on Figure 3.14. All measurements with the Razor diode detector were done with the long axis of the detector aligned parallel to the direction of propagation of the beam.

The measured beam data were converted to w2CAD file format (Dumitru, 2019) with the myQA Accept software and imported into the Eclipse TPS to help commissioned the TPS. Implementation of Enhance dynamic wedge (EDW) were verify with the 2D array detector. Plans with various angles of EDWs that are likely to be used clinically were created with TPS and the plans executed on the treatment machine. Measured profiles and transmission factors of the EDWs were compared to those calculated generated from the TPS to check their congruencies.

Dynamic leave gap (DLG) and leaf transmission for the MLC were measured with dedicated treatment plans provided by Varian Medical Systems that would simulate treatment effects needed for the effective determination of those MLC parameters. Measurements were done on the CAX in the water phantom with the CC13 IC connected to the UNIDOS electrometer. The depth of measurement was 10 cm and SPD was 90 cm. For the leaf transmission, measurements were done for both MLC bank A and bank B, and the average of the two values determined as the leaf transmission. For DLG, CAX doses for dynamic MLC (DMLC) with rectangular gaps of 2, 1 and 0.5 cm that slide over the detector were measured. Correlation between gap and detector response was determined and extrapolating the resulting linear dose, DLG was found out. A test plan was created and its DMLCs imported to the treatment machine. The plan was replicated on the treatment machine and the TPS calculated dose distribution compared to those measured. The leaf transmission and the DLG were fine-tuned to improve the precision and accuracy of the doses.

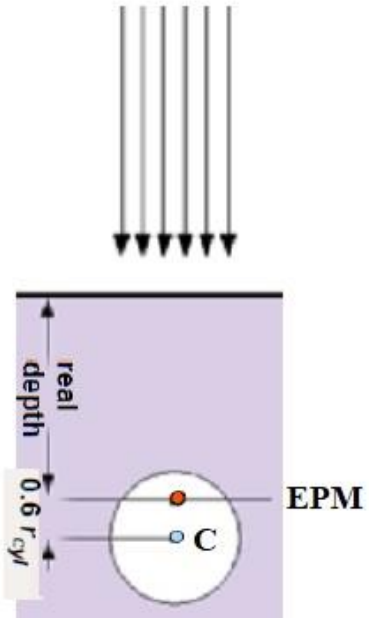

Figure 3.13. Schematic diagram illustrating effective point measurement

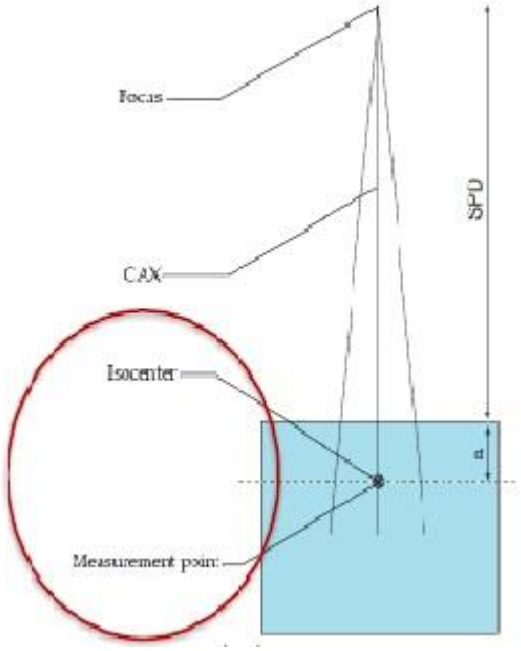

Figure 3.14. Output factor geometry

3.4.2 Absolute Dose Determination

Absorbed dose at a depth of 10 cm was measured, and the value was compared against the baseline data acquired during acceptance and commissioning tests before the patient – specific IMRT verification measurements. This enabled the variation of the MatriXX response and the linac output to be factored into the IMRT QA measurement.

The calibration was performed using a FC65-G farmer – type ionization chamber and an associated PTW Freiburg electrometer following TRS 398 protocol for the calculation of absorbed dose in water (D_w) (IAEA, 2000).

This exercise involved recording temperature and pressure of the room at the beginning and the end of measurements. The temperature and pressure were calibrated using the temperature – pressure correction factor before starting the measurement for the output measurements. The absolute dose calibration was done using a Blue Phantom^2. The water phantom was filled to a level appropriate for the measurements, as illustrated in Figure 3.12.

The procedure was based on the Tissue – Phantom Ratio ($TPR_{20,10}$), using SSD technique at a depth of 10 cm and 20 cm, where the quality of the beam was typically measured by calculating the dose rate at a depth of 20 cm compared with that at 10 cm in water as demonstrated by the schematic illustration of Figure 3.15.

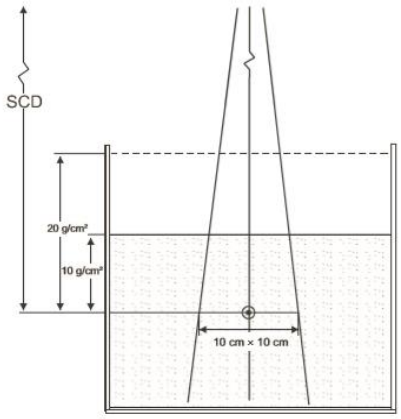

Figure 3.15: Schematic illustration $TPR_{20/10}$ (IAEA TRS 398, 2000)

The FC65-G IC was kept at a depth of 10cm in a Blue Phantom^2, perpendicular to the central axis of the beam with the source – to – surface distance (SSD) of 100 cm for point dose measurements. The IC was later kept at a depth of 20 cm in the water phantom for the same measurement.

The chamber was exposed to 6 MV photon beam of the linac using a field size of 10 × 10 cm with the lateral and longitudinal movement of the treatment couch. The charges deposited were displayed by the electrometer, which were then used to calculate for the absorbed dose to water at a depth of 10 cm ($D_{w,10}$).

Figure 3.16: Electrometer readings of charges deposited (Korle – Bu Teaching Hospital)

Calculations for the absorbed dose to water were done manually following IAEA TRS 398 protocols.

3.4.3 Calibration of Patient – Specific Device

Beam output of the Unique linear accelerator was measured with the FC65-G Farmer type IC based on the IAEA-TRS 398 protocol (Medin, et al., 2006). The dose rate obtained was used to cross calibrate the 2D array detector to obtain calibration factor (K_{user}) for the 2D array detector. This was verified with a treatment plan generated with the miniPhantom with the 2D array embedded in it as illustrated in Figure 3.17.

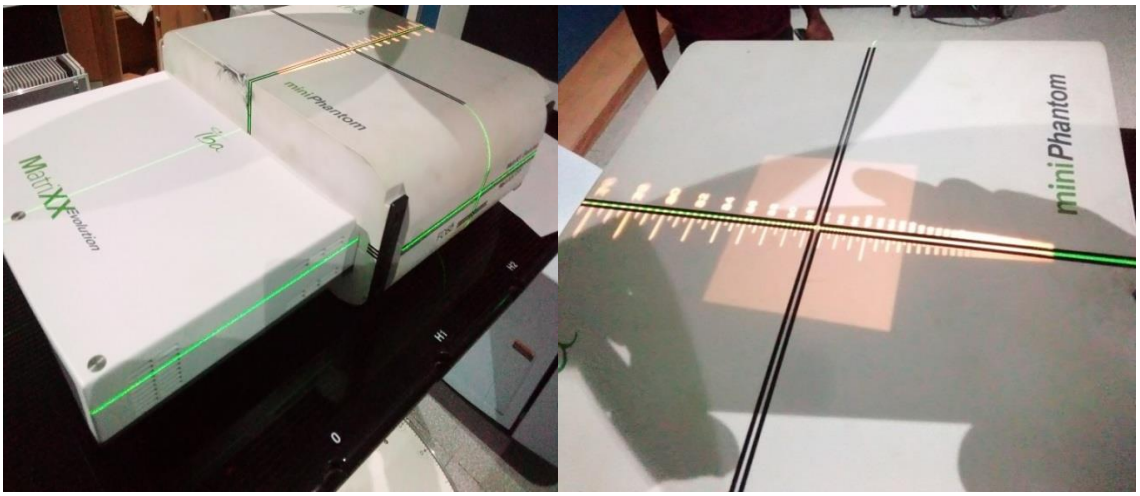

(a) *(b)*

Figure 3.17: miniPhantom with MatriXX embedded in it (Korle – Bu Teaching Hospital)

The miniPhantom was placed on the treatment couch, and the MatriXX was inserted in it as displayed by Figure 3.17. The MatriXX was positioned in the miniPhantom to be able to measure scattering. The room lasers in conjunction with the side cross markers of the miniPhantom were used to position the MatriXX in the centre of the beam. The MatriXX

was aligned using the spirit level placed on the miniPhantom, showing the detector area of the device.

At the accelerator, the light field size was put to $20 \times 20\ cm$. The adjustment capabilities of the treatment couch were used to position the MatriXX, so that the cross – hairs at the sensor area and the light field cross – hairs were superimposed. The cables to the PC were properly connected, the power cord was plugged into the mains power outlet, and the MatriXX was switched on. This was confirmed by the green LED illumination. Warm – up time was allowed, within which the device was pre – irradiated.

The doses were recorded using the MatriXX inserted in the miniPhantom. On the myQA platform, the output calibration dialog was opened. In the machine group, the machine drop down box was clicked, and machine was selected. In the Reference Value group, the reference value was entered in dose mode. The absolute dose calibration were measured and entered for a defined reference point for the reference field size.

The detector response of the MatriXX was converted into dose when the same reference MU was used. The reference dose was measured using the FC65-G IC in the same measurement set up of $10 \times 10\ cm$, 100 MU, 100 SSD and same build up. The effects of the variation of the linac output were accounted for, by following the AAPM TG 51 protocol (Almond, et al, 1999).

Correction factor to account for the uniformity in response of the various detectors within the sensitive area of the 2D array detector had been determined by the manufacturer, but this was verified with a large field size and was found to be within tolerance.

3.4.4 Treatment Planning for IMRT

The treatment planning procedure was guided by the AAPM TG 218 recommendations on IMRT methodologies and constraints (Miften, et al., 2018). Analysis of IMRT QA measurements and the corresponding treatment plans were performed in absolute dose mode.

The miniPhantom with 2D array detector inserted in it was scanned with the GE CT simulator in Figure 3.18, based on departmental protocol in use for patients.

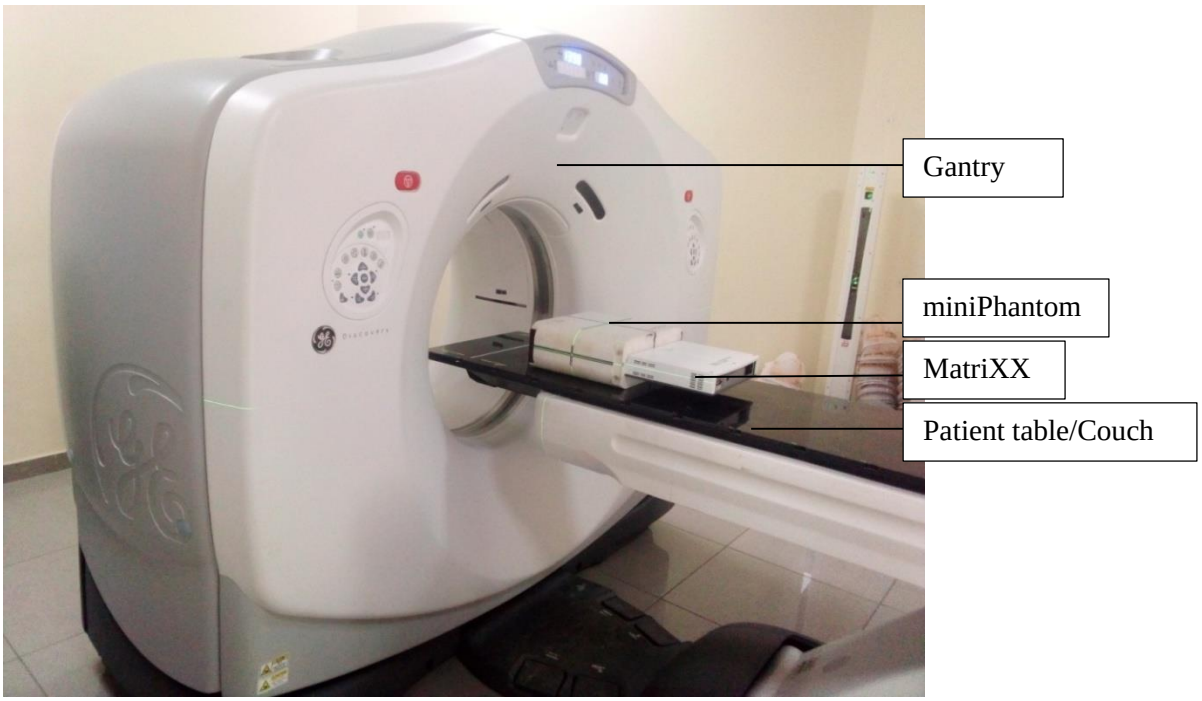

Figure 3.18: CT scanning of miniPhantom with MatriXX embedded in it (Korle – Bu Teaching Hospital)

The axial DICOM images as illustrated in figure 3.19 were imported to the Eclipse TPS.

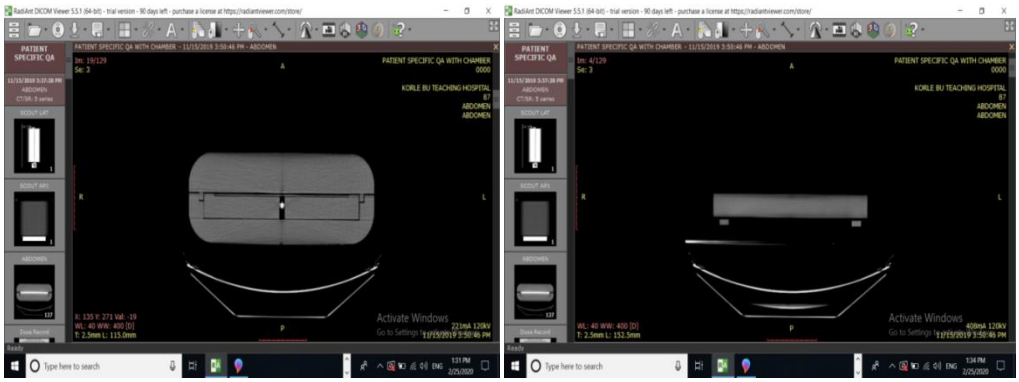

Figure 3.19: CT scans of miniPhantom

The IMRT treatments in this study were planned with inversely – planned IMRT techniques. 3D Varian Eclipse TPS with inverse plan optimization was used to create the treatment plans, where analytical anisotropic algorithm (AAA) was used for optimization.

The study was designed such that prostate and head – and – neck cancers were mimicked by 5 cases each. All 10 plans were generated for the study using 3, 5, 7 or 8 fields IMRT based on clinical objectives, demonstrated by figure 3.20, using 6 MV photon energies.

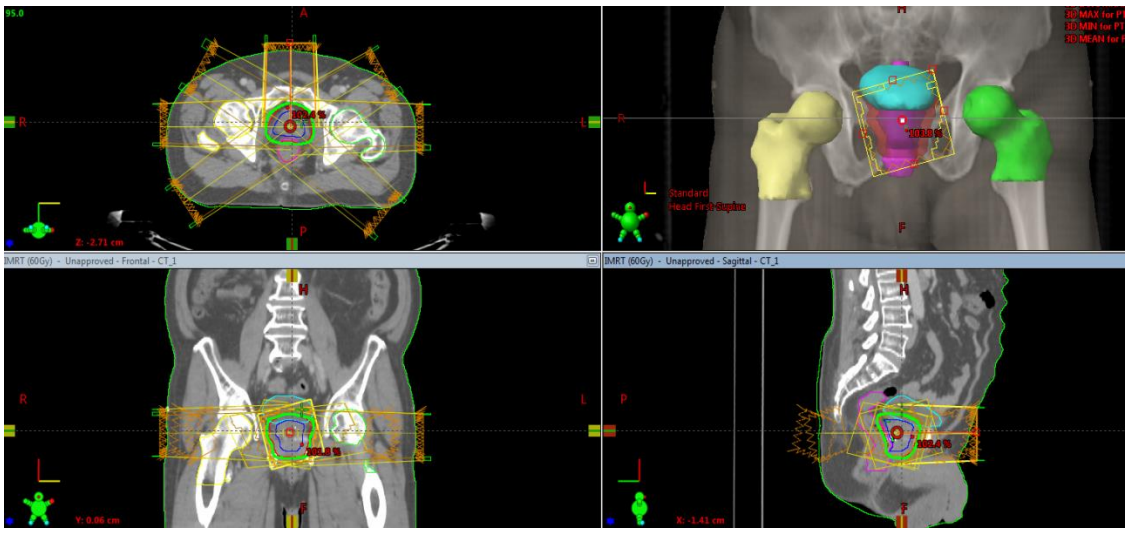

(a)

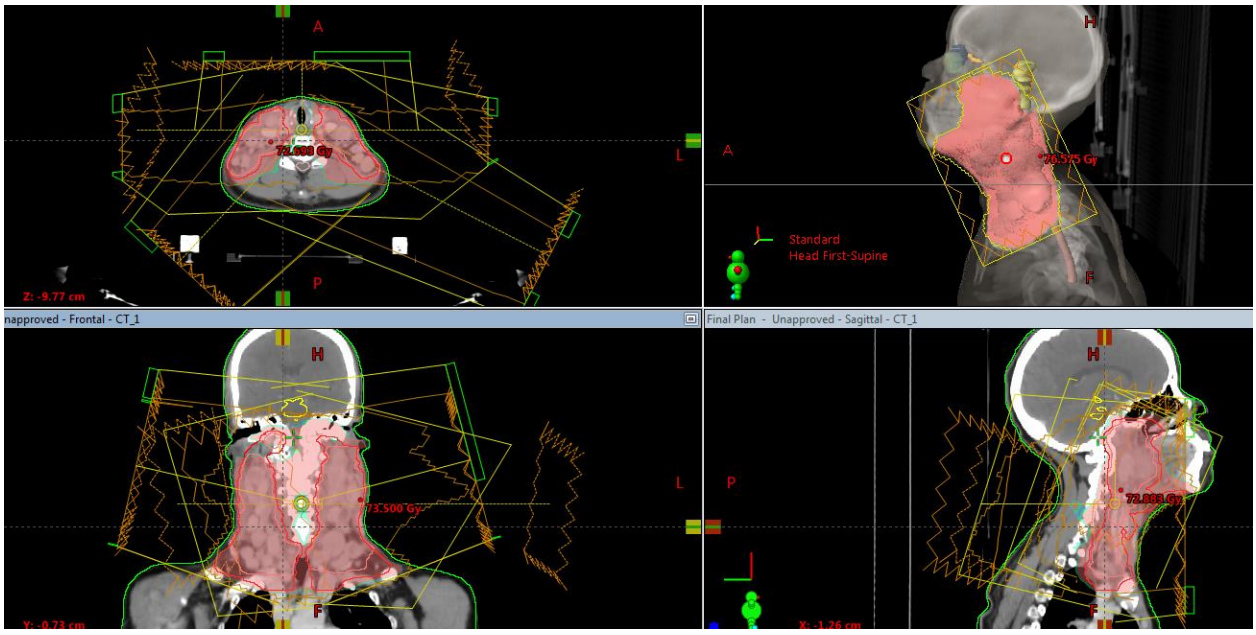

(b)

Figure 3.20: 7 fields IMRT plans: (a) Prostate IMRT (b) Head – and - Neck plan

3.4.5 IMRT Plan Verification

Verification treatment plan for each patient to be treated with IMRT was generated with the miniPhantom. Verification treatment plan was obtained by creating a template of the DMCLs for the patient treatment plan and placing them on the phantom for the TPS to recalculate the dose distributions based on the patient's treatment with DMLCs.

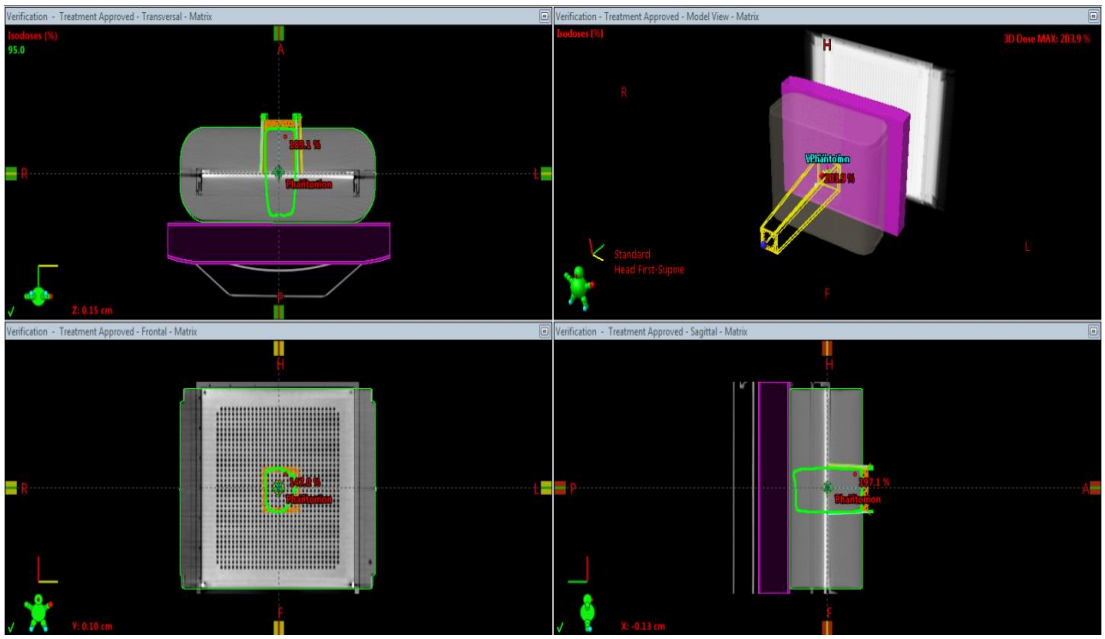

Figure 3.21: Verification plan of a 7 fields prostate IMRT

The pretreatment verifications were performed for all cases at zero degree gantry angle as in Figure 3.21 since the actual treatment angles could not be delivered due to lack of angle sensors for the MatriXX.

3.4.6 Treatment Delivery

Each verification plan was transferred including all corresponding treatment parameters to the ARIA Version 13.6 MR 1.2 for delivery.

The setup of the miniPhantom and the MatriXX were done exactly as the set up used for the scan at the CT. The MatriXX was inserted until it reached the L – shape stoppers in the back, and the plastic block was placed under the electronic part of the MatriXX as a support. The parameters for pre – irradiation were 100 cm SSD, $24 \times 24\ cm$, field size and 500 MU.

The orientation of the MatriXX, the gantry and collimator angles of the linear accelerator were set at 0^0. The vertical orientation of the MatriXX was obtained with the help of the laser and the side markers of the miniPhantom, indicating the exact position of the measurement level. The MatriXX was connected to the PC. The MatriXX was turned on after connecting it. In the Equipment group, the correct machine and detector were selected, and connected by a click. Background measurements were taken, settings were defined and the detector was pre – irradiated. Measurements mode was then set, and the beam was turned on.

The verification plan was executed on the linac, using the 4DITC with all systems networked through ARIA networking system. Treatment was delivered by a sliding window multileaf sequencing method, using the 6 MV linac as displayed in Figure 3.22.

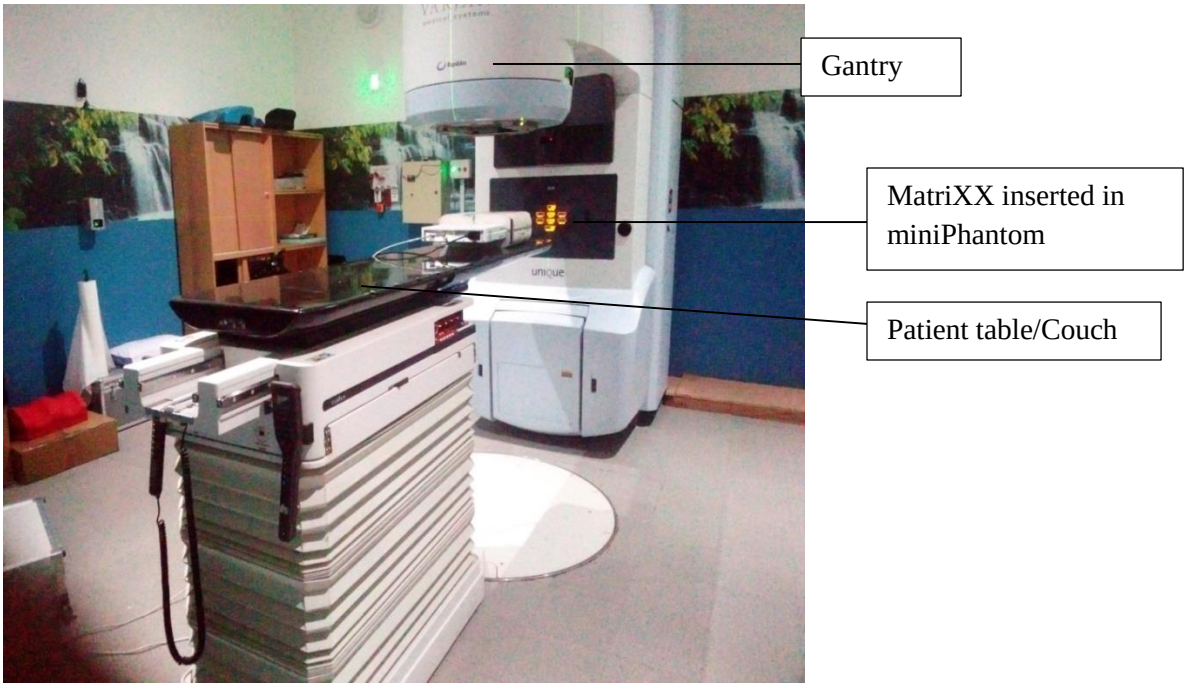

Figure 3.22: Treatment delivery of the miniPhantom with MatriXX embedded in it

Each miniPhantom irradiation was repeated three times for each plan at different times to check for fluctuations in the MatriXX.

3.4.7 Verification Data Analyses with myQA Patients Software

The planar dose deposited were analyzed using myQA Patients SW, where the doses were imported and retrieved. The connection settings were set up to select the patient from a list, where a patient was created with the DICOM patient.

The measurement data was pressed and dragged to the compare pane, to be verified, and the dose plan was pressed and dragged to the reference pane, to be compared with. The images in the reference and compare panes were aligned so they would overlap. The calculated and measured dose distributions were co – registered for comparison. The registration presented the dose distribution positions in a common coordinate system. The Gamma Index calculation was performed in the results pane and verification results were saved.

Planned and measured data were presented based on TG 119 recommendations. (Ezzell, et al., 2009). Point dose calculations at the location of the MatriXX were repeated with the myQA Patients SW for all composite treatment plans. Dose planes were compared with calculations for all 10 IMRT plans.

Verifications were made using global normalization as per TG – 218 recommendations (Miften, et al., 2018). The gamma (γ) evaluation method was used to compare the planned dose in TPS and delivered dose. Passing rates were calculated using dose DD/DTA, γ

evaluation, and absolute dose comparison with global normalization. Consequently, the value of γ calculated by myQA Patients SW was used.

The gamma passing rate used for the gamma evaluation was 95% passing rate with 3% DD and 3 mm DTA. Doses calculated using the TPS were compared with doses measured by the MatriXX for all 10 cases based on gamma evaluation (3%/3 mm, threshold 5%). Per the passing criteria, the percentage of detectors with $\gamma < 1$ was recorded.

The IMRT treatment process was monitored and thoroughly investigated to check if the γ passing rate was systematically lower than the tolerance limits or higher than the action limits.

In order to demonstrate the dosimetric fluctuations in the MatriXX, passing rates for three consecutive measurement results were assessed based on gamma index values for all 10 cases, which meant that patient – specific QA was confirmed three times for each case.

CHAPTER FOUR

4.0 RESULTS AND DISCUSSIONS

4.1 Introduction

This chapter outlines pertinent information on two principal components of the study. It presents the research findings from the QA verifications performed. The linear accelerator commissioning falls out of the scope of this work, hence commissioning results was not presented. Since the linear accelerator commissioning was very relevant and interrelated to this research work, it was imperative to throw a light on how the commissioning was done in Chapter Three.

The reference doses calculated by the treatment planning system (TPS) to be delivered by the medical linear accelerator and the compared doses measured by the MatriXX for all cases of IMRT is presented. It also highlights on the dose differences, and some comparison and relationships between reference and measured doses recorded in the study. The passing rates recorded for each IMRT case verified in the study have as well been presented, and the comparison of the data obtained with results from literature and other international protocols have also been discussed.

The primary aim was to assess the pass rates and the dose differences, and compare them to the recommendations made by international professional bodies as yardstick to evaluate the credibility of the treatment facilities for IMRT implementation.

Due to the absence of local guidelines on the implementation of pretreatment patient – specific QA for IMRT in Ghana, comparison of the findings have been made against the recommendations by the International Atomic Energy Agency (IAEA), American

Association of Physicist in Medicine (AAPM) and the European Society for Radiotherapy and Oncology (ESTRO).

4.2 Trend of IMRT Implementation in Ghana

IMRT began in Ghana firstly at the Korle – Bu Teaching Hospital in June 2020, with just one patient for a period of one month. The number has since been increasing after the clinical observation of the patient – specific verification results at the centre. Table 4.1 presents the trend of IMRT implementation and the frequency of IMRT cases at the centre.

Figure 4. 1 is a graphical illustration of the trend of IMRT implementation in Ghana. It is a plot of the number of IMRT cases treated per month, from the beginning of its first treatment at the National Centre for Radiotherapy and Nuclear Medicine. In April 2020, the facility commenced the treatment of its first case of IMRT.

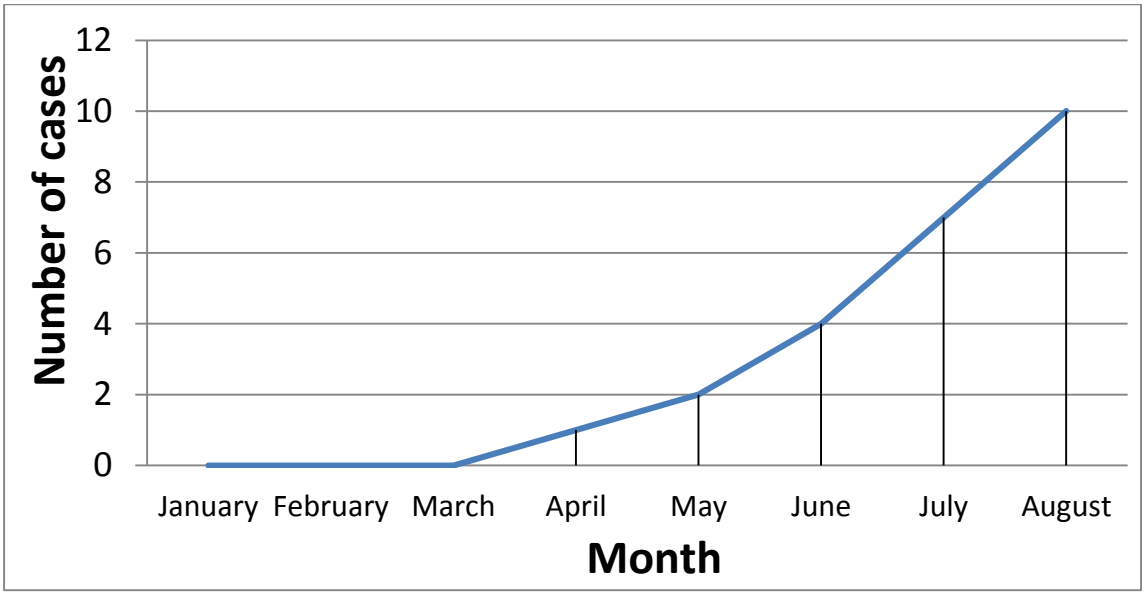

Figure 4.1: Data on IMRT procedures in Ghana

The graph explains the sudden rise of its usage at the centre, resulting in an increment of three more cases in two months, and a total of 10 cases in four months from the beginning. The trend indicates the prospects of the technique in the country and the need to implement patient – specific verification QA prior to treatment at the centre.

4.3 myQA SW Verification Results

The resulting ionization chamber array measurements have been displayed by myQA software. Reference and compare planar dose distributions have been presented based on the {3% (global), 3 mm} gamma analysis, as illustrated by Figure 4.2.

Fig. 4.2 (a) and (b) display the results for prostate and head – and – neck IMRT verification respectively;

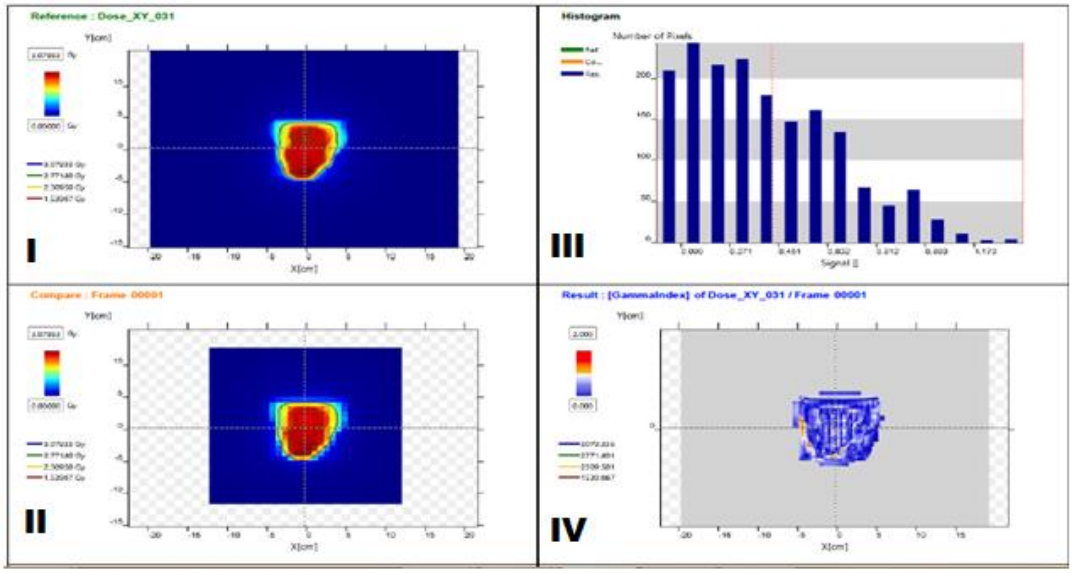

Figure 4.2 (a): A prostate result of a gamma evaluation of dose differences between doses measured by MatriXX and a calculated dose distribution using 3%/3 mm criteria: (I) Coronal dose distribution for MatriXX; (II) Coronal dose distribution for TPS calculated; (III) Dose histogram; (IV) Gamma evaluation results by the MatriXX

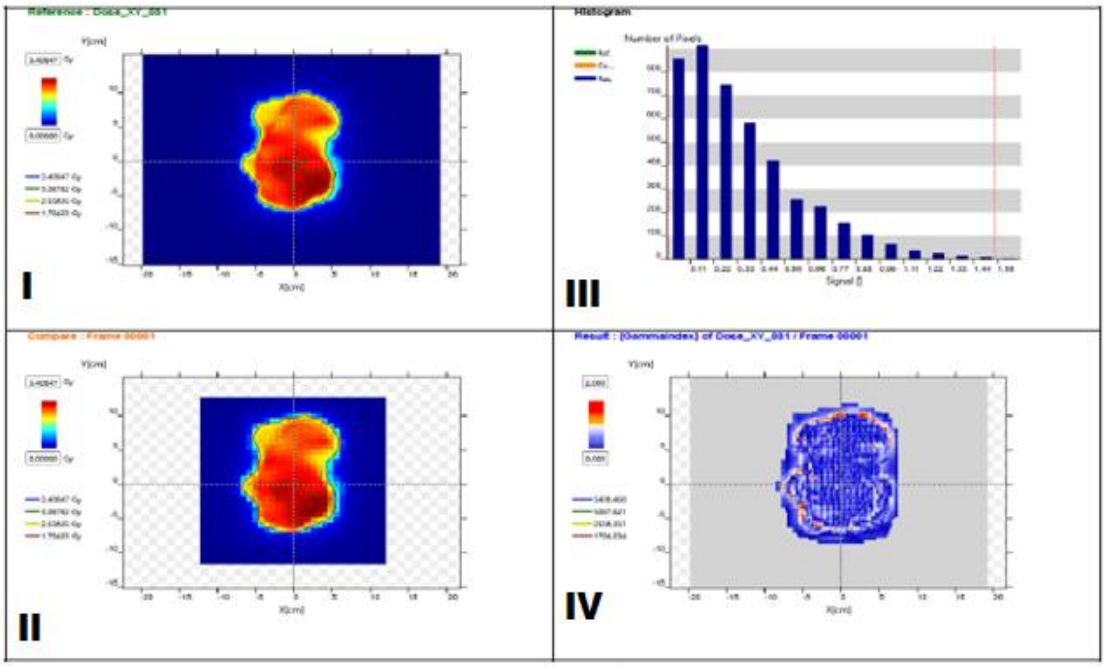

Figure 4.2 (b): A Head-and-Neck result of a gamma evaluation of dose differences between doses measured by MatriXX and a calculated dose distribution using 3%/3 mm criteria: (I) Coronal dose distribution for MatriXX; (II) Coronal dose distribution for TPS calculated; (III) Dose histogram; (IV) Gamma evaluation results by the MatriXX

In Figure 4.2 (a) and (b), the coronal dose distributions for TPS calculation and MatriXX measurement have displayed very close values for both prostate and head – and – neck verifications, illustrating the accuracy of planned dose delivery. The result of the comparison of the reference and measured doses is displayed in IV for both cancer types, demonstrating credibility of dose delivery.

Figure 4.2 (c) displays dose profiles with the orange and green profiles being reference and compared doses respectively.

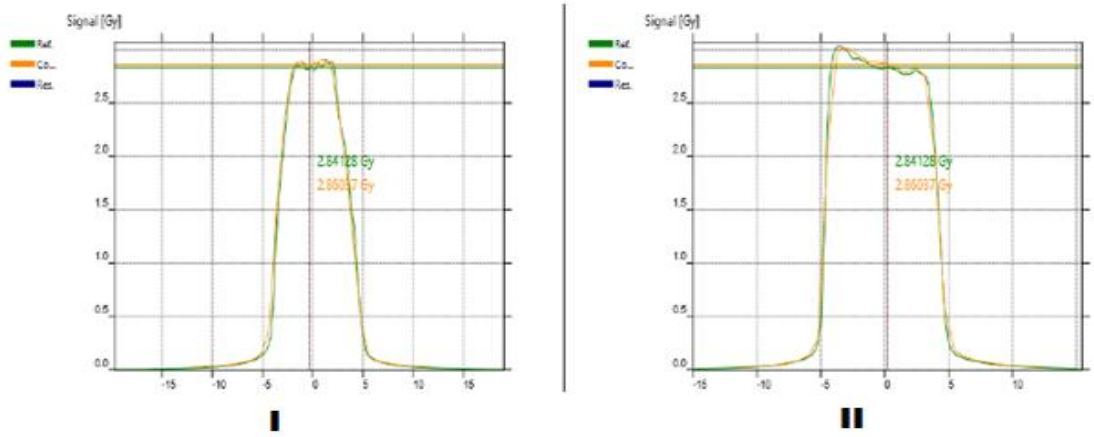

Figure 4.2 (c): Display of dose profiles for a gamma evaluation of dose differences between doses measured by MatriXX and a calculated dose distribution: (I) Profile in the X – axis; (II) Profile in the y – axis;

The dose profile for the gamma evaluation show extremely identical pattern for reference (green line) and measured (orange line) doses for both axes in both cancer types, indicating accurate dose delivery by the linac.

4.4 Comparison of TPS Calculated Dose Distribution and Dose Measured by MatriXX

Table 4.1 (a) and (b) are the representation of dose distributions calculated by TPS and those measured by MatriXX, for various cases of prostate and head – and – neck IMRT respectively. The tabular representations display the results of reference dose distributions calculated by the treatment planning system for each five cases of prostate and head – and – neck IMRT. They also display the results of verification dose distributions measured by MatriXX for all the repeated exercises performed throughout the verification of the dose distributions. It also shows the mean values of the measured dose distributions for all cases of both prostate and head – and – neck IMRT.

Table 4.1 (a): Prostate dose distribution verification

Cases	Dose calculated by TPS/Gy	Dose measured by MatriXX/Gy			Mean Dose measured by MatriXX/Gy
		1st verification	2nd verification	3rd verification	
1	3.08	3.06	3.07	3.07	3.07
2	3.08	3.04	3.06	3.07	3.06
3	4.47	4.47	4.45	4.47	4.46
4	3.37	3.33	3.33	3.36	3.34
5	2.58	2.57	2.59	2.58	2.58
Mean value	3.32	3.30	3.30	3.31	3.30

Figure 4.3 (a) and (b) are graphical demonstrations of the comparison of TPS calculated dose distributions and the mean values of the dose distributions measured by MatriXX for prostate and head – and – neck IMRT respectively. They are plots of dose distributions calculated and measured for each of the cases for both anatomical representations of the research.

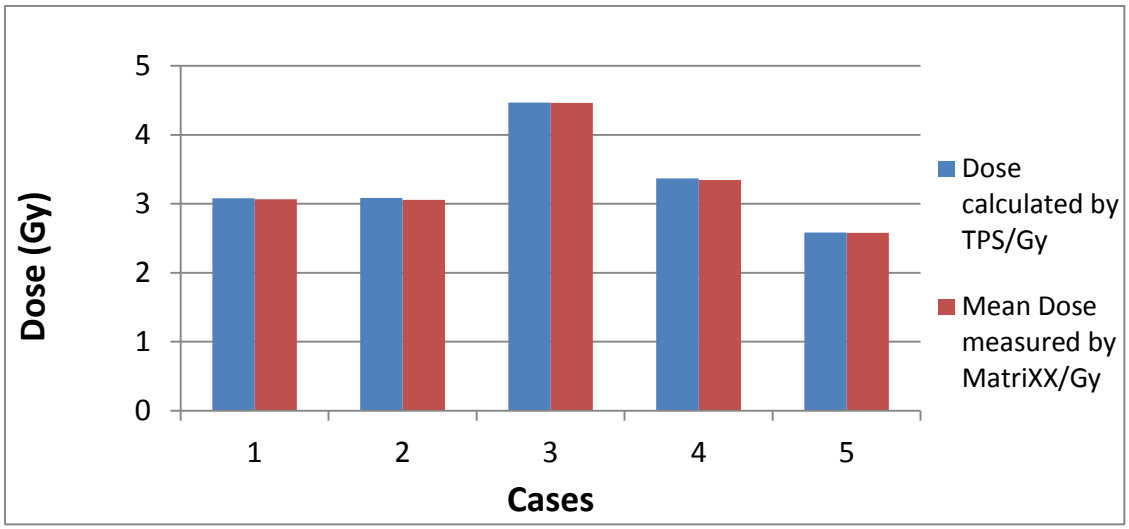

Figure 4.3 (a): Comparison of Calculated and Measured Dose Distributions for Prostate IMRT

The dose distributions calculated at TPS and the mean values of the dose distributions measured by the MatriXX for each of the prostate cases as illustrated in Figure 4.3 (a) are very close. A t – test analysis of the two sets of doses reveals a p – value = 0.029, sufficiently small to demonstrate that the data is statistically significant. A descriptive analysis has also demonstrated that the two data sets show very close values for the mean values of the measured doses with its overall mean dose of 3.30 Gy and a standard deviation of 0.70 Gy to doses calculated, with a mean value of 3.31 Gy and a standard deviation of 0.70 Gy.

Table 4.1 (b): Head – and - Neck dose distribution verification

Cases	Dose calculated by TPS/Gy	Dose measured by MatriXX/Gy			Mean dose measured by MatriXX/Gy
		1st verification	2nd verification	3rd verification	
1	2.72	2.74	2.72	2.72	2.73
2	2.85	2.89	2.84	2.81	2.85
3	3.41	3.38	3.40	3.42	3.40
4	2.24	2.19	2.24	2.24	2.22
5	3.11	3.11	3.10	3.11	3.11
Mean value	2.87	2.86	2.86	2.86	2.86

The dose distributions calculated at TPS and the mean values of the dose distributions measured by the MatriXX for each of the head – and – neck cases as illustrated in Figure 4.3 (b) are very close. A t – test analysis of the two sets of doses reveals a p – value =0.030,

demonstrating that the data is statistically significant. A descriptive analysis has also demonstrated that the two data sets show very close values for the mean values of the measured doses with its overall mean dose of 2.86 Gy and a standard deviation of 0.44 Gy to doses calculated, with a mean value of 2.87 Gy and a standard deviation of 0.44 Gy.

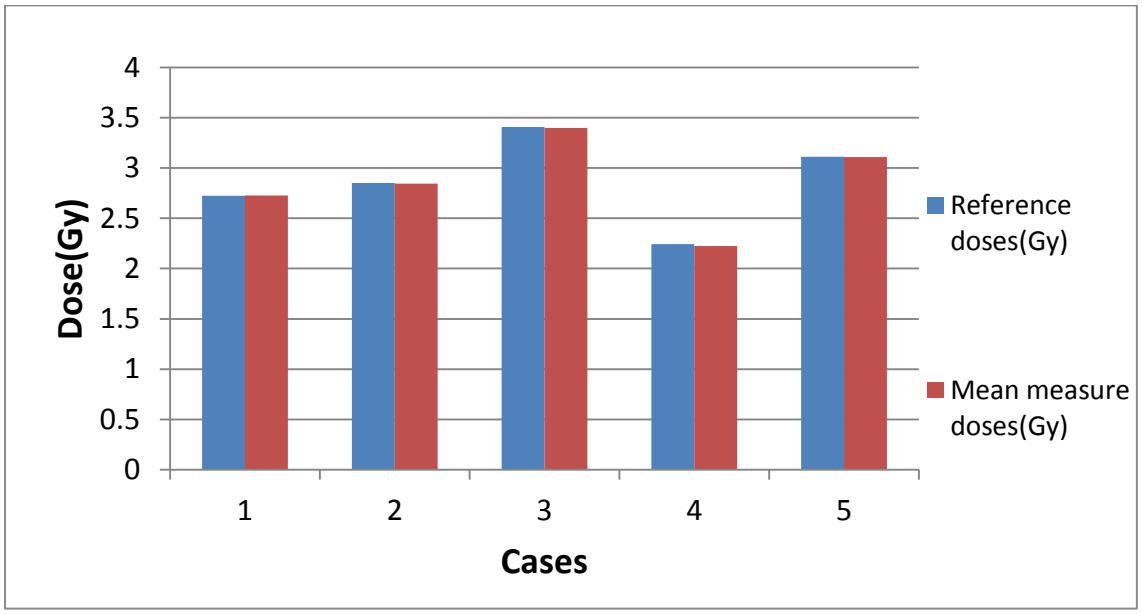

Figure 4.3 (b): Comparison of Calculated and Measured Dose Distributions for Head-and-Neck IMRT

Each of the graphs displayed in Figure 4.2 indicates that there is almost a negligible amount of difference between the reference and the measured dose distributions. This result is an indication of the accuracy of the TPS used for the planning of the IMRT cases. It also reveals the credibility of the medical linear accelerator used for the exposure of the QA phantoms as well as the reproducibility of the phantom setup between CT imaging and treatment delivery.

4.5 Repeated Results of MatriXX Measured Dose Distributions

Figure 4.4 (a) and (b) are bar charts displaying measured dose distributions for the repeated verification exercises performed for prostate and head – and – neck IMRT respectively. They are plots of dose distributions measured for all repeated verifications performed.

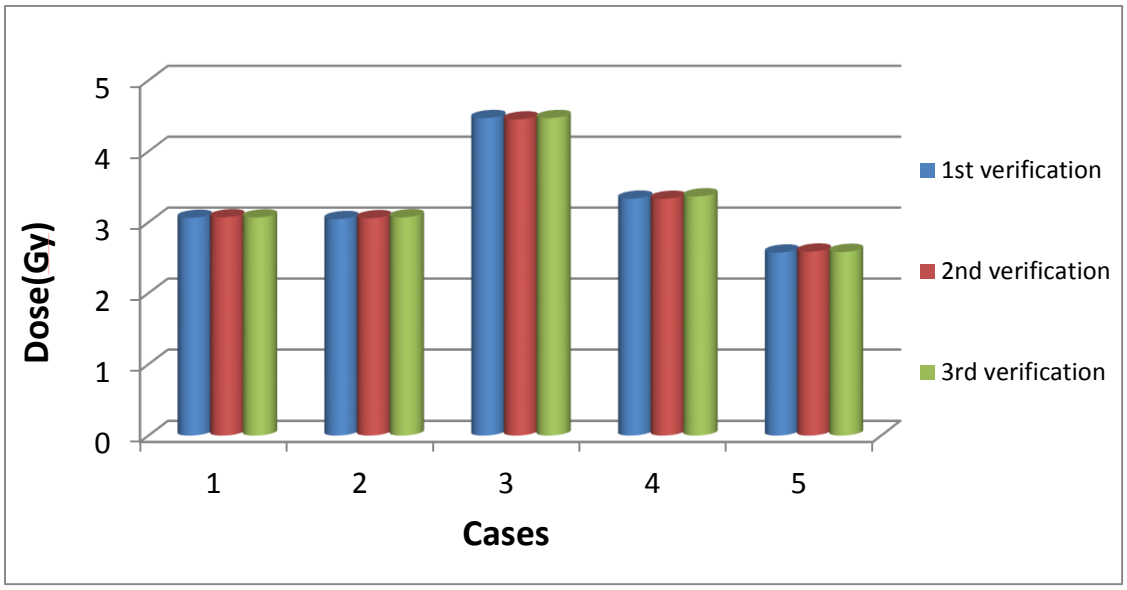

Figure 4.4 (a): Comparison of measured dose distributions for repeated prostate IMRT verification

Analysis of variance for the results of the repeated verification exercises as shown in Figure 4.4 (a), for same cases of prostate IMRT display very close values to each other for measured dose distributions with a p – value = 0.00, and a standard deviation of 0.01 Gy, indicating an extreme value of statistical significance.

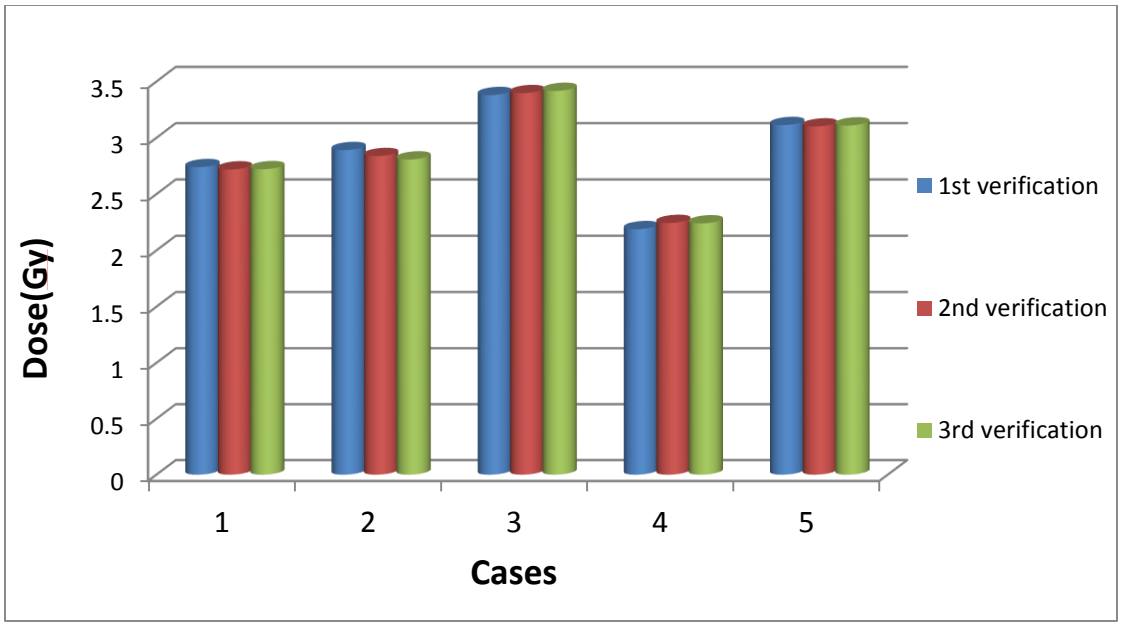

Figure 4.4 (b): Comparison of measured dose distributions for repeated head-and-neck IMRT verification

In Figure 4.4 (b), the results of the repeated verification exercises for same cases of head – and – neck IMRT display extremely close values to each other for measured dose distributions with a standard deviation of 0.00Gy, and a p – value of 0.00.

These results confirm the reproducibility of the phantom setup between CT imaging and treatment delivery. It also confirms constancy in the performance of the MatriXX 2D array used for the patient – specific QA at the centre.

4.6 Consistency of dose differences

Table 4.2 (a) and (b) are the results of the dose differences between reference and measured dose distributions for various cases of prostate and head – and – neck IMRT respectively. The tabular representations display the dose differences resulting from the impreciseness of dose distributions between the doses calculated by TPS and the doses measured by MatriXX for the five selected cases of prostate and head – and – neck IMRT each. They

display the resulted dose differences recorded for each of the repeated exercises performed throughout the verification of the dose distributions.

Table 4.2 (a): Dose differences between reference and measured dose distributions for prostate

Cases	Dose differences/Gy			
	1st verification	2nd verification	3rd verification	Mean
1	0.02	0.01	0.01	0.01
2	0.04	0.03	0.01	0.03
3	0.00	0.02	0.00	0.01
4	0.03	0.04	0.00	0.02
5	0.01	0.00	0.00	0.00
Mean value	0.02	0.02	0.01	0.02

Table 4.2 (b): Dose differences between reference and measured dose distributions for head – and – neck

Cases	Dose differences/Gy			
	1st verification	2nd verification	3rd verification	Mean
1	0.02	0.00	0.00	0.01
2	0.04	0.01	0.04	0.03
3	0.03	0.01	0.01	0.02
4	0.06	0.00	0.00	0.02
5	0.00	0.01	0.00	0.00
Mean value	0.01	0.01	0.01	0.02

The values recorded in Table 4.3 (a) and (b) indicate that the dose differences between reference doses calculated at TPS and the doses measured by MatriXX for all prostate and head – and – neck IMRT cases were very small values. In spite of the fact that the MatriXX failed to record the exact values of the prescribed doses in both cases, it is evident that the dose differences are within the internationally acceptable range of deviations.

It is as well relevant to mention that the repeated verification exercises performed for each case to check for fluctuations in the measurement detectors have also recorded accurate values for dose differences in all the measurements. A summarized descriptive statistical test for these repeated verification values have exposed a standard deviation of 0.01Gy for the dose difference of prostate and 0.00Gy for the dose difference of head – and – neck

IMRT verifications. This constancy in the recorded values demonstrates the consistency in the methodology employed and points to the fact that the detectors are in good shape.

Table 4.3 (a) and (b) highlight the mean values of the resulting dose differences from the repeated verification exercises for all cases of both prostate and head – and – neck IMRT. In addition to that, they provide the percentage value of the dose differences to their reference doses calculated by TPS.

Table 4.3 (a): Percentage dose differences (%DD) recorded for prostate

Cases	Dose calculated by TPS/Gy	Mean Dose measured by MatriXX/Gy	Mean dose difference/Gy	Percentage dose difference/%
1	3.08	3.07	0.01	0.43
2	3.08	3.06	0.03	0.90
3	4.47	4.46	0.01	0.16
4	3.37	3.34	0.02	0.70
5	2.58	2.58	0.00	0.17
Mean value	3.32	3.30	0.02	0.47

Figure 4.5 (a) and (b) are graphical illustrations of the percentage dose differences computed from the mean dose differences as a percentages of the reference doses for each case of prostate and head – and – neck IMRT respectively.

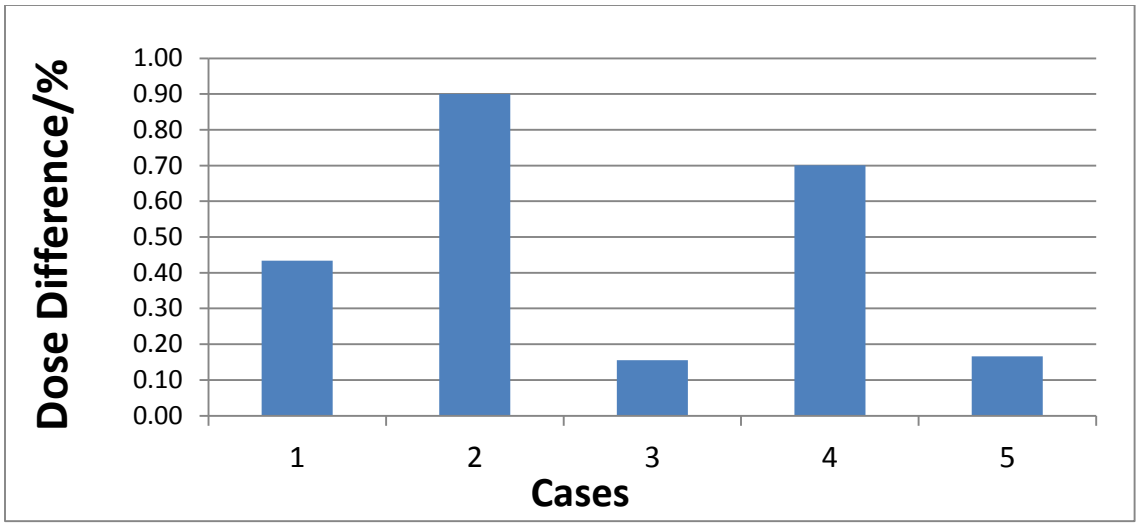

Figure 4.5 (a): Percentage of the mean dose difference for prostate

The percentage dose differences illustrated in Figure 4.5 (a) demonstrate a narrow range of mean dose differences for all prostate IMRT cases. The values range from 0.16 to 0.90% with the average percentage dose difference for all prostate IMRT cases being 0.46% with a standard deviation of 0.33%. Such a range of values indicate that for each prostate case, the percentage value of the mean dose difference is less than 1%.

Table 4.3 (b): Percentage dose differences (%DD) recorded for head – and – neck

Cases	Dose calculated by TPS/Gy	Mean Dose measured by MatriXX/Gy	Mean dose difference/Gy	Percentage dose difference/%
1	2.72	2.73	0.01	0.24
2	2.85	2.85	0.00	0.16
3	3.41	3.40	0.01	0.36
4	2.24	2.22	0.02	0.71
5	3.11	3.11	0.00	0.07
Mean value	2.87	2.86	0.01	0.31

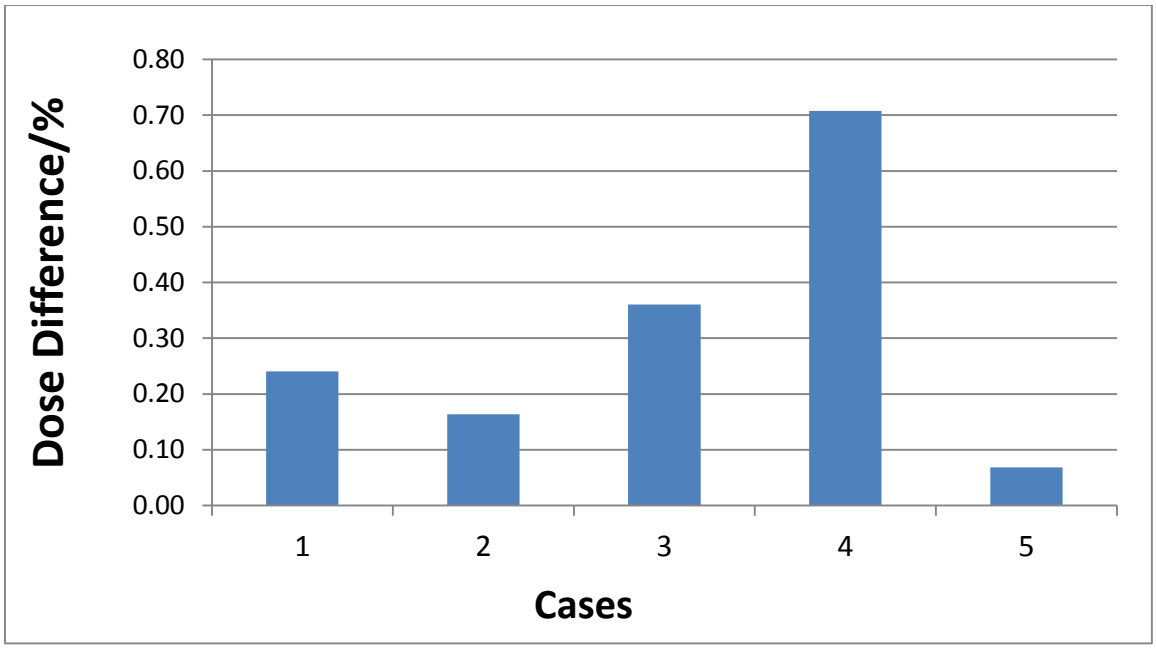

Figure 4.5 (b): Percentage of the mean dose difference for head – and - neck

The percentage dose differences illustrated in Figure 4.4 (b) present an increasingly controversial scenario. This follows the consistency of the unexpected accuracy of the percentage dose difference of the first head – and – neck case considering the fact that it particularly failed the passing criteria of the general verification exercise. Subsequent results on IMRT passing rates will throw more light on this argument. Despite this controversy, the general percentage dose differences for the head – and – neck cases also display a narrow range of mean dose differences for all cases. The values range from 0.07% to 0.71% with the average percentage dose difference for all head – and - neck IMRT cases being 0.31% with a standard deviation of 0.25%.

Considering the 3% tolerance limit acceptability of dose difference recommended by the AAPM TG 218 and the European Society for Radiotherapy and Oncology (ESTRO), the graphs in Figure 4.4 demonstrate highly accurate verification results, since all percentage

values of the mean dose differences are less than 1% (Miften, et al., 2018). The results therefore present an additional confirmation of the accuracy of the TPS and the treatment delivery.

4.7 Acceptance Criteria Passing Rate

The resulting ionization chamber array measurements have been evaluated based on TG 119 recommendations, using myQA software. Planned and measured planar dose distributions have been analyzed using the {3% (global), 3 mm} criteria. The passing gamma index values corresponding to points with gamma ≤ 1.0 are presented in the Table 4.5 (a) and (b).

Table 4.4 (a) and (b) relate the values of the passing rates of the various prostate and head – and – neck IMRT cases respectively in percentages. They give full accounts of the pass rates recorded for each case in all the repeated verification exercises performed and their corresponding mean values.

Table 4.4 (a): Results of MatriXX planar dose distributions using the point of maximum dose as global normalization point with percentage of points passing the {3% (global), 3 mm} gamma criteria for prostate IMRT.

Cases	Pass rates/%			
	1st verification	2nd verification	3rd verification	Mean
1	97.50	97.20	98.10	97.60
2	95.40	95.40	96.60	95.80
3	96.10	96.80	97.40	96.77
4	98.30	97.90	99.10	98.43
5	95.40	96.00	95.10	95.50
Mean value	96.54	96.66	97.26	96.82

Figure 4.5 (a) and (b) are charts displaying values of the passing rates of various cases for prostate and head – and – neck IMRT respectively. It is an illustration of the mean values of the pass rates recorded over the repeated verifications performed for each case.

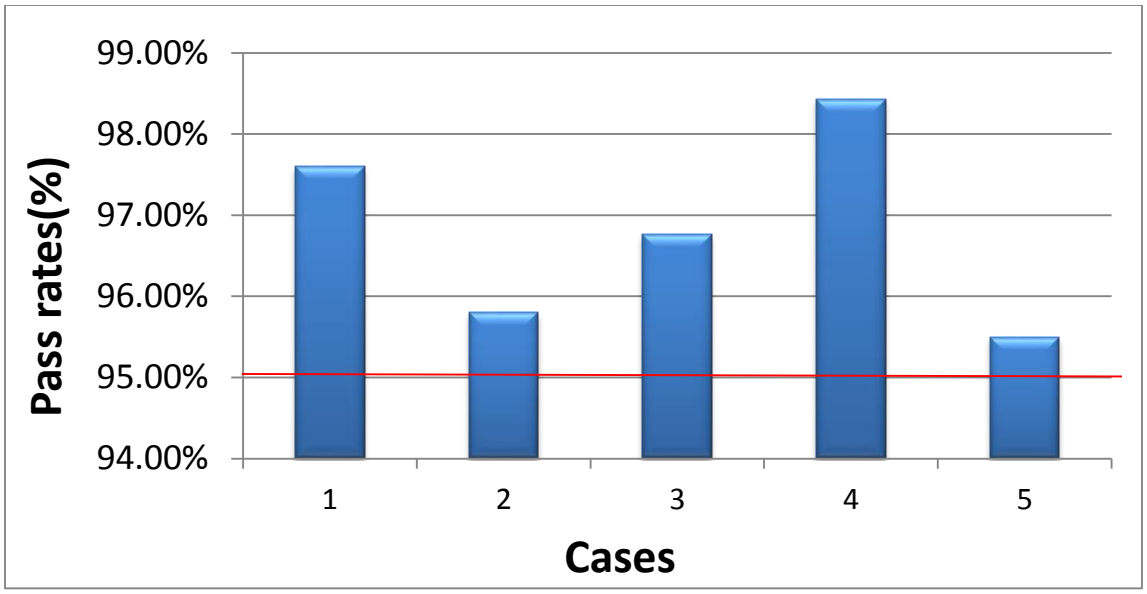

Fig. 4.6 (a): Plot of a gamma evaluation demonstrating prostate IMRT verification pass rate in percentages

The evaluation of 5 prostate IMRT plans with 6MV photon beam using gamma index method with TPS calculated dose distribution has produced passing values ranging from 95.50 to 98.43% for$\gamma \leq 1$. The results of the gamma evaluation method based on 95% passing criteria with {3% (global), 3 mm}, as plotted in Figure 4.5 (a) demonstrate that all prostate IMRT cases passed the acceptance criteria.

The mean passing rate, based on the gamma index method ($\gamma \leq 1$) for the treatment fields of each case using the MatriXXis $96.82 \pm 1.22\%$, showing good agreement with the calculated values for all 5 cases.

Table 4.4 (b): Results of MatriXX planar dose distributions using the point of maximum dose as global normalization point with percentage of points passing the {3% (global), 3 mm} passing criteria for head – and – neck IMRT.

Cases	Pass rates/%			
	1st verification	2nd verification	3rd verification	Mean
1	93.70	95.00	95.10	94.60
2	96.50	96.90	96.90	96.77
3	96.50	97.10	96.80	96.80
4	96.30	95.80	96.60	96.23
5	97.10	97.80	98.20	97.70
Mean value	96.02	96.52	96.72	96.42

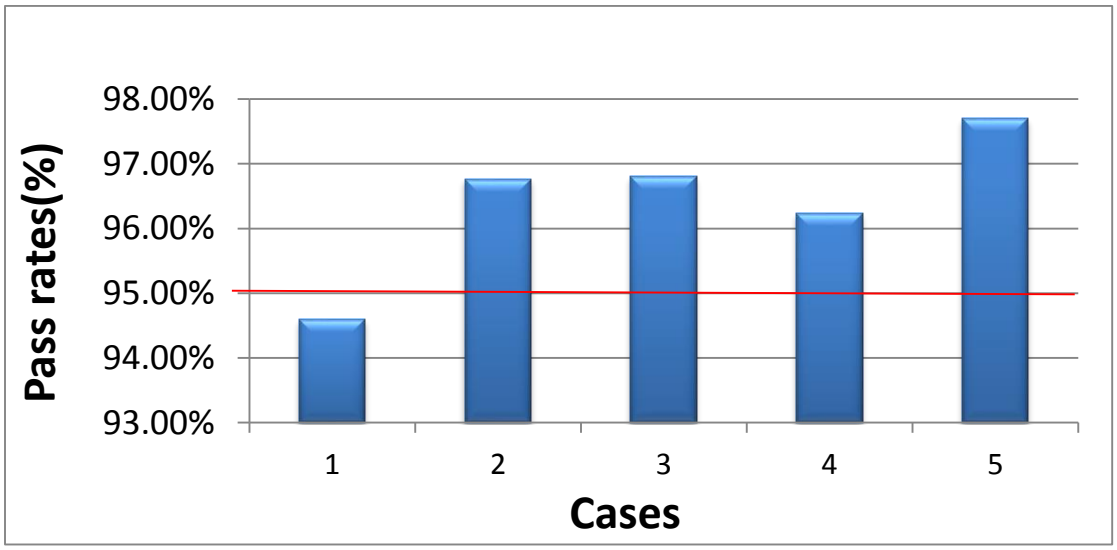

Figure 4.6 (b): Plot of a gamma evaluation demonstrating head – and – neck IMRT verification pass rate in percentages

The mean value for the pass rate of the Head - and - neck IMRT cases is 96.42% with one case failing the acceptance criteria of the gamma evaluation method as illustrated in Figure 4.5 (b). The passing values vary from 94.60 to 97.70% with standard deviation of 1.14%.

It is extremely relevant to state that the failure of the mean value of this particular case was affected by the passing rate recorded in the first verification exercise in which the very case had 93.70% pass rate. However, subsequent verifications of this case all passed the acceptance criteria with 95.00 and 95.10% respectively. It is as well important to mention that, the case in question was the first head – and – neck verification performed at the centre, and the results could be affected by lack of confidence and experience. Meanwhile, the passing values obtained in the subsequent verification of the same case suggest that the failure in the first verification could also be attributed to a technical source of error such tongue – and – groove effect.

Since the effectiveness of a treatment plan is estimated through the evaluation of the gamma passing rate, it was therefore established that the treatment planning generated are effective for implementation.

The credibility of IMRT implementation at the centre is evidenced by juxtaposing the data acquired from the study with the 95% passing rate, using as criteria a tolerance of dose difference of 3% and a tolerance of distance – to – agreement of 3 mm, as acceptable by majority of international protocols. Considering the report of AAPM TG 119 and other papers confirming that the 3% DD and 3 mm DTA is the most commonly used by physicists in pretreatment IMRT QA, it is satisfactory to state that the criteria used for the acceptance in this work is a suitable (Ezzell, et al., 2009).

4.8 Setup Accuracy from Reproducibility of Passing Rate Values

In order to check for fluctuations in the 2D array, a plot of values for pass rates obtained from repeated IMRT verification results have been displayed, demonstrating the variation of the detector response for same plan parameters and phantom setup at different times.

Figure 4.7 (a) and (b) are plots of values for pass rates recorded from repeated verification exercises for prostate and head – and – neck IMRT respectively. They provide detailed comparison of results obtained for same cases over the repeated verifications.

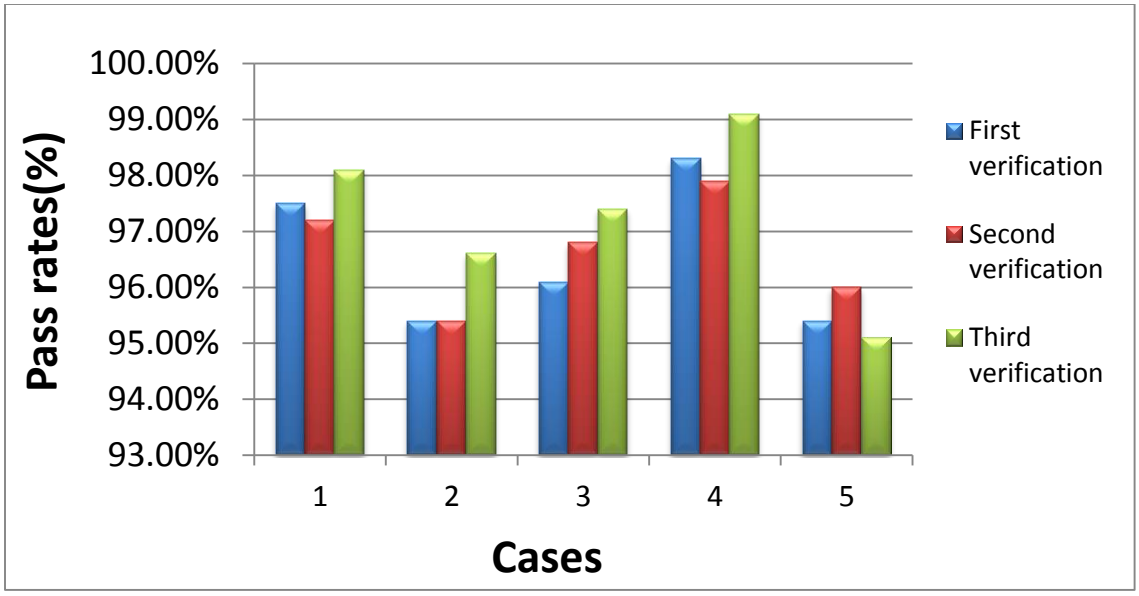

Figure 4.7 (a): Plot of gamma evaluation results comparing pass rate values over repeated verifications for prostate IMRT

In spite of the tabular information in Table 4.5 (a), that all prostate cases passed the acceptance criteria throughout the verifications performed, the graphical display of the pass rate values of same cases of prostate IMRT in Figure 4.7 (a) signifies inexactness of dose delivery to the prescribed targets and depths.

However, the pass rate values obtained from the repeated verification of all prostate IMRT cases do not suffer so much difference from their first verification values, with one particular case of the second verification precisely repeating the value of the first verification result. An ANOVA statistical tool has expressed a p – value = 0.039, indicating the statistical significance of the repeated verification results. This is an indication that the MatriXX used for the verification exercises does not suffer from fluctuations.

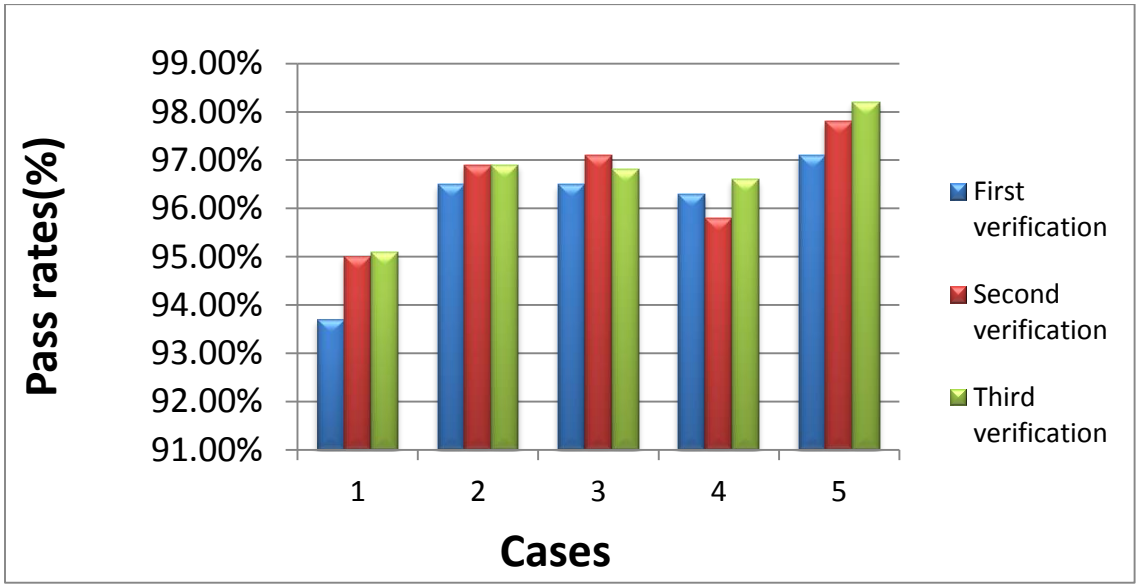

Figure 4.7 (b): Plot of gamma evaluation results comparing pass rate values over repeated verifications for head – and – neck IMRT

Despite the observed imprecision of dose delivery in both Figure 4.7 (a) and (b), the graphical comparison of the pass rate values obtained from the repeated verification of same cases of head – and – neck IMRT in Figure 4.7 (b) demonstrates closeness to the first verification values than observed in Figure 4.7 (a) for prostate IMRT. An ANOVA statistical tool has also revealed a p – value = 0.001, indicating the statistical significance of the resulting data.

Except for the case of the first head – and – neck IMRT case, which passed the acceptance criteria in its subsequent verifications only, the other head – and IMRT cases passed the gamma criteria in all the rounds of verification. This observation also explains the possibility of all cases passing the acceptance criteria with increasing experience. It is therefore suspected that the failure of the first head – and – neck case was caused by lack of confidence and experience at the beginning of the head – and – neck delivering.

The observations made above demonstrate the accuracy of the treatment setup, the TPS used for IMRT plans at the centre and the dose delivery of the medical linear accelerator. These observations also confirm the credibility of the MatriXX detector and its compatibility with the miniPhantom at the centre. It has also demonstrated the facility's readiness for implementation of pretreatment patient – specific QA for IMRT. Meanwhile, the impreciseness of pass rate values over the repeated exercises is possibly due to set up errors incurred at the different verification times.

4.9 Cause of failure of acceptance criteria

The actual cause of the failure of the acceptance criteria of the first head – and – IMRT is not certain. This is because, it is very difficult to establish whether differences between measurement and calculation are caused by planning or delivery or even measurement technique. According to TG 82 of the AAPM (Low, et al., 2003), dose measurements in IMRT is more difficult owing to the presence of localized dose gradients.

Based on explanations given by TG 119 of the AAPM, "differences between measurements and prediction may be caused by measurement uncertainty, limitations in the accuracy of dose calculations, and limitations in the dose delivery mechanisms" (Ezzell, et al., 2009).

It is however possible that the error might not even come from the accuracy of the dosimetric components of the treatment planning process. The TG 63 of the AAPM specifies copious sources of uncertainties in treatment planning alone, starting from patient localization, imaging definition of anatomy, establishment of beam geometry, dose calculation, dose display and plan evaluation (Reft, et al., 2003).

4.10 Influence of Different Anatomical Sites over Passing Rates

Table 4.5 presents the mean pass rate values obtained for all cases over each set of the verifications performed for prostate and head – and – neck IMRT.

Table 4.5: Mean pass rate values for prostate and head - and - neck IMRT verifications

Case type	First verification/%	Second verification/%	Third verification/%
Prostate	96.54	96.66	97.26
Head - and – neck	96.02	96.52	96.72

Figure 4.8 demonstrates the comparison of the mean values of the pass rates recorded for all IMRT cases of prostates and head – and – neck over the set of verifications performed. It outlines the values of the mean pass rate of prostate versus head – and – neck for each set of verifications.

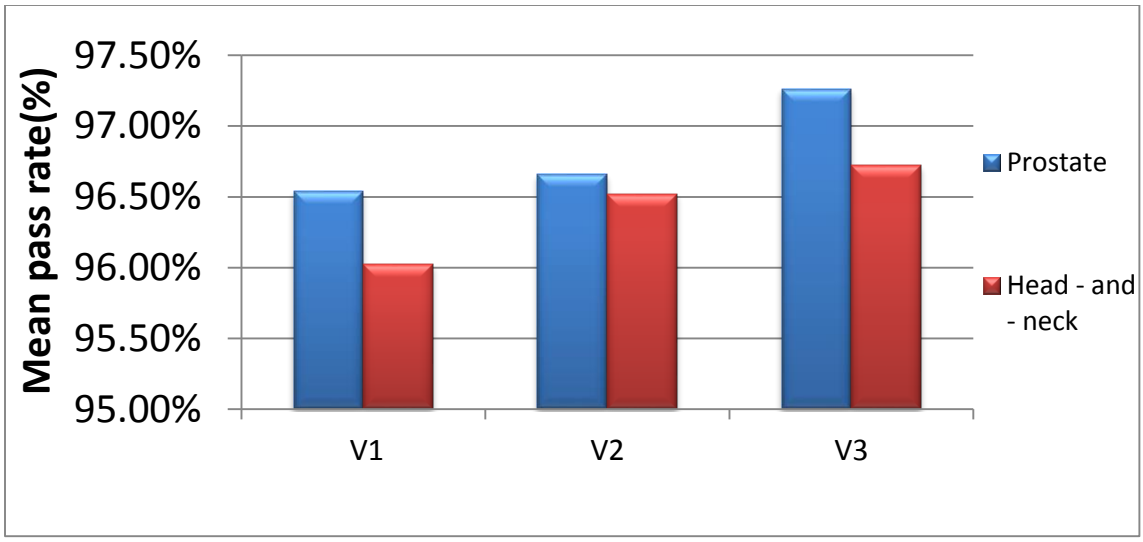

Figure 4.8: A plot comparing mean pass rate values for prostate and head – and – neck IMRT verifications

The plots indicate that the mean value of the pass rates of the prostate IMRT are generally greater than that of head – and – neck over all the sets of verifications. The overall mean value for the pass rates of prostate IMRT was $96.82 \pm 1.22\%$ and $96.42 \pm 1.14\%$ for head – and – neck IMRT.

This is possibly due to the complexity associated with the treatment planning and delivery of head – and – neck IMRT plans, and calls for a review in the planning and treatment protocols of head – and – neck IMRT cases at the centre to be able to meet the 95% passing criteria.

This is also an indication that results for patient – specific verifications of IMRT cases can be influenced by complexity of the treatment planning and delivery of the different anatomical sites. There is therefore the need to set different acceptance criteria for the verification of diverse body parts.

4.11 Relationship between Pass Rates and Dose Differences

Table 4.6 provides mean pass rate values for both prostate and head – and – neck with their corresponding percentage dose differences.

Table 4.6: Dose difference and their corresponding passing values

Cases	Mean pass rate/%		Percentage dose difference/%	
	Prostate	Head - and – neck	Prostate	Head - and – neck
1	97.60	94.60	0.43	0.24
2	95.80	96.77	0.90	0.16
3	96.77	96.80	0.16	0.36
4	98.43	96.23	0.70	0.71
5	95.50	97.70	0.17	0.07

Figure 4.9 (a) and (b) gives a visual demonstration of the relationship between dose differences and their corresponding pass rates for prostate and head – and – neck IMRT respectively.

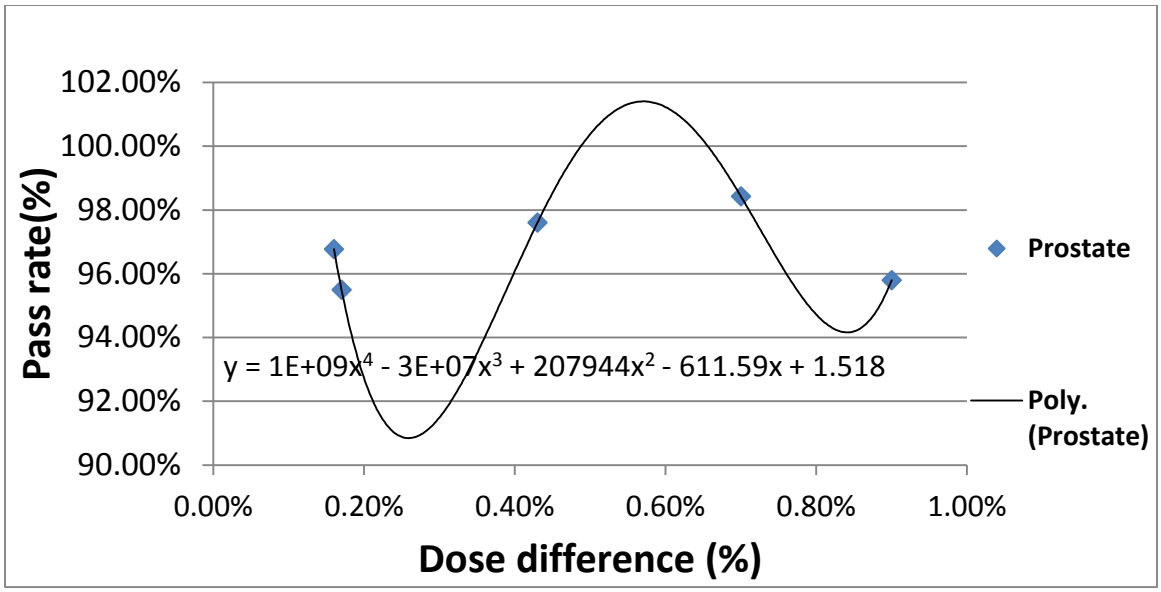

Figure 4.9 (a): A scatter plot revealing the possibility of influence of dose difference on prostate IMRT passing rate values

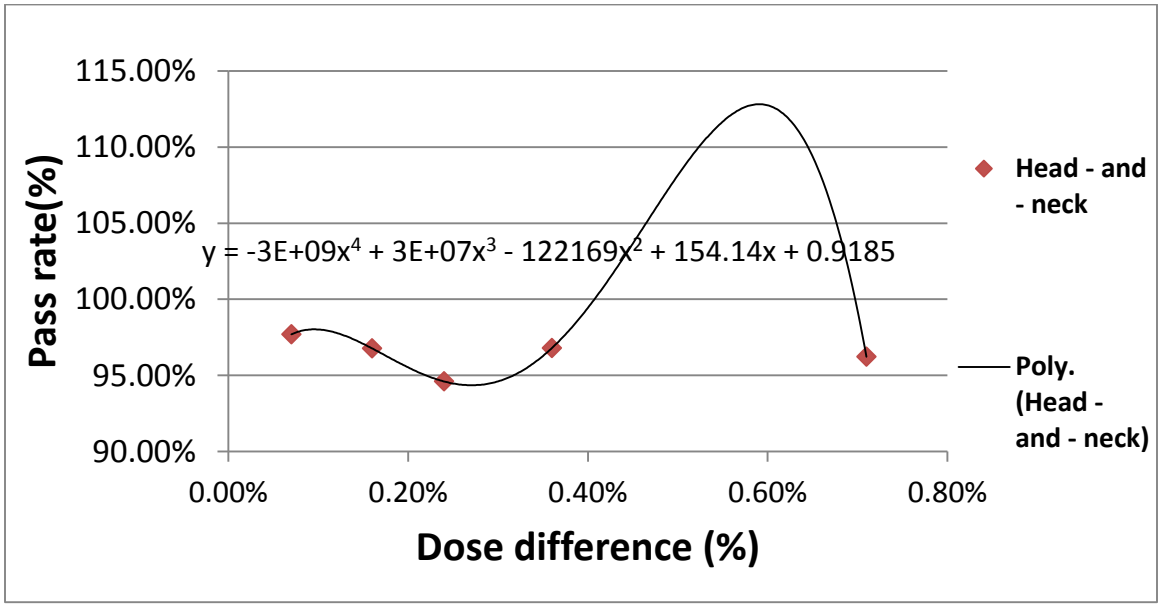

Figure 4.9 (b): A scatter plot revealing the possibility of influence of dose difference on head – and – neck IMRT passing rate values

The data presented in Table 4.7 as plotted in both (a) and (b) of Figure 4.9 reveal the unlikely influence of the dose difference on the passing values of the verification QA. Meanwhile, the gamma passing rate represents the fraction of dose points per plan that conform to the acceptance criteria. This points to the fact that the dose difference should basically have influence on the gamma passing rate.

Considering the gamma index as a representation of the multidimensional distance that can least possibly be between the measured and calculated dose points in a space comprising of dose and coordinates of distance, relevant information on both the dose and spatial resolution are required to establish a well-founded relationship.

However, as part of its major limitations, the gamma index method, fails to provide information about their spatial resolution. This makes this procedure quite difficult, however, it is well understood that the passing rate is influenced by both factors, and only one of such factors known cannot have significant influence over the pass rate.

4.12 Research Limitations

This research has been met with several limitations, making progress quite difficult. Mostly among these are:

a) Inaccessibility of different types of 2D detector arrays and corresponding software to compare measured dose distributions recorded with MatriXX for a variety of relevant information on detector response to the measured dose distributions;
b) Less frequency of IMRT cases to the centre limits the sample population to the research. Results from larger populations will yield better outcomes for the work;

c) The limitation of GI method is that it only determines the number of points out of tolerance without giving any information about their spatial location. It is therefore extremely difficult for one to assume that the %GP of the entire plan corresponds to that of the single organ;

d) Restrictions to one type of medical linear accelerator. Inaccessibility of different brands of medical linear accelerators in the facility restricted the study to only a varian linac for the work, making recommendations from the findings difficult to be justified.

CHAPTER FIVE

CONCLUSIONS AND RECOMMENDATIONS

5.1 Introduction

This chapter presents the conclusion made from the results obtained, and the necessary recommendations to stakeholder institutions.

5.2 Conclusion

The prescribed doses calculated at TPS were accurately delivered by the medical linear accelerator, and the gamma criteria for acceptance were mostly satisfied by the selected cases throughout the research for both cancer sites under study.

The analysis made demonstrates that these IMRT results are consistent with peer reviewed baseline data for a well-commissioned IMRT program, taken into consideration the limitations of the medical linear accelerator at the centre.

The results also demonstrate that the delivery equipment, the treatment planning system, the QA tools and their corresponding software are accurate and therefore acceptable for IMRT implementation at the centre. The protocol followed for the dosimetric pretreatment verification and the analytical software used are also proven to be authentic.

Guidelines on IMRT and protocols that can ensure safe implementation of patient-specific IMRT QA in Ghana based on available resources have been recommended.

5.3 Recommendations

In view of the findings of the study, and the challenges encountered during the course of the work, a number of recommendations for improving the available systems have been derived.

5.3.1 To the Radiation Oncology Departments

1. The National Centre for Radiotherapy and Nuclear Medicine is recommended to acquire other 2D detectors and software to facilitate further studies in patient – specific IMRT QA using other tools in comparison to the MatriXX.

5.3.2 To the Ghanaian Clinical Physicist

- With IMRT, the Ghanaian medical physicist is recommended to balance patient-specific tests described with routine equipment-QA.
- All IMRT treatment plans should be verified prior to treatment delivery;
- Analysis of IMRT QA measurements and the corresponding treatment plans should be performed in absolute dose mode;
- DD and DTA of 3%/ 3 mm should be adopted for all cases, but may be reviewed to 2% / 2 mm for other cases with the exception of head – and – neck;
- Gamma passing rate of 95% should be used for all cases with the exception of very complex treatment plan where a passing rate of 90% is acceptable;
- Dose threshold of 10% should be used;
- Global gamma assessment criteria should be adopted;
- Treatment plans that fail to pass the gamma passing rate should be investigated;
- Use of very large fields for IMRT should be discouraged.

REFERENCES

Abdel-Wahab, M., Bourque, J. M., Pynda, Y., Iżewska, J., Van der Merwe, D., Zubizarreta, E., & Rosenblatt, E. (2013). Status of radiotherapy resources in Africa: an International Atomic Energy Agency analysis. *The lancet oncology*, *14*(4), e168-e175.

Almond, P. R., Biggs, P. J., Coursey, B. M., Hanson, W. F., Huq, M. S., Nath, R., & Rogers, D. W. O. (1999). AAPM's TG-51 protocol for clinical reference dosimetry of high-energy photon and electron beams. *Medical physics*, *26*(9), 1847-1870.

Azangwe, G., Grochowska, P., Georg, D., Izewska, J., Hopfgartner, J., Lechner, W., ... & Fukumura, A. (2014). Detector to detector corrections: a comprehensive experimental study of detector specific correction factors for beam output measurements for small radiotherapy beams. *Medical physics*, *41*(7), 072103.

Cheung, K. Y. (2006). Intensity modulated radiotherapy: advantages, limitations and future developments. *Biomed Imaging Interv J*, *2*(1), e19.

Cho, B. (2018). Intensity-modulated radiation therapy: a review with a physics perspective. *Radiation oncology journal*, *36*(1), 1.

Cyriac, S., Musthafa, M. M., Ganapathi Raman, R., Abdul Haneefa, K., & Hridya, V. T. (2014). Pretreatment patient specific quality assurance and gamma index variation study in gantry dependent EPID positions for IMRT prostate treatments. *Journal of Radiotherapy*, *2014*.

De Los Santos, J., Popple, R., Agazaryan, N., Bayouth, J. E., Bissonnette, J. P., Bucci, M. K., ... & Langen, K. (2013). Image guided radiation therapy (IGRT) technologies for radiation therapy localization and delivery. *International Journal of Radiation Oncology• Biology• Physics*, *87*(1), 33-45.

De Wagter, C. (2006). QA-QC of IMRT: European Perspective. In *Image-guided IMRT* (pp. 117-128). Springer, Berlin, Heidelberg.

Dumitru, N. (2019). Commissioning and Acceptance Testing of a Varian TrueBeam.

Ebert, M. A., Howlett, S. J., Harrison, K., Cornes, D., Hamilton, C. S., & Denham, J. D. (2008). Linear-accelerator X-ray output: a multicentre chamber-based intercomparison study in Australia and New Zealand. *Australasian Physics & Engineering Sciences in Medicine*, *31*(4), 268-279.

Ezzell, G. A., Burmeister, J. W., Dogan, N., LoSasso, T. J., Mechalakos, J. G., Mihailidis, D., ... & Shi, J. (2009). IMRT commissioning: multiple institution planning and dosimetry comparisons, a report from AAPM Task Group 119. *Medical physics*, *36*(11), 5359-5373.

Guerreiro, S. F. C. (2018). *Automating daily Llnac quality control using Portal Images* (Doctoral dissertation).

Hernandez, V., Hansen, C. R., Widesott, L., Bäck, A., Canters, R., Fusella, M., ... & Koniarová, I. (2020). What is plan quality in radiotherapy? The importance of evaluating dose metrics, complexity, and robustness of treatment plans. *Radiotherapy and Oncology*.

Intensity Modulated Radiation Therapy Collaborative Working Group. (2001). Intensity-modulated radiotherapy: current status and issues of interest. *International Journal of Radiation Oncology* Biology* Physics*, *51*(4), 880-914.

Klein, E. E., Hanley, J., Bayouth, J., Yin, F. F., Simon, W., Dresser, S. & Liu, C. (2009). Task Group 142 report: Quality assurance of medical acceleratorsa. *Medical physics*, *36*(9Part1), 4197-4212.

Knutson, N. C. (2018). *A Cost Effective and Efficient Methodology for Collecting Radiation Therapy Beam Data* (Doctoral dissertation, University of Massachusetts Lowell).

Low, D. A., Moran, J. M., Dempsey, J. F., Dong, L., & Oldham, M. (2011). Dosimetry tools and techniques for IMRT. *Medical physics*, *38*(3), 1313-1338.

Magli, A., Moretti, E., Tullio, A., Giannarini, G., Tonetto, F., Urpis, M., ... & De Giorgi, G. (2018). Hypofractionated simultaneous integrated boost (IMRT-SIB) with pelvic nodal irradiation and concurrent androgen deprivation therapy for high-risk prostate cancer: results of a prospective phase II trial. *Prostate cancer and prostatic diseases*, *21*(2), 269-276.

Mans, A., Schuring, D., Arends, M. P., Vugts, C. A., Wolthaus, J. W., Lotz, H. T., ... & van de Kamer, J. B. (2016). The NCS code of practice for the quality assurance and control for volumetric modulated arc therapy. *Physics in Medicine & Biology*, *61*(19), 7221.

Medin, J., Ross, C. K., Klassen, N. V., Palmans, H., Grusell, E., & Grindborg, J. E. (2006). Experimental determination of beam quality factors, kQ, for two types of Farmer chamber in a 10 MV photon and a 175 MeV proton beam. *Physics in Medicine & Biology*, *51*(6), 1503.

Miften, M., Olch, A., Mihailidis, D., Moran, J., Pawlicki, T., Molineu, A., ... & Papanikolaou, N. (2018). Tolerance limits and methodologies for IMRT measurement-based verification QA: recommendations of AAPM Task Group No. 218. *Medical physics*, *45*(4), e53-e83.

Mijnheer, B. (Ed.). (2017). *Clinical 3D dosimetry in modern radiation therapy*. CRC Press.

Page, A. A. (2016). Intensity Modulated Radiation Therapy (IMRT) AHM.

Pan, Y., Yang, R., Zhang, S., Li, J., Dai, J., Wang, J., & Cai, J. (2019). National survey of patient specific IMRT quality assurance in China. *Radiation Oncology*, *14*(1), 69.

Ravichandran, R., Bhasi, S., Binukumar, J. P., & Davis, C. A. (2011). Need of patient-specific quality assurance and pre-treatment verification program for special plans in radiotherapy. *Journal of Medical Physics/Association of Medical Physicists of India*, *36*(3), 181.

Reft, C., Alecu, R., Das, I. J., Gerbi, B. J., Keall, P., Lief, E., ... & Van Dyk, J. (2003). Dosimetric considerations for patients with HIP prostheses undergoing pelvic irradiation. Report of the AAPM Radiation Therapy Committee Task Group 63. *Medical physics*, *30*(6), 1162-1182.

Saboori, M. (2015). Development of a daily dosimetric control for radiation therapy using an electronic portal imaging device (EPID).

Solberg, T. D., Agazaryan, N., Goss, B. W., Dahlbom, M., & Lee, S. P. (2004). A feasibility study of 18F-fluorodeoxyglucose positron emission tomography targeting and simultaneous integrated boost for intensity-modulated radiosurgery and radiotherapy. *Journal of neurosurgery*, *101*(Supplement3), 381-389.

Son, J., Baek, T., Lee, B., Shin, D., Park, S. Y., Park, J., ... & Yoon, M. (2015). A comparison of the quality assurance of four dosimetric tools for intensity modulated radiation therapy. *Radiology and oncology*, *49*(3), 307-313.

Stasi, M., Bresciani, S., Miranti, A., Maggio, A., Sapino, V., & Gabriele, P. (2012). Pretreatment patient-specific IMRT quality assurance: a correlation study between

gamma index and patient clinical dose volume histogram. *Medical physics*, *39*(12), 7626-7634.

Stojadinovic, S., Ouyang, L., Gu, X., Pompoš, A., Bao, Q., & Solberg, T. D. (2015). Breaking bad IMRT QA practice. *Journal of applied clinical medical physics*, *16*(3), 154-165.

Stucki, G., Muench, W., & Quintel, H. (2002). *The METAS absorbed dose to water calibration service for high energy photon and electron beam radiotherapy* (No. IAEA-CN--96).

Tagoe, S. N. A., Mensah, S. Y., Fletcher, J. J., & Sasu, E. (2018). Telecobalt Machine Beam Intensity Modulation with Aluminium Compensating Filter Using Missing Tissue Approach. *Iranian Journal of Medical Physics*, *15*(1), 48-61.

Tagoe, S. N., Mensah, S. Y., & Fletcher, J. J. (2018). Implementation of compensator-based intensity modulated radiotherapy with a conventional telecobalt machine using missing tissue approach. *Polish Journal of Medical Physics and Engineering*, *24*(4), 171-179.

Wegener, S., & Sauer, O. A. (2019). The effective point of measurement for depth-dose measurements in small MV photon beams with different detectors. *Medical Physics*, *46*(11), 5209-5215.

World Health Organization. (2020). WHO report on cancer: setting priorities, investing wisely and providing care for all.

APPENDIX A

Table A1: Prostate fail rate values

Cases	**Fail rates/%**			
	1st verification	2nd verification	3rd verification	Mean
1	2.50%	2.80%	1.90%	2.40%
2	4.60%	4.60%	3.40%	4.20%
3	3.90%	3.20%	2.60%	3.23%
4	1.70%	2.10%	0.90%	1.57%
5	4.60%	4.00%	4.90%	4.50%
Mean value	3.46%	3.34%	2.74%	3.18%

Table A2: Head – and – Neck fail rate values

Cases	**Fail rate/%**			
	1st verification	2nd verification	3rd verification	Mean
1	6.30%	5.00%	4.90%	5.40%
2	3.50%	3.10%	3.10%	3.23%
3	3.50%	2.90%	3.20%	3.20%
4	3.70%	4.20%	3.40%	3.77%
5	2.90%	2.20%	1.80%	2.30%
Mean value	3.98%	3.48%	3.28%	3.58%

Table A3: Prostate IMRT verification results

Cases	Dose ratio/Gy	Plane position/cm	Delta dose abs/Gy	Delta dose ratio/%	Delta distance/cm	Threshold/ %	Search distance/cm
1	3.07933	0.17	0.09238	3	0.3	5	0.45
2	3.08476	0.17	0.12026	3	0.3	5	0.45
3	4.46913	0.17	0.13407	3	0.3	5	0.45
4	3.36598	0.17	0.10098	3	0.3	5	0.45
5	2.58407	0.17	0.07752	3	0.3	5	0.45

Table A4: Head – and – Neck IMRT verification results

Cases	Dose ratio/Gy	Plane position/cm	Delta dose abs/Gy	Delta dose ratio/%	Delta distance/cm	Threshold/ %	Search distance/cm
1	2.72351	0.17	0.08171	3	0.3	5	0.45
2	2.84981	0.17	0.08549	3	0.3	5	0.45
3	3.40487	0.17	0.10225	3	0.3	5	0.45
4	2.24384	0.17	0.06732	3	0.3	5	0.45
5	2.58407	0.17	0.07752	3	0.3	5	0.45

Table A5: Summary of Prostate and Head - and - Neck verification results

	Prostate		Head - and – Neck	
Cases	Dose ratio/Gy	Delta dose abs/Gy	Dose ratio/Gy	Delta dose abs/Gy
1	3.07933	0.09238	2.72351	0.082
2	3.08476	0.12026	2.84981	0.085
3	4.46913	0.13407	3.40487	0.102
4	3.36598	0.10098	2.24384	0.067
5	2.58407	0.07752	2.58407	0.078

Table A6: Prostate histogram information

Cases	Average value	Passing values/%	Failing values /%	Threshold T1/Gy	Threshold T2/Gy	Values < T1/%	T1 < values < T2/%	Values > T2/%
1	0.398	97.5	2.5	0.425	1.353	58.8	41.1	0.1
2	0.00072	95.4	4.6	4E-04	0.00135	4.2	95.8	0
3	0.434	96.1	3.9	0.425	1.353	54.4	45.2	0.4
4	0.301	98.3	1.7	0	1.534	0.1	99.9	0.1
5	0.411	95.4	4.6	0	1.534	0.1	99.8	0.1

Table A7: Head – and – Neck histogram information

Cases	Average value	Passing values/%	Failing values /%	Threshold T1/Gy	Threshold T2/Gy	Values < T1/%	T1 < values < T2/%	Values > T2/%
1	0.449	93.7	6.3	0	1.534	0	99.2	0.8
2	0.405	96.5	3.5	0	1.534	0	99.5	0.5
3	0.355	96.5	3.5	0	1.534	0	99.9	0
4	0.345	96.3	3.7	0	1.534	0.1	99.8	0.1
5	0.411	97.1	2.9	0	1.534	0.1	99.9	0.1

Table A8: Data showing the trend of IMRT implementation in Ghana

Month	**Number of cases**
January	0
February	0
March	0
April	1
May	2
June	4
July	7
August	10

APPENDIX B

DEPARTMENT OF MEDICAL PHYSICS
SCHOOL OF NUCLEAR AND ALLIED SCIENCES
University of Ghana – Atomic

Phone: +233 264 945 805
Fax: +233 302 400 807
Website: http://snas.edu.gh

Office of the Head
P. O. Box AE 1
Atomic Energy
Accra – GHANA

Our Ref: SNAS / MPHY/40
Your Ref:

Date: 19th August, 2020.

National Centre for Radiotherapy
And Nuclear Medicine
Korle – Bu
Accra.

National Centre For Radiotherapy
RECEIVED
Date 25/08/20
KORLE-BU
And Nuclear Medicine

Dear Sir,

LETTER OF INTRODUCTION – MR. ALHASSAN MOHAMMED BAIDOO

I am writing to introduce to you Mr. Alhassan Mohammed Baidoo, a second year MPhil student of the Department of Medical Physics SNAS, with student identification number 10702652.

Mr. Alhassan is undertaking his research study under the supervision of Dr. Samuel Tagoe and Mr. Eric Addison. His research study is titled "Implementation of pretreatment Patient specific quality Assurance for Intensity Modulated Radiotherapy." As part of the workplan, he will be using Medical Linear Accelerator, Radiotherapy CT, Blue Phantom 2, SLAB Phantom, IBA Mini Phantom, 0.6cc ion chamber, Varian Eclipse TPS, MYQA SW.

It will be appreciated if Mr. Alhassan Mohammed Baidoo is granted permission to undertake the study at the Radiotherapy Department.

Looking forward to your kind support.

Yours faithfully,

Head of Physics
Approved

DR. FRANCIS HASFORD
(HEAD)